1-1-2010

# Assessment of an acoustic chamber for testing structure-borne sound transmission in a double-panel assembly

Peter Bulski
*Ryerson University*

# ASSESSMENT OF AN ACOUSTIC CHAMBER FOR TESTING STRUCTURE-BORNE SOUND TRANSMISSION IN A DOUBLE-PANEL ASSEMBLY

By

Peter Bulski

B.Eng., Ryerson University, 2007

A thesis

Presented to Ryerson University

In partial fulfillment of the

Requirement for the degree of

Master of Applied Science

In the Program of

Mechanical Engineering

Toronto, Ontario, Canada, 2010

# AUTHOR'S DECLARATION

I hereby declare that I am the sole author of this thesis.

I authorize Ryerson University to lend this thesis to other institutions or individual for the purpose of scholarly research.

_____ _____

Date Peter Bulski

I further authorize Ryerson University to reproduce this thesis by photocopying or by other means, in total or in part, at the request of other institutions or individuals for the purpose of scholarly research.

_____ _____

Date Peter Bulski

# BORROWER

Ryerson University requires the signature of all persons using or photocopying this thesis. Please sign below, and give address and date.

# ABSTRACT

## ASSESSMENT OF AN ACOUSTIC CHAMBER FOR TESTING STRUCTURE-BORNE SOUND TRANSMISSION IN A DOUBLE-PANEL ASSEMBLY

by
Peter Bulski
Masters of Applied Science
2010
Mechanical Engineering
Ryerson University

An acoustic chamber was designed for testing structure-borne sound transmission in a double-panel assembly induced by point connectors. Several vibration isolators were tested and the overall effects on the noise transmitted through the assembly were predicted by establishing the link between the vibratory acceleration level (VAL) and the sound pressure level (SPL). A detailed assessment of the acoustic chamber showed that a major modification of the double-panel assembly is required before the acoustic performance of this assembly could be evaluated directly using insertion loss (IL) measurements where the sound pressure level (SPL) difference is the performance indicator. This thesis describes the assessment findings and retrofitting options. It is concluded that adjustments to the VAL-to-SPL relation are required to account for distance, radiation efficiency, and room effects. Further adjustments to the acoustic chamber are required to enhance its performance.

# ACKNOWLEDGMENTS

Many thanks are due to many people. I could not have completed this work without the help that was freely offered. Help was given throughout many stages of this research work.

1. Many thanks are due to Dr. Greg Kawall who developed the original idea for this work. He had devoted a good portion of his busy schedule to assist me in this work. He has answered many questions, and I have been given encouragement throughout.
2. Dr. Shudong Yu has provided a data acquisition system for me and has given me many good suggestions in his area of expertise.
3. Thanks are due to most of the Ryerson University Technical Officers, but especially, Joseph Amankrah, who must be thanked for his advice and his generosity in providing raw materials and assistance with wood working and machining.
4. Graduate students who have helped and answered questions include: Xuan Zhang, Farzin Abbasian, Ravi Peri, and Wen Li.

# TABLE OF CONTENTS

# LIST OF TABLES

# LIST OF FIGURES

# NOMENCLATURE

| | |
|---|---|
| $(\langle\ \rangle)$ | Spaced averaged value |
| $\overline{(\ )}$ | Mean square value |
| $a$ | Side length of the square plate, m |
| $a'$ | Characteristic structural dimension - spherical radius in this case, m |
| $A$ | Plate area, $m^2$ or room sound absorption, $m^2$ Sabine |
| $A_R$ | Sound absorption of the receiving room with test specimen in place, $m^2$ Sabine |
| $B$ | Bending stiffness per unit length of the plate, Nm |
| $BW$ | Half-power bandwidth, Hz |
| $c_0$ | Speed of sound in air, $m/s^2$ |
| $d$ | Depth of the air space confined by two panels, m |
| d | The rate of decay of sound pressure level, dB/s |
| $df$ | Mean modal separation, Hz |
| D | Mode coefficient for edges conditions |
| $e$ | Distance between point forces, m |
| $E$ | Young's modulus of the plate, $N/m^2$ |
| $f$ | Frequency, Hz |
| $f_B$ | Bridging frequency, Hz |
| $f_{ijk}$ | Resonant frequencies of the modes of vibrating in a rectangular cavity, Hz |
| $f_l$ | Upper frequency limit, Hz |
| $f_{r,\,0}$ | Normal-incidence fundamental natural frequency of a mass-spring-mass system, Hz |
| $f_{r,\,r}$ | Random-incidence fundamental natural frequency of a mass-spring-mass system, Hz |
| $f_s$ | Sampling rate, Hz |
| $f_S$ | Schroeder frequency, Hz |
| $f_0$ | Fundamental natural frequency of a flat, homogenous, thin finite-size panel, Hz |

$f_1$ First axial mode resonant frequency of an air space between two parallel plates, Hz

$F(\omega_n)$ Fourier Transform

$|F_n|$ Fourier Spectrum multiplied by equivalency constant

$|F_n|^2$ Spectral Density Function or the Spectrum

$h$ Plate thickness, m

$i$ Index of a particular mode along the length, or an imaginary number

$j$ Index of a particular mode along the width

$k$ Index of a particular mode along the height

$k'$ Acoustic wavenumber, $m^{-1}$

$IL$ Insertion loss, dB

$K_a$ Equivalent stiffness of an air space, $N/m^3$

$K_p$ Equivalent stiffness of square panel, $N/m^3$

$L_e$ Sum of all edge lengths, m

$L_{eq}$ Equivalent continuous sound pressure level

$\bar{L}$ Average sound pressure level, dB

$\bar{L}_a$ Adjusted signal level, dB

$\bar{L}_b$ Background noise level, dB

$\bar{L}_R$ Average sound pressure level in the receiving room, dB

$\bar{L}_{R_a}$ Average sound pressure level after the installation, dB

$\bar{L}_{R_b}$ Average sound pressure level before the installation, dB

$\bar{L}_S$ Average sound pressure level in the source room, dB

$\bar{L}_{sb}$ Level of signal and background combined, dB

$L_X$ Length of the rectangular cavity, m

$L_Z$ Height of the rectangular cavity, m

| | |
|---|---|
| $L_Y$ | Width of the rectangular cavity, m |
| $m$ | Surface mass or mass per unit area of the plate, kg/m$^2$ |
| $M$ | Total mass per unit area of the construction, kg/m$^2$ |
| $m_c$ | Mass per unit area of the side supported by point connections, kg/m |
| $m_1$ | Mass per unit area of the inside panel, kg/m$^2$ |
| $m_2$ | Mass per unit area of the outside panel, kg/m$^2$ |
| $m_{12}$ | Effective surface mass for plates 1 and 2, kg/m$^2$ |
| $n$ | Number of individual sound pressure levels |
| n | Number of excitation point forces applied to the plate area $A$ |
| $N$ | Number of sampling points |
| $N_f$ | Number of modes of vibrations |
| $NR$ | Noise reduction, dB |
| $p_a$ | Sound pressure after installation at the same location relative to the sound source, Pa |
| $p_b$ | Sound pressure before installation at the same location relative to the sound source, Pa |
| $p_i$ | Incident sound pressure, Pa |
| $p_o$ | Sound pressure outside of the enclosure along a linear path same location relative to the sound source, Pa |
| $p_t$ | Transmitted sound pressure, Pa |
| $p_w$ | Sound pressure within the enclosure along a linear path same location relative to the sound source, Pa |
| $PWL$ | Sound power level referenced to $W_0 = 10^{-12}$ Watts |
| $Q$ | Directivity, dimensionless |
| $S_p$ | Surface area of the plate, m$^2$ |
| $S_R$ | Area of test specimen that is exposed in the receiving room, m$^2$ |
| $SPL_i$ | Individual sound pressure level referenced to $p_0 = 2 \times 10^{-5}$ Pa, dB |

$t$ Time, s

$t_k$ Discrete-time or $k^{th}$ sampling instant, s

$T$ Period of a sample signal, s

$TL_{\mathrm{f}}$ Field-incidence mass law transmission loss, dB

$TL_{\mathrm{r}}$ Random-incidence mass law transmission loss, dB

$TL_{\mathrm{r},\,M}$ Random-incidence composite mass law transmission loss, dB

$TL_0$ Normal-incidence mass law transmission loss, dB

$TL_{0,\,M}$ Normal-incidence composite mass law transmission loss, dB

$TL_1$ Mass law transmission loss of the inside panel, dB

$TL_2$ Mass law transmission loss of the outside panel, dB

$TL_{1+2}$ Sum of mass law transmission loss of the inside and outside panel, dB

$TSL$ Total signal energy, dB

$T_{60}$ Reverberation time in the receiving room, s

$\langle \overline{v^2} \rangle$ Spaced averaged, normal vibration velocity at any point, $m/s^2$

$V$ Volume of the rectangular room, $m^3$

$VAL$ Vibratory acceleration level referenced to $\alpha_0 = 10^{-5}$ $m/s^2$

$W$ Radiated noise power, Watts

$x_k$ Input signal amplitude (real or complex) as a function of time

$X_n$ Complex spectrum value at frequency $\omega_n$

$\bar{X}_n$ Conjugate of the spectrum

$|X_n|$ Fourier Spectrum

$\sqrt{\overline{x^2}}$ Root mean square value (RMS) for two sided FFT

$z$ Measurement distance from the surface, m

$\Delta f$ Bandwidth of the relevant 1/3 octave band center frequency, Hz

$\Delta t$ Sample spacing, s

$\Delta TL_M$ Change in transmission loss of a double panel system due to point connections, dB

$\Delta TL_{nr}$ Non-resonant transmission loss correction for low frequencies, dB

$\eta$ Mechanical damping loss factor of the plate

$\nu$ Poisson's ratio of the plate, dimensionless

$\omega_n$ $N^{th}$ frequency, rad/s

$\rho$ Plate density, $kg/m^3$

$\rho_0$ Density of the air, $kg/m^3$

$\sigma$ Radiation ratio or radiation efficiency

# CHAPTER 1 INTRODUCTION

## 1.1 Noise Exposure Regulations

The effects of environmental noise[1] in residential neighbourhoods on hearing impairment cannot be easily determined. As such, potential hearing damage has been extrapolated from industrial exposures [1]. Noise exposure regulations were first published under the Walsh-Healey Public Contracts Act and later adopted under the Occupational Safety and Health Act (OSHA) on May 29 1971 [2]. The OSHA imposed an 85 dBA[2] permissible noise intensity limit for an eight hour daily dose to protect employees in industrial settings from permanent hearing impairment. In addition, it was recommended that one's daily noise exposure averaged over the whole year should not exceed 70 dBA. One of the major effects of environmental noise is interference with speech communication. Table 1.1 summarizes optimum maximum noise levels acceptable for various activities requiring adequate level of speech clarity. As background noise levels decrease from 75 to 35 dBA, the quality of speech communication and the acceptable distance between nearby listeners increases. For an intelligible conversation, the speech level should be at least 10 dBA greater than the environmental noise level, a minimum sound attenuation found in a typical household with closed doors and windows. Another major effect of environmental noise is sleep disturbance. Noise exposure during sleep or leisure time may cause stress that can cause some physiological conditions such as hypertension, change in heart rate and respiration pattern, vasoconstriction[3] and cardiac arrhythmia[4]. The aftermath of sleep deprivation from noise exposure may include increased fatigue and decreased performance and sense of well-being. The optimum maximum noise level acceptable inside bedrooms is 30 dBA. Sound-related community annoyance is the most frequent effect of environmental noise. Such sounds are found to be aesthetically unpleasant and may be dependent on the nature of the noise (single tones or random signals), and/or the temporal variation (constant, intermittent or random) and intensity. Regulatory programs for noise control exist at local, provincial and federal levels.

---

[1] Environmental noise is the summary of noise from transport, industrial and recreational activities.

[2] dBA is A-weighted equivalent continuous noise level which is used as a descriptor of both occupational and environmental noise. A-weighting attempts to match the response of the human ear to noise.

[3] Vasoconstriction is narrowing of blood vessels. Symptoms include pale skin.

[4] Cardiac arrhythmia is abnormal electrical activity in the heart. Symptoms may include irregular heartbeat or abnormal awareness of heart beat.

These levels have adopted quantitative ordinances and bylaws limiting the sound crossing real property boundaries [3]. The limit imposed is usually determined by the use of the property through which sound is traveling. For instance, the Ontario Ministry of the Environment (MOE) regulates power industry noise in residential neighbourhoods. Most regulated facilities must comply with the maximum facility sound level contribution between 40 to 50 dBA at the nearby residences [4].

TABLE 1.1 Some optimum maximum noise level acceptable for various activities [2]

| Maximum Levels (dBA) | Activity |
|---|---|
| 75 | audible shouted warnings in industrial locations, often necessary for work safety |
| 65 | close range communication in workshops and plant control rooms |
| 55 | non-critical speech among nearby listeners in public areas of buildings like lobbies and restaurants |
| 48 | background masking noise inside general, open plan, office |
| 40 | good speech quality among groups of nearby listeners inside private offices and libraries |
| 35 | high quality speech among groups of nearby listeners in classrooms and meeting rooms |

## 1.2 Noise Transmission Paths and Control Method

The most recurring challenge faced by engineers is to devise an appropriate noise control plan for a customer so that a satisfactory noise reduction is attained at an acceptable cost. Noise reduction can only be achieved at two locations, either at the noise source or in the noise transmission path. Controlling noise levels at the source is very effective in reducing unwanted noise, but it needs to be implemented during the design stage. In situations where the noise is emitted from fluid motion in building system, such as from fans, pumps and compressors, obstructing the flow would result in lost performance to the system. In these instances, the best solution would be to select the equipment so that it operates at speeds that produce disturbance frequencies that are different from the natural frequencies of the supporting structure, but such measures are not always feasible [5]. If direct attenuation of the noise source is not a valid option, attention is directed towards the noise transmission path. Noise transmission paths are either airborne or structure-borne, either or both of which can be present in any situation. Passive

control of noise is the traditional noise control method; over the past fifty years, research in this field has advanced a variety of commercially available sound isolation, sound absorption, and vibration damping materials. The passive noise control method utilizes sound barriers and absorption materials to control airborne noise, while structure-borne noise is treated with vibration isolation materials [6]. Minimizing the vibration transfer from the mounting of the source to the surrounding structural assembly is a regularly occurring corrective action taken in noise control problems.

### 1.3 Industrial Noise: Power Generation Units

Peaking power generating units, commonly referred to as “peakers”, are power generating units that run only when there is a high demand for electricity or unexpected power outage. Peakers generally consist of gas turbine installations or a network of diesel generators. Unlike base-load generating stations, i.e., nuclear or hydroelectric plants, peakers are usually constructed near residential neighbourhoods (Figure 1.1). Their main function is to increase the power supply to local homes and businesses, as well as maintain normal voltage levels during times of strain and imbalance in the local distribution grid [7]. Power generating units have a significant noise impact on the surrounding environment. To comply with noise exposure regulations at residential locations for one-third octave frequency bands between 50 and 8000 Hz, power generating units rely on various outdoor attenuation effects, such as atmospheric absorption, ground effects and sound barriers, all of which are frequency dependent.

Atmospheric absorption is mainly a high frequency attenuator; it depends on distance, temperature and humidity, e.g., atmospheric absorption at 1000 meters, 20°C and 70% relative humidity would have at least 5 dB noise reduction at 1000 Hz octave and an astonishing 75 dB at 8000 Hz octave. The ground effects can either reduce or amplify the noise levels at the receiver location. The attenuation of the ground effects depends on the elevation and the composition (absorption) of the ground surface, where the practical limit for ground absorption is about 20 dB relative to hard ground. Sound barriers are one of the most reliable tools in the passive noise control method. For a single barrier, where the sound propagation path includes each of the vertical sides and the top of the barrier, the maximum attenuation that can be obtained is around 20 dB. Addition of a second barrier at sufficient distance increases the attenuation to 25 dB [8].

Reasonable levels of noise attenuation can be obtained from outdoor effects as long as they are feasible with regard to the topography of the peaker site. A general practice, however, is

to first suppress as much of the noise as economically feasible by insulating the power generating units by means of double-panel enclosures with cavity absorbent filling. A double-panel construction has proved to have best efficiency with a floor-to-ceiling barrier and an enclosure [9]. A considerable variety of commercially available sound absorbing, temperature and corrosion resilient materials can be selected for this purpose; however, the full attenuation potential of these enclosures is controlled by the de-coupling (vibration isolation) technique used in reducing the structure-borne vibration. The vibration is transmitted through the structural links which cause re-radiation of noise on the adjacent panel: casing-radiated noise. Low frequency noise, know as infra sound, in many cases causes vibration in homes and is often a primary complaint from neighbours near peaker installations. Audible noise (20 - 20000 Hz) at mid-and-high frequencies is reduced using vibration isolator assemblies that incorporate rubber or neoprene elements [10].

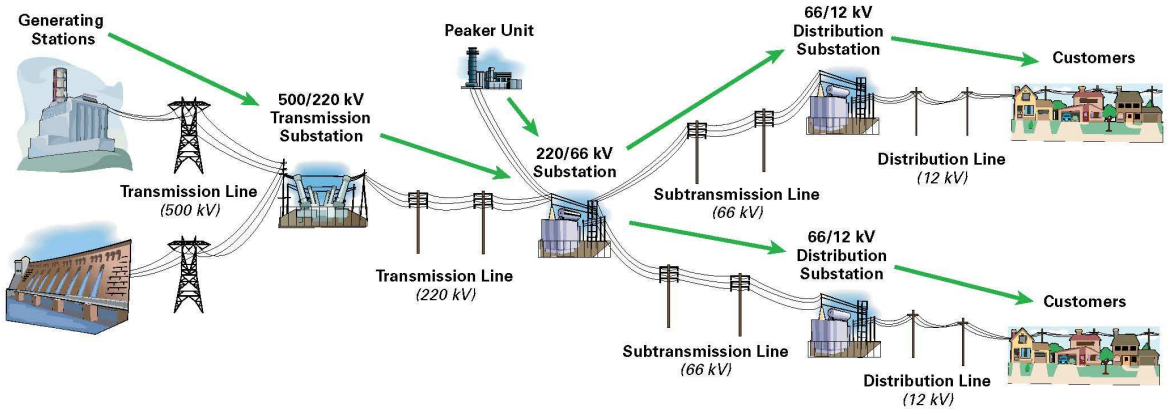


FIGURE 1.1 Path of Electricity [7]

## 1.4 Acoustic Chamber in the Ryerson Aeroacoustic Research Facility

At present, the Ryerson Aeroacoustic Research Facility is equipped with an acoustic chamber designed specifically for investigating the acoustical effects of varying the structure-borne vibration transmitted through point connections in a double-panel assembly. The acoustic chamber can be viewed as an inexpensive alternative to an electrodynamic shaker used in product testing of small automotive components and connectors. An electrodynamic shaker uses a construction similar to a common loudspeaker to convert electrical current into mechanical force. In a moving-coil loudspeaker, the forced oscillations of the conical diaphragm produce

fluctuations in the air pressure that radiate away from the driver as sound waves. At sufficient distance, these sound waves propagate as a uniform pressure wavefront, the frequency range of which is limited by the precision of the driver and nature of the listening environment. In an electrodynamic shaker, however, the diaphragm is replaced by a lightweight rigid fixture which holds the test samples. The force is uniform over the fixture surface and consistent throughout the excitation period. An electrodynamic shaker is an expensive capital investment for a research laboratory, especially when integrated with head expenders for testing large fixtures. In addition, the complete test facility takes up a considerable amount of lab space and requires a permanent location within the lab. With these constraints in mind and considering the nature of the various studies to be investigated in the Ryerson Aeroacoustic Research Facility, the decision was made to exploit the most practical and economic alternative while trying to maintaining survey grade performance. The solution was a custom-built acoustic chamber. The principles behind its function are very similar to that of the electrodynamic shaker, except there is an additional force transmission path, air. Knowing that a common loudspeaker set in a reverberant enclosure is capable of producing a uniform pressure field, a chamber can be constructed with a hood fixed in such a way as to transmit only the sound-borne vibration from the internal pressure wavefront. The hood of the enclosure serves as the mounting surface for test specimens; its size and mass are predetermined by the upper limit of the acoustic power produced by the loudspeaker in the reverberant enclosure. By controlling the amount of electrical current entering the loudspeaker, vibration levels of the hood can be controlled either at a single excitation frequency or over a band of frequencies. Although the level of performance of the acoustic chamber is distinctively lower than that of a precision instrument such as the electrodynamic shaker, more practical experimental conditions are obtained with the acoustic chamber. For instance, the loudspeaker has a capacity to excite the hood with random signals such as white and pink noise, whereas the electrodynamic shaker only works with a sinusoidal signal. Previous work involved various acceleration measurements on vibration isolators, which were ranked according to the amount of reduction in the vibratory acceleration level (VAL) on the second panel, were the VAL of a solid connection was the basis of comparison [11]. The acoustical effects of varying the structure-borne vibration could not be measured directly because the acoustic chamber was not designed to confine the airspace between the two panels to focus the energy radiated from the hood at the second panel. The only course of action was to predict the noise reduction of the assembly by

establishing a link between the VAL and the sound pressure level (SPL). The assumption here was that by lowering the structure-born vibration, there would be a corresponding reduction in noise.

### 1.5 Research Objective

The work done by Raasch [11] suggested that the test facility located in the Ryerson Aeroacoustic Research Facility was capable of single panel transmission loss testing but required a modification for direct acoustical analysis of the double-panel assembly. The primary objective of this thesis was to evaluate the test facility and recommend feasible alterations to meet the performance requirements of transmission loss testing facilities based on industry standards. Recognising the fact that the acoustic chamber design was not required to meet the accreditation criteria outlined in these standards at the time of construction, the information found in these standards was only used as a guide in determining the lowest reliable frequency limit and the upper limit of acceptable transmission loss measurements. Formerly, the predicted sound attenuation level of the double-panel assembly was based on the difference between the measured SPL inside the acoustic chamber near the surface of the hood and the estimated SPL from VAL recorded at the external surface of the second panel. This approach, although effective in demonstrating a use of noise predictions from vibration measurements, cannot be used to predict transmission loss of a specimen because the measurements should be taken at sufficient distance from the reflective surface to avoid scatter in results caused by near-field[5] effects of the radiated sound. For this reason, the equation describing the relationship between VAL and SPL was revisited and adjusted to account for distance, radiation efficiency, and room effects. Furthermore, a theoretical characterization of transmission loss for a single-panel and double-panel with sound bridges was devised to aid in the comparison between the estimates of sound attenuation levels obtained from VAL data and those obtained directly from SPL data. Acoustic performance of a single-panel (hood) was evaluated using various performance measures to verify the potential of this test facility. Relevant adjustments to the single-panel transmission loss

[5] Near field is a region near the sound source where the SPL fluctuates about a mean. In the near field, sound waves emitted from different points in the source vibrate with different amplitudes and phases and thus interfere constructively and destructively. The depth of the near field is dependent on the frequency, source geometry, and measurement location.

theory were included to establish a theoretical confidence region into which measured values should fall.

## 1.6 Scope of Research

The material in this thesis is organized as follows. Chapter 1 provides an introduction to the research. The theory of transmission loss of a single-panel and a double-panel is reviewed in Chapter 2. Chapter 3 discusses how transmission loss is measured in practice, as well as introduces the relationship between VAL and SPL. A brief discussion on acoustic test chambers and standard material testing methods is given in Chapter 4. The construction and performance requirements of the test facility are presented in Chapter 5. Appropriate ISO[6] and ASTM[7] standards were selected for this purpose, but not before structural evaluations were completed for the acoustic chamber and chambers used in standard material testing methods. Chapter 6 discusses the instrument setup, as well as signal processing techniques used in this research. Chapter 7 compares the vibratory acceleration levels of various connectors and compares the transmission loss results obtained theoretically with those obtained directly from average sound pressure level measurements. Chapter 8 provides the main conclusion and presents recommendations for future research.

[6] International Organization for Standardization

[7] American Society for Testing and Materials

# CHAPTER 2 THEORY OF SOUND SUPPRESSION

## 2.1 Transmission Loss of a Single Panel

Although equations used to predict sound transmission loss are continuously evolving, thanks to the development in multilayer systems of panels and the invention of composite panels, the theoretical work done on thin, homogenous, panels has been fairly complete for at least 60 years. This section will provide the reader with a selection of equations used to predict the sound transmission loss of a single panel excited by a diffuse sound field and/or one which sustains acoustic standing waves.

### 2.1.1 Natural & Resonant Frequencies

The natural frequency is an inherent property of a system to vibrate without the influence of external periodic forcing. The fundamental or the first mode natural frequency $f_0$ of a flat, homogenous, thin finite-size panel is given by [12]:

$$f_0 = \frac{1}{2\pi}\sqrt{\frac{K_p}{m}} \tag{2.1}$$

where $K_p = 4B\pi^4/a^4$ = equivalent stiffness of square panel, N/m$^3$

$B = Eh^3/\left[12\left(1-\nu^2\right)\right]$ = bending stiffness per unit length of the plate, N·m

$E$ = Young's modulus of the plate, N/m$^2$

$h$ = plate thickness, m

$\nu$ = Poisson's ratio of the plate

$a$ = side length of the square plate, m

$m$ = surface mass or mass per unit area of the plate, $m = \rho h$, kg/m$^2$

$\rho$ = plate density, kg/m$^3$

Substituting the above variables into equation (2.1) gives:

$$f_0 = \frac{\mathrm{D}}{2\pi}\sqrt{\frac{Eh^2}{\rho a^4\left(1-\nu^2\right)}} \tag{2.1a}$$

where $\mathrm{D} = \pi^2/\sqrt{3}$ = first mode coefficient for all edges simply supported

To calculate natural frequencies for other modes and/or different edge conditions, D is substituted with an appropriate value from Table 2.1.

TABLE 2.1 Natural frequencies of thin, flat square plates of uniform thickness [12]

| EDGE CONDITIONS | VALUE OF D FOR MODE: | | | | | |
|---|---|---|---|---|---|---|
| | 1 | 2 | 3 | 4 | 5 | 6 |
| One edge clamed-three edges free | 1.01 | 2.47 | 6.20 | 7.94 | 9.01 | |
| **All edges clamped** | **10.40** | **21.21** | **31.29** | **38.04** | **38.22** | **47.73** |
| Two edges clamped-two edges free | 2.01 | 6.96 | 7.74 | 13.89 | 18.25 | |
| All edges free | 4.07 | 5.94 | 6.91 | 10.39 | 17.80 | 18.85 |
| One edge clamed-three edges simply supported | 6.83 | 14.94 | 16.95 | 24.89 | 28..99 | 32.71 |
| Two edges clamed-two edges simply supported | 8.37 | 15.82 | 20.03 | 27.34 | 29.54 | 37.31 |
| All edges simply supported | 5.70 | 14.26 | 22.82 | 28.52 | 37.08 | 48.49 |

The resonant frequency, on the other hand, is excited by periodic forcing, and it is almost equal to, but less than, the natural frequency of a system. Resonance will occur if the excitation frequency corresponds to the resonant frequency of the system.

### 2.1.2 Coincidence Effect

The coincidence effect is a form of acoustic resonance phenomena which describes the optimal radiation efficiency of a panel. Since the sound radiation efficiency of a panel is dependent upon the coupling of bending (flexural) waves in a panel and compression (longitudinal) waves in the air, as depicted in Figure 2.1, a maximum energy transfer from

vibration to sound is achieved when the speed of the free bending wave[8] in the panel coincides with the speed of the acoustic wave in the air. The coincidence or critical frequency of radiation is given by [13]:

$$f_c = \frac{c_0^2}{2\pi}\sqrt{\frac{m}{B}} \tag{2.2}$$

where $c_0 = 20.047\sqrt{273.15 + T}$ = speed of sound in air, m/s;

$T$ = temperature in degree Celsius

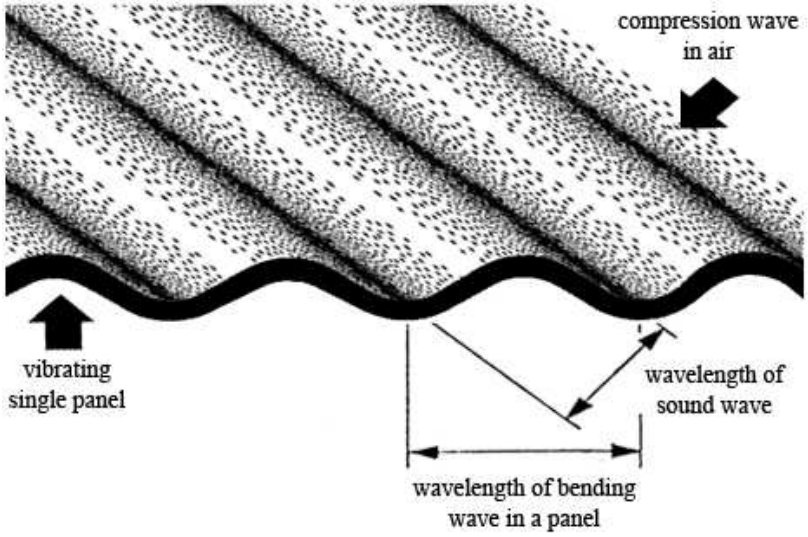


FIGURE 2.1 Coincidence Effect

### 2.1.3 Transmission Loss Characteristics of a Single Panel

Transmission loss characteristics of a single thin panel excited by an acoustic field can be separated into four frequency regions, as depicted in Figure 2.2, where each region is controlled by a single or several mechanism(s) such as stiffness, resonance, mass or damping; furthermore, approximate governing equations have been developed to predict the transmission loss response in those regions and are summarized below [13].

[8] Free bending waves are not restricted by some structural discontinuities.

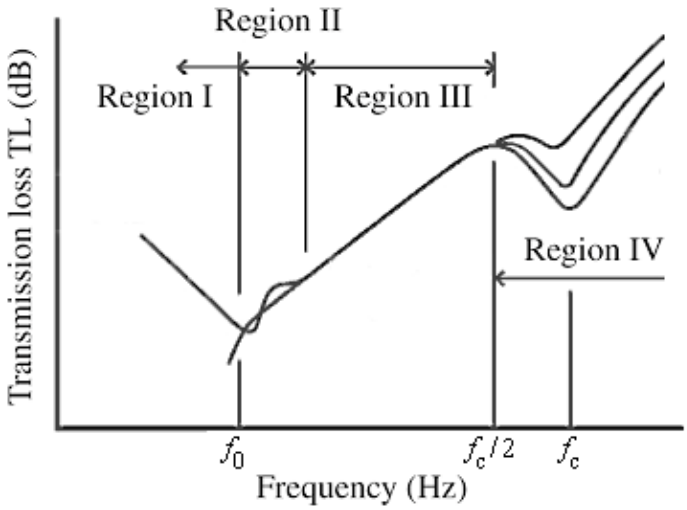


FIGURE 2.2 Transmission loss characteristics of a single panel [13]

**Region I**: When $f \ll f_0$, transmission loss is controlled by the stiffness of the panel. The stiffness law of transmission loss for a finite-size panel is given by:

$$TL = TL_0 - 40 \log_{10}\left(\frac{f}{f_0}\right) \tag{2.3}$$

where $TL_0$ = normal-incidence mass law, further described below

**Region II**: When $f \approx f_0$ , transmission loss is controlled by the fundamental mode associated with the first natural frequency. For an unbounded panel, transmission loss at resonance equals zero dB provided that radiation damping exceeds mechanical damping $\left(\rho_0 c_0 / 2\pi fm \gg \eta\right)$. When the opposite is true, i.e., mechanical damping exceeds radiation damping $\left(\eta \gg \rho_0 c_0 / 2\pi fm\right)$, transmission loss is given by:

$$TL = TL_0 + 20 \log_{10}(\eta) \tag{2.4}$$

where $\eta$ = mechanical damping loss factor of the panel.

**Region III**: When $f_0 \ll f \leq f_c/2$ , transmission loss is controlled by the surface mass of the infinite panel and, for sound waves incident at a single angle, θ, is given by:

$$TL_\theta = 10 \log_{10}\left( \left| 1 + \frac{m\pi f \cos(\theta)}{\rho_0 c_0} \right|^2 \right) \tag{2.5}$$

where $\rho_0$ = density of the air, kg/m$^3$

There are several forms of the mass law [13] of transmission loss, each dependent on the incident angle of the incoming waves. The first one is the ***normal-incidence mass law***, which represents the transmission loss at the normal angle of incidence, $\theta = 0$, and simplifies to the following form when $m\pi f \gg \rho_0 c_0$.

$$TL_0 = 10 \log_{10}\left( \left| 1 + \frac{m\pi f}{\rho_0 c_0} \right|^2 \right) \cong 20 \log_{10}\left( \frac{m\pi f}{\rho_0 c_0} \right) \tag{2.5a}$$

When transmission loss is taken at the angle averaged over a range, $0 \leq \theta \leq 90^o$, the sound field is assumed to be perfectly diffused and represented by the ***random-incidence mass law***, which is given by:

$$TL_r \cong TL_0 - 10 \log_{10}\left(0.23 TL_0\right) \tag{2.5b}$$

In practice, however, an empirical correction is used to attain a better agreement between the calculated and measured values of the actual sound field when the transmission loss is taken at the angle averaged over a range $0 \leq \theta \leq 78^o$. Transmission loss is represented by the ***field-incidence mass law*** and is given by:

$$TL_{\mathrm{f}} = 20 \log_{10}\left( \frac{m\pi f}{1.8\rho_0 c_0} \right) \tag{2.5c}$$

The three variations of mass law transmission losses are compared in Figure 2.3.

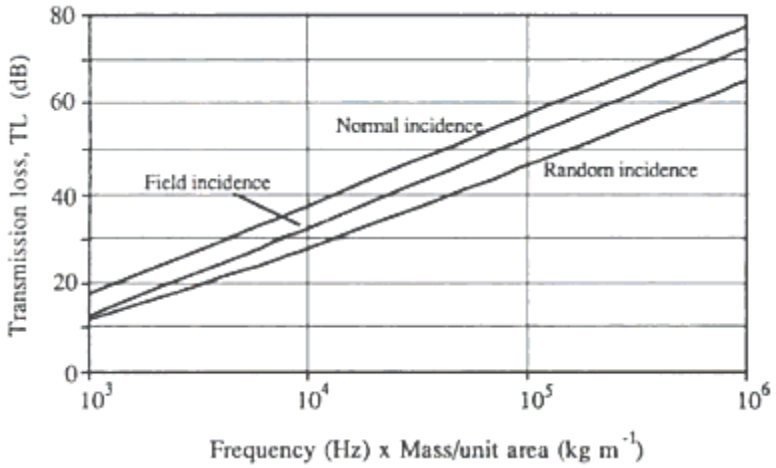


FIGURE 2.3 Mass law transmission losses [14]

The lowest frequency applicable to the mass law is not well defined $\left(f_0 \ll f\right)$. Every so often, the mass law under-estimates the transmission loss at this frequency. Sewell [15] derived the following correction to assist the normal-incidence mass law in those instances.

$$\Delta TL_{nr} = -10 \log_{10}\left( \ln\left( \frac{2\pi f\sqrt{A}}{c_0} \right) + 0.16 + \frac{c_0^2}{16\pi^3 f^2 A} \right) + 20 \log_{10}\left( 1 - \frac{f^2}{f_{\mathrm{c}}^2} \right) \tag{2.6}$$

where $A = a^2$ = plate area, m$^2$.

Sewell's expression is based upon the theoretical consideration of the forced transmission; contributions from resonant transmission were omitted since, below the critical frequency, resonant frequencies have very low radiation efficiency and thus are poor sound

transmitters. For this reason, transmission loss predictions are not significantly affected since the resonant component is several decibels lower than the forced component [14, 16].

The random- and field-incidence mass law equations assumed that the panel was located in an aperture in an infinite, rigid plane baffle separating two semi-infinite volumes of fluid and that the incident sound was diffuse. However, the diffuse-field transmission performance of the real bounded panel in a rigid baffle can differ significantly from the theoretical performance when acoustic standing waves are sustained within the enclosed fluid volume. The acoustic standing-wave modes can couple with the structural modes in the panel if their natural frequencies are in close proximity to each other or if there is good special matching between the acoustic mode pressure distribution over the panel and the distribution of panel mode displacements. Fahy [17] derived the following relationship for the transmission loss below the critical frequency when room modes are present (modified here for square panels).

$$TL = TL_0 - 10\log_{10}\left(\left[1.5 + \ln\left(\frac{2f}{\Delta f}\right)\right] + \frac{8c_0^2}{\eta\pi^2 A\sqrt{ff_c^3}}\left[1 + 2\left(\frac{f}{f_c}\right) + 3\left(\frac{f}{f_c}\right)^2\right]\right) \quad (2.7)$$

where $\Delta f$ = bandwidth of the relevant one-third octave band, Hz

When coupling exists between the acoustic and structural modes, a 3-6 dB reduction in transmission loss will result if the coupling is resonant (the term in braces which contains η) or roughly represent that of the field-incident mass law if it is non-resonant (5.6 dB reduction based on a 1/3 octave band filter) [14, 17].

**Region IV**: When $f > f_c/2$, transmission loss is controlled by the surface mass and damping of the panel. The relation describing the general form of theoretical diffuse field transmission loss for an infinite panel above coincidence $\left(f > f_c\right)$ was first derived by Cremer [18] and is given by:

$$TL_r = TL_0 + 10\log_{10}\left(\frac{2\eta f}{\pi f_c}\right) \quad (2.8a)$$

Several authors have developed approximate relations at the diffuse-field coincidence point, $\left(f=f_c\right)$. Fahy [17] approximated it as:

$$TL_{\mathrm{r}} = TL_0 + 10\log_{10}\left(\frac{2\eta\Delta f}{\pi f_{\mathrm{c}}}\right) \tag{2.8b}$$

There is a well known disparity in the transmission loss predictions obtained with the field-incidence mass law (2.5c) and Cremer's expression (2.8a) near the coincidence dip $\left(f_c/2 < f \le f_c\right)$. Sharp [19] suggested using a linear interpolation scheme to correct this discontinuity until more accurate expressions are available. A better prediction of transmission loss is obtained when a straight line is drawn between the field-incidence mass law value at $f=f_{\mathrm{c}}/2$ and the value obtained with Fahy's expression (2.8b) at $f=f_{\mathrm{c}}$.

Several variations of the mass law transmission loss with relevant adjustments were described in this section. The complete theoretical transmission loss characteristics of the hood are illustrated in Figure 2.4. The material constants used in the simulation of transmission loss are listed in Table 2.2.

TABLE 2.2 Hood transmission loss simulation constants

| SIMULATION CONSTANTS | SYMBOL | VALUE | UNIT |
|---|---|---|---|
| **Air at T = 27.5°C** | | | |
| Speed of sound | $c_0$ | 347.50 | m/s |
| Density | $\rho_0$ | 1.174 | $kg/m^3$ |
| **Steel Hood** | | | |
| Density | $\rho$ | 7695 | $kg/m^3$ |
| Young's modulus | E | 200 | GPa |
| Poisson's ratio | $\nu$ | 0.30 | |
| Loss factor [11] | $\eta$ | 0.01 | |
| Thickness | $h_1$ | $6.35\cdot10^{-3}$ | m |
| Side length | $a_1$ | 0.91 | m |
| Surface mass | $m_1$ | 48.86 | $kg/m^2$ |
| $1^{st}$ mode coefficient for all edges clamped | D | 10.40 | |
| Bending stiffness per unit length | B | 4690 | Nm |

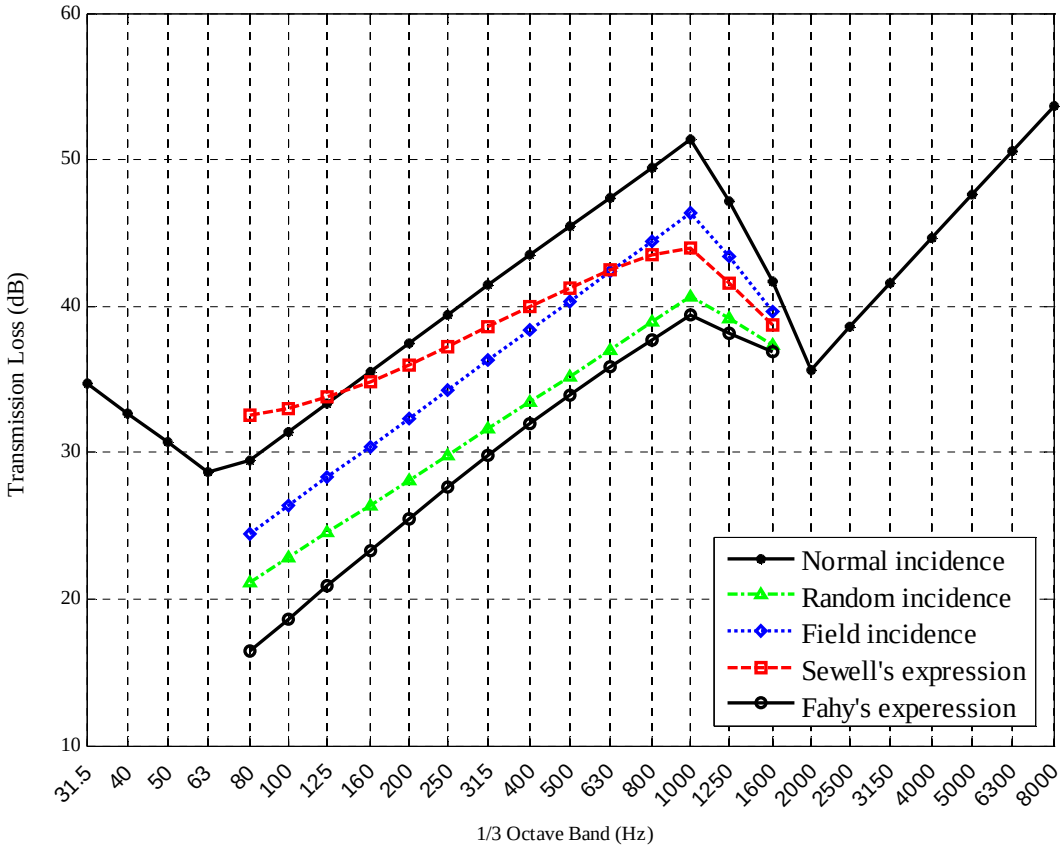


FIGURE 2.4 Complete theoretical transmission loss characteristics of the single panel

## 2.2 Transmission Loss of Double Panels

It is a known fact that better sound attenuation performance of a multi-panel system can be realized with proper selection of insulation and absorbing materials. Theoretically, the simplest case of such a system is the ideal-double-panel system composed of two impermeable, homogenous panels of infinite extent separated by an air gap: an air-mass sandwich. Practically, such a system would require some kind of connectors between the panels, which inevitable introduce a path for structure-born vibration: these connectors act as sound-bridges [19].

### 2.2.1 Resonant Frequency of Mass-Spring-Mass System

The vibration of an ideal-double-panel system can be modeled as a mass-spring-mass system with the normal-incidence fundamental natural frequency of [13]:

$$f_{\mathrm{r,\,0}} = \frac{1}{2\pi}\sqrt{\frac{K_a}{m_{12}}} \tag{2.9a}$$

or a random-incidence fundamental natural frequency of [20]:

$$f_{\mathrm{r,\,r}} = \frac{1}{2\pi}\sqrt{\frac{3.6K_a}{m_{12}}} \tag{2.9b}$$

where $K_a = \rho_0 c_0^2 / d$ = equivalent stiffness of an air space, N/m$^3$

$d$ = depth of the air space confined by two panels, m

$m_{12} = \left(2m_1 m_2\right) / \left(m_1 + m_2\right)$ = effective surface mass for plates 1 and 2, kg/m$^2$ [19]

### 2.2.2 Resonant Frequencies of an Air Cavity

A standing wave, or a mode of vibration, is a phenomenon that occurs when progressive waves of the same frequency and kind interfere to produce a periodic wave having fixed distribution in space with distinct locations of maxima and minima [20]. Acoustic standing waves are a common occurrence in an air space bounded by parallel surfaces. The resonant frequencies of the modes of vibration in a rectangular cavity, as cited by Beranek [21], are given by:

$$f_{ijk} = \frac{c_0}{2}\sqrt{\left(\frac{i}{L_X}\right)^2 + \left(\frac{j}{L_Y}\right)^2 + \left(\frac{k}{L_Z}\right)^2} \tag{2.10}$$

where $i, j, k$ = are the indices of a particular mode, the harmonics of the resonant frequency

$L_X, L_Y, L_Z$ = are the length, width, and height of the rectangular cavity

The number of modes of vibration, $N_f$, between zero and a given upper frequency limit, $f_l$, can be estimated from [22].

$$N_f = \frac{4\pi}{3} V \left( \frac{f_l}{c_0} \right)^3 + \frac{\pi}{4} S_w \left( \frac{f_l}{c_0} \right)^2 + \frac{L_e}{8} \left( \frac{f_l}{c_0} \right) \tag{2.11}$$

where $V = L_X L_Y L_Z$ = volume of the rectangular room, $m^3$

$S_w = 2\left( L_X L_Y + L_X L_Z + L_Y L_Z \right)$ = surface area of the walls, $m^2$

$L_e = 4\left( L_X + L_Y + L_Z \right)$ = sum of all edge lengths, m

with mean modal separation $df$, at $f_l$, of

$$df = \frac{c_0^3}{4\pi V f_l^3} \tag{2.11a}$$

The modes of vibration can belong to a different class, which is determined by the number of surfaces involved in creating a standing wave. Axial modes involve two parallel surfaces; tangential modes involve four surfaces, while oblique modes involve all six surfaces. The energy level of modes in each class decreases when more surfaces are involved, that is, the tangential modes have about half the energy of axial modes, while the oblique modes have about one quarter. Axial modes are the most important, since they carry a large amount of energy and are the easiest to compute. For example, equation (2.12) defines the first axial mode of equation (2.10) simplified for a 1-DoF system consisting of two parallel plates separated by an air space *d* [13].

$$f_1 = \frac{c_0}{2} \sqrt{\left( \frac{1}{d} \right)^2} = \frac{c_0}{2d} \tag{2.10}$$

### 2.2.3 Transmission Loss Characteristics of Double Panel

Sharp [19] was the first one to compile the approximate equations for the normal incidence

transmission loss characteristics of a double panel. He separated the transmission loss response into three principle frequency regions listed below and defined in Figure 2.5:

**Region I**: When $f < f_r$, the transmission loss complies with the normal-incidence mass law of a single panel, except a sum of surface masses of both panels is used.

$$TL_{0,\,M} = 20\,\log_{10}\left(\frac{M\pi f}{\rho_0 c_0}\right) \tag{2.13a}$$

where $M$ = total mass per unit area of the construction, $M = m_1 + m_2$, kg/m$^2$

$m_1$, $m_2$ = mass per unit area of each panel, kg/m$^2$

For a random-incidence transmission loss of a composite panel, the term in brackets is divided by an additional constant.

$$TL_{r,\,M} = 20\,\log_{10}\left(\frac{M\pi f}{3.6\rho_0 c_0}\right) \tag{2.13b}$$

**Region II**: When $f_r \le f < f_1/\pi$, transmission loss is given by:

$$TL = TL_{1+2} + 20\,\log_{10}\left(\frac{4\pi df}{c_0}\right) \tag{2.14}$$

where $TL_1$, $TL_2$ = normal- or random-incidence mass law transmission losses for each panel, dB

$TL_{1+2} = TL_1 + TL_2$

**Region III**: When $f > f_1/\pi$, or to be exact when interpolation between peaks at $f = (2n-1)c_0/4d$ is used, transmission loss is given by:

$$TL = TL_{1+2} + 6 \tag{2.15}$$

The theory that was presented above has assumed that the air cavity between the two panels was well damped; thus, the two lines above the composite mass law in Figure 2.5 represent the upper limit for such a condition. In the absence of absorptive material between the panels, the panels are so coupled by the air cavity resonance that the transmission loss follows the composite mass law below the first cavity resonance, as shown in Figure 2.6.

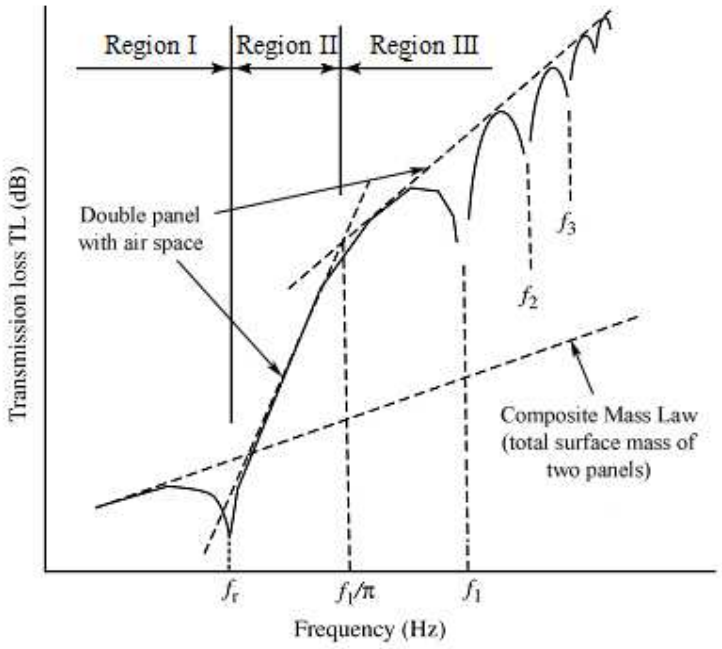


FIGURE 2.5 Transmission loss of the double panel with air space [13]

### 2.2.4 Transmission Loss of Double Panels with Sound Bridges

In the previously presented theory, a simple model for predicting the sound transmission in a double panel structure with an air cavity was devised by considering the structural independence of each panel and thus focusing only on the air-borne transmission path. In actual building partitions, connections between adjacent walls/plates are used for structural support and act as paths for the structure-born vibration. These mechanical links, such as steel sections, stud bolts, and the like, are commonly referred to as sound bridges and are illustrated in Figure 2.7

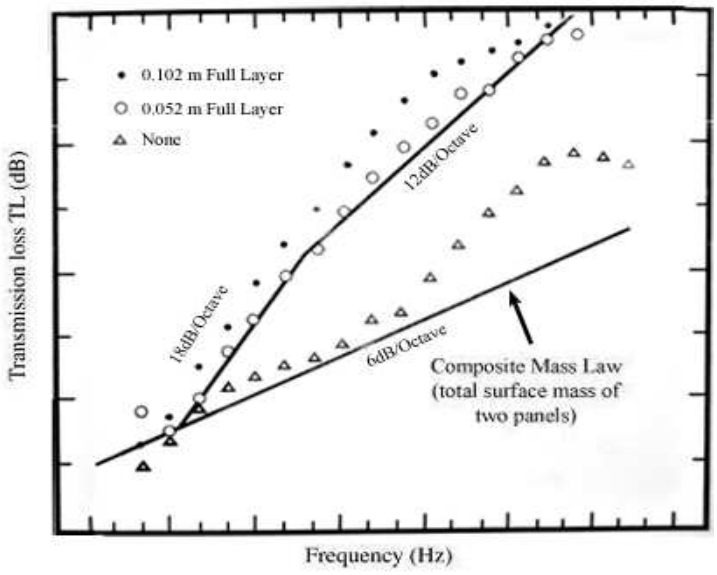


FIGURE 2.6 Measured values of transmission loss of an isolated double panel construction with and without full layer cavity absorption [19]

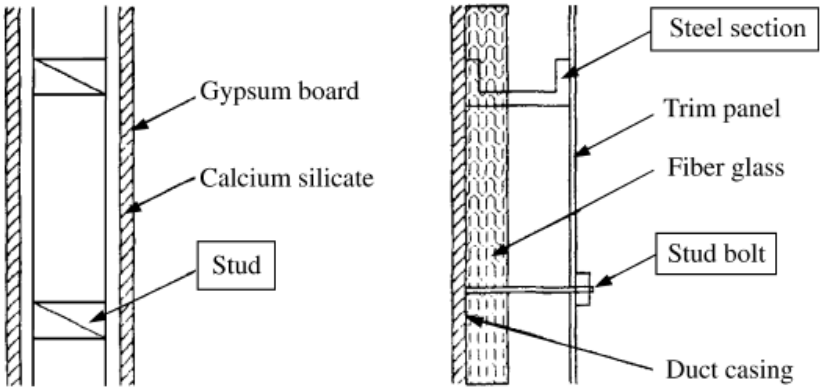


FIGURE 2.7 Example of actual building partition with sound bridges [12]

A key interest of this thesis is to explore the acoustical effect of vibration isolators on the transmission loss when substituted for the conventional mechanical links, such as stud bolts, in a double-panel system subjected to the acoustic loading. For this reason, only the theory for point forces will be considered when deriving the transmission loss relation. Sharp [19] developed relatively simple expressions for the transmission loss above the composite mass law for a double-panel system with point connections, namely,

$$\Delta TL_M = 20\log_{10}(ef_c) + 20\log_{10}\left(\frac{m_1}{m_1 + m_c}\right) + 10\log_{10}\left(\frac{\pi^3}{8c_0^2}\right) \tag{2.16}$$

where n = number of excitation point forces applied to the plate area $A$

$e$ = distance between point forces, $e = \sqrt{A/n}$, m

$m_c$ = mass per unit area of the side supported by point connections, kg/m$^2$

The bridging frequency [20] for point connections is:

$$f_B = f_0\sqrt{\frac{ef_c}{c_0}} \tag{2.17}$$

The overall transmission loss of a typical double-panel system with point connections is illustrated in Figure 2.8 and is summarized below:

$$TL = \begin{cases} TL_M & f < f_r \\ TL_{1+2} + 20\log_{10}\left(\frac{4\pi df}{c_0}\right) & f_r < f < f_B \\ TL_M + \Delta TL_M & f_B < f < f_c/2 \end{cases} \tag{2.18}$$

The prediction of the transmission loss of the double-panel with four solid connections is illustrated in Figure 2.9 for normal and random incidence cases. The material constants used in the simulation of double-panel transmission loss are listed in Table 2.2 (Section 2.1.3) and Table 2.3 below.

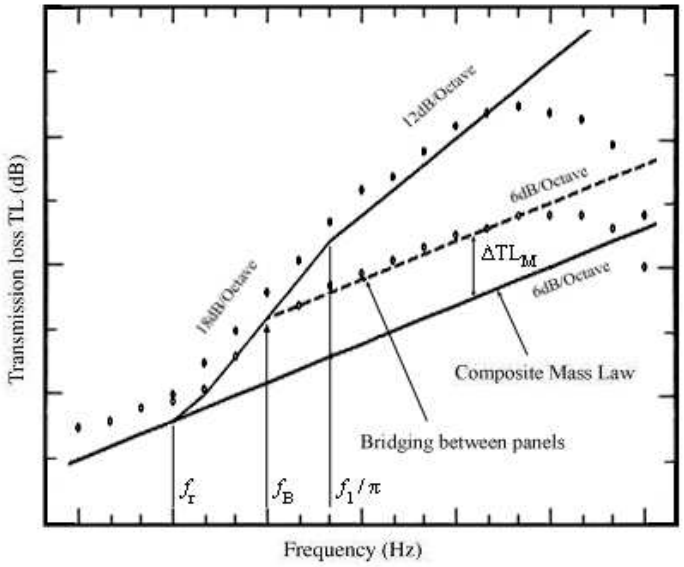


FIGURE 2.8 General form of transmission loss of a double panel system with point connections [20]

TABLE 2.3 Additional double-panel transmission loss simulation constants

| SIMULATION CONSTANTS | SYMBOL | VALUE | UNIT |
|---|---|---|---|
| **Air at T = 27.5°C** | | | |
| Equivalent stiffness of an air space | $K_a$ | $2.84 \cdot 10^{+6}$ | $N/m^3$ |
| Air gap | d | 0.05 | m |
| **Steel Panel** | | | |
| Thickness | $h_2$ | $3.18 \cdot 10^{-3}$ | m |
| Side length | $a_2$ | 0.91 | m |
| Surface mass | $m_2$ | 24.43 | $kg/m^2$ |
| Equivalent surface mass | $m_{12}$ | 32.57 | $kg/m^2$ |
| Surface mass of side supported by point connections | $m_c$ | 24.43 | $kg/m^2$ |
| Distance between point forces | e | 0.455 | m |

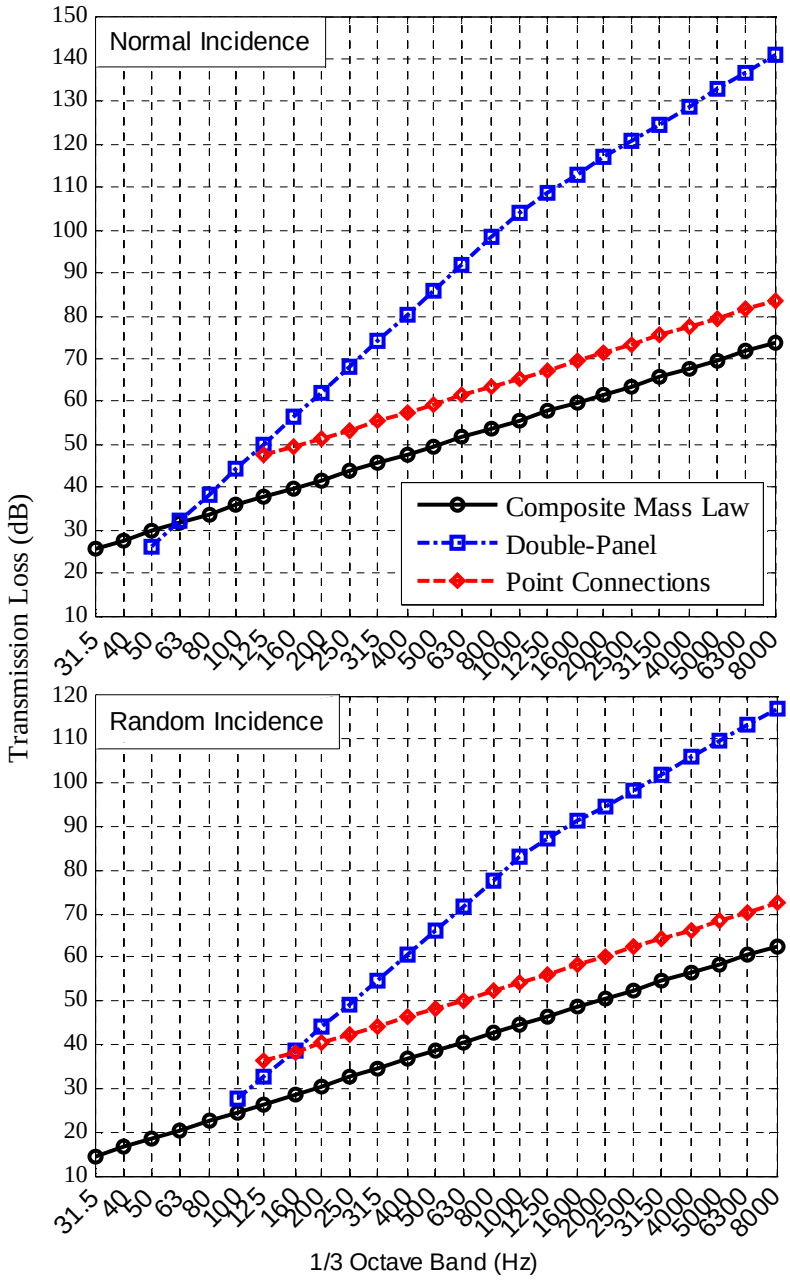


FIGURE 2.9 Complete theoretical transmission loss of a double panel with point connections

# CHAPTER 3 MEASURE OF ACOUSTIC PERFORMANCE AND NOISE EMISSION FROM VIBRATORY ACCELERATION LEVEL

## 3.1 Measure of Acoustic Performance

The acoustic performance of a system can be assessed using one of the following three main performance measures: transmission loss (TL), noise reduction (NR), and insertion loss (IL). All three use an average sound pressure level difference as a performance indicator, with the slight differences that are outlined below [21]. The TL represents the loss of airborne sound power[9] due to transmission of energy through the specimen; more precisely, it is defined as the difference between the average sound pressure level[10] in the source room and the receiving room plus ten times the common logarithm of the ratio of the test specimen area exposed on the receiving side and sound absorption in the receiving room with the test specimen in place [23, 24].

$$TL\,(dB) = \bar{L}_S - \bar{L}_R + 10\log_{10}\left(\frac{S_R}{A_R}\right) \tag{3.1}$$

where $\bar{L}_S$ = average sound pressure level in the source room, dB

$\bar{L}_R$ = average sound pressure level in the receiving room, dB

$$\bar{L} = 10\log_{10}\left(\frac{1}{n}\sum_{i=1}^{n} 10^{SPL_i/10}\right) = 10\log_{10}\left(\frac{1}{n}\sum_{i=1}^{n} p_i^2/p_0^2\right)$$

$n$ = number of individual sound pressure levels

$SPL_i$ = individual sound pressure level referenced to $p_0 = 2 \times 10^{-5}$ Pa, dB

$S_R$ = area of test specimen that is exposed in the receiving room, $m^2$

---

[9] Sound power is the rate at which acoustic energy is emitted from a sound source. It is not affected by environment; thus, it is an absolute value.

[10] Average sound pressure level is defined as ten times the common logarithm of the arithmetic mean of the squared pressure ratios from which the individual levels were derived, measured at different times (also known as equivalent continuous sound pressure level) or different positions or both.

$A_R = 55.4V/c_0T_{60}$ = sound absorption of the receiving room with test specimen in place, $m^2$ Sabin

$V$ = volume of the receiving room, $m^3$

$T_{60} = 60/d$ = reverberation time in the receiving room, s

$d$ = the rate of decay of sound pressure level, dB/s

The NR is defined as the difference between the average sound pressure levels measured in two enclosed spaces or rooms due to the sound source in one of the spaces. The individual observations in each room should be randomly distributed about a mean, with no systematic variations with position within the permissible measurement region [25].

$$NR(dB) = \bar{L}_S - \bar{L}_R \tag{3.2}$$

The IL represents the decrease in the radiated sound power, measured at the same relative location (distance and orientation) to the receiver, resulting from installation of a barrier or an enclosure between the source and the receiver. It is defined as the difference between the average sound pressure levels before and after the installation at the same location relative to the sound source [21].

$$IL(dB) = \bar{L}_{R_b} - \bar{L}_{R_a} \tag{3.3}$$

where $\bar{L}_{R_b}$ = average sound pressure level before the installation, dB

$\bar{L}_{R_a}$ = average sound pressure level after the installation, dB

Theoretically, TL is the easiest one to predict, but is difficult to obtain during actual field tests. In general, good agreement can be reached between the TL predictions and the experimental results obtained in a specially designed acoustic test chamber, but these predictions are only approximations of the actual performance of the acoustic system. In practice, the design of sound attenuating structures is usually based on the TL predictions, while the final

performance of the completed structure during the field test is based on the measured NR and IL [21].

### 3.2 Estimation of Noise Emitted by the Vibration of the Plate

This section will provide the reader with a detailed derivation of the expression that relates the vibratory acceleration level (VAL) of a large finite-plate type structure to the sound pressure level (SPL) that was originated by the surface vibration.

The acoustic power radiated from an arbitrary structure excited by sound pressure is given by:

$$W = \sigma \rho_0 c_0 S_p \langle \overline{v^2} \rangle \tag{3.4}$$

where $W$ = radiated noise power, *Watts*

$\sigma$ = radiation ratio or radiation efficiency

$S_p$ = surface area of the plate, $m^2$

$\langle \overline{v^2} \rangle$ = spaced averaged ($\langle\ \rangle$) mean square ($\overline{\ }$) normal vibration velocity at any point, $m/s^2$

The radiation ratio is a function of the parameter *k'a'* and/or of the ratio of the bending wave frequency to the critical frequency, $f/f_c$. If the sound source is modeled as a uniform spherical radiator, provided that the dimensions of the source are small compared to the wavelength of the generated sound, $\lambda$, and the source is located at a large distance from the receiver, $a \gg \lambda$, the radiation ratio is given by [26]:

$$\sigma = \frac{(k'a')^2}{1 + (k'a')^2} \tag{3.5}$$

where $k' = 2\pi f / c$ = acoustic wavenumber, $m^{-1}$

$a'$ = characteristic structural dimension such as spherical radius in this case, m

If the sound source is modeled as an infinite plate vibrating flexurally, the radiation ratio is given by:

$$\sigma = \frac{1}{\sqrt{1 + f_c / f}} \tag{3.6}$$

The radiation ratios for a spherical sound source (A) and for bending waves on an infinite, undamped flat plate (B) are illustrated in Figure 3.1. An important observation is that, at sufficient distance from the sound source and at high frequencies, the radiation ratio approaches unity. For infinite plates, no sound is radiated acoustically below the critical frequency, although, in practice, some radiation does occur for finite plates due to the radiation of excited edge and corner vibration modes. This situation is illustrated in Figure 3.2 (A), from which it is evident that the radiation ratio of a finite-plate type structure is a function of both *k'a'* and $f/f_c$. Furthermore, the severe scatter in the radiation amount of the edge and corner modes, as much as 10-15 dB, makes precise determination of radiation amounts impossible. In the case where the edges of the plate are sealed, as in a wall partition, sound waves cannot flow around the edges of the plate but can only flow along it. In this case, σ is only a function of frequency ratio [26].
Taking the logarithm of each side, we can express equation (3.4) as a level, as follows:

$$PWL = 10 \log_{10} \sigma + 10 \log_{10} \rho_0 c_0 S_p + 10 \log_{10} \langle \overline{v^2} \rangle + 120 \tag{3.7}$$

where $PWL = 10 \log_{10} W / W_0$ = sound power level referenced to $W_0 = 10^{-12}$ Watts, dB

Expressing vibration velocity in terms of acceleration ($v = \alpha/2\pi f$), the above expression reduces to:

$$PWL = 10 \log_{10} \sigma + 10 \log_{10} \rho_0 c_0 S_p + VAL - 20 \log_{10} f + 4.04 \tag{3.8}$$

where $VAL = 20 \log_{10} \alpha / \alpha_0$ = vibratory acceleration level referenced to $\alpha_0 = 10^{-5}$ m/s$^2$, dB

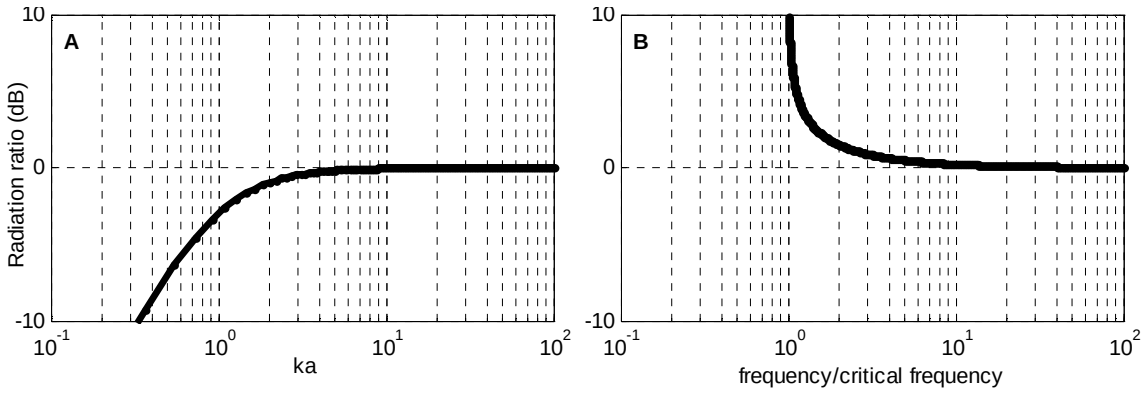


FIGURE 3.1 Radiation ratios for a spherical sound source (A) and bending waves on an infinite plate (B)

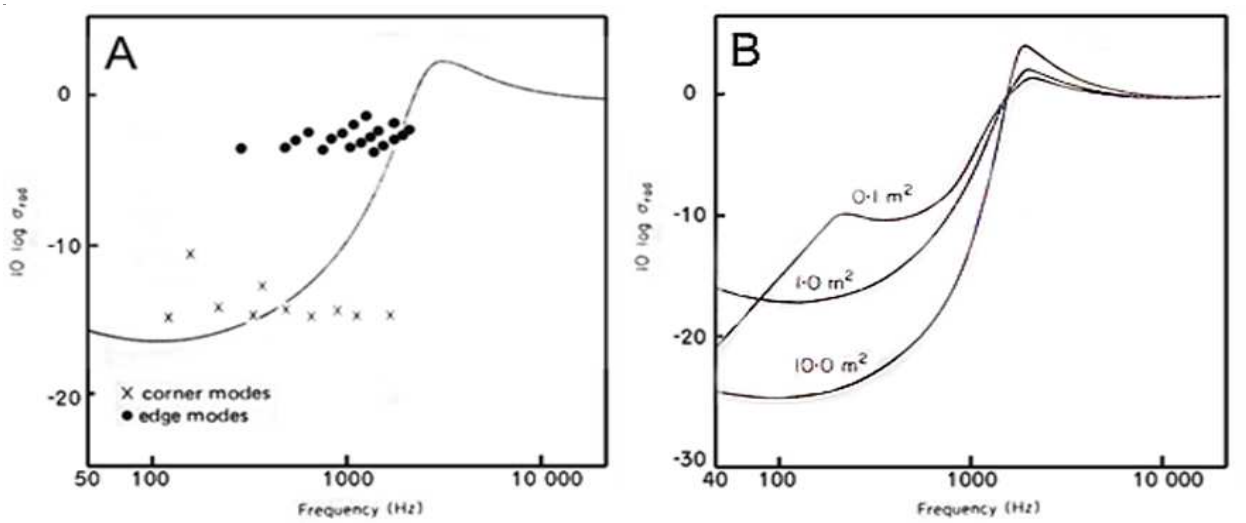


FIGURE 3.2 Radiation ratios of a ¼ inch thick steel plate simply supported at its edges when excited at one of its natural frequencies. Plate with an area of 1.0 $m^2$ (A) and areas: 0.1, 1.0 and 10.0 $m^2$ (B) [26].

The next step is to obtain the relationship between the SPL[11] and PWL emitted from a planar source in the semi-reverberant-field[12], exemplified by an ordinary room or laboratory. A planar source is a two-dimensional surface that is large compared with the measurement distance. The phase relationship between different vibrating points on the surface of the planar source is assumed to be decoupled, thus allowing omission of the effects of mode shapes. It is

[11] Under field test conditions, SPL should be space- and time-averaged: $\bar{L}$

[12] In a semi-reverberant-field, sound is neither free nor diffuse

suggested that measurements should be taken over a sufficient area at a distance of at least λ/4 (far-field[13]) away from the sound source or reflective surface. The relationship is given by:

$$SPL = PWL + 10\log_{10}\left(\frac{Q}{4\pi\left[z+\sqrt{\frac{S_p Q}{4\pi}}\right]^2}\right) + 10\log_{10}\left(\frac{\rho_0 c_0}{400}\right) \qquad (3.9)$$

where $Q$ = directivity, dimensionless

$z$ = measurement distance from the surface, m

The expression relating SPL to VAL is obtained by inserting equation (3.8) into equation (3.9) and substituting numerical values of $\rho_0$ (= 1.20 kg/ m$^3$), $c_0$ (= 343 m/s), $S_p$ (= 0.83 m$^2$) and D(=1 near the source)

$$SPL = VAL - 20\log_{10} f + 10\log_{10}\sigma + 10\log_{10}\left(\frac{1}{4\pi[z+0.26]^2}\right) + 29.50 \qquad (3.10)$$

From the above equation it is clear that SPL is affected by many factors. Although equation (3.10) accounts for directivity and distance effects, enabling one to compare the predicted and measured SPLs at any location in a room, it does not account for characteristics of the space such as the size of the room and the nature of its walls, ceiling, and furniture, if any. The room effects are included by adding *4/R* in the term in braces which includes *z*. Thus the complete equation becomes:

$$SPL = VAL - 20\log_{10} f + 10\log_{10}\sigma + 10\log_{10}\left(\frac{1}{4\pi[z+0.26]^2}+\frac{4}{R}\right) + 29.50 \qquad (3.11)$$

[13] A far field is a region far from the sound source where the sound pressure diminishes gradually with distance and obeys the inverse square law. In the far field, sound waves arriving from different points on the source are in phase. On the contrary, below λ/4, the near field region prevails.

where $R$ = room constant which defines total absorption in a room including air absorption. If the absorption of the room, $A_R$, is not adjusted to exclude air absorption then $R = A_R$

Equation (3.11) was confirmed by comparing the predicted and measured time-averaged sound pressure levels at 0 (location of hood surface), 0.2, 0.5 and 1.0 meters from the panel. The findings are illustrated in Figures 3.3 to 3.6. The radiation ratio values were estimated for each one-third octave from the curve in Figure 3.2B for a 1.0 $m^2$, ¼ inch thick, steel plate. The room effects, or receiving room absorption, were taken from Table 4.2. The vibratory acceleration levels were measured with an accelerometer positioned at the center of the panel. The sound pressure level predictions using vibratory acceleration levels appear to be in good agreement with the measured sound pressure levels at various distances from the specimen. These results support the hypothesis that it is feasible to predict the transmission loss of a specimen using the sound pressure difference between measured SPL values and SPL values estimated from VAL measurements.

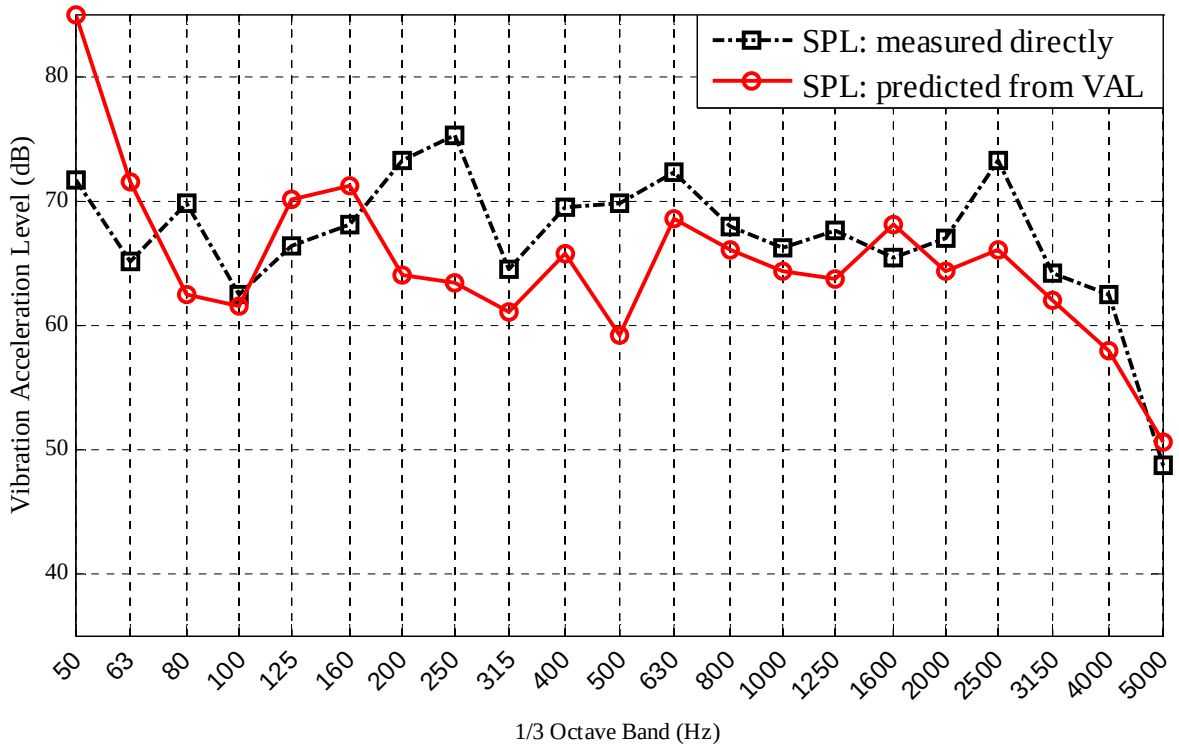


FIGURE 3.3 Measured and predicted time-averaged sound pressure level at the hood surface

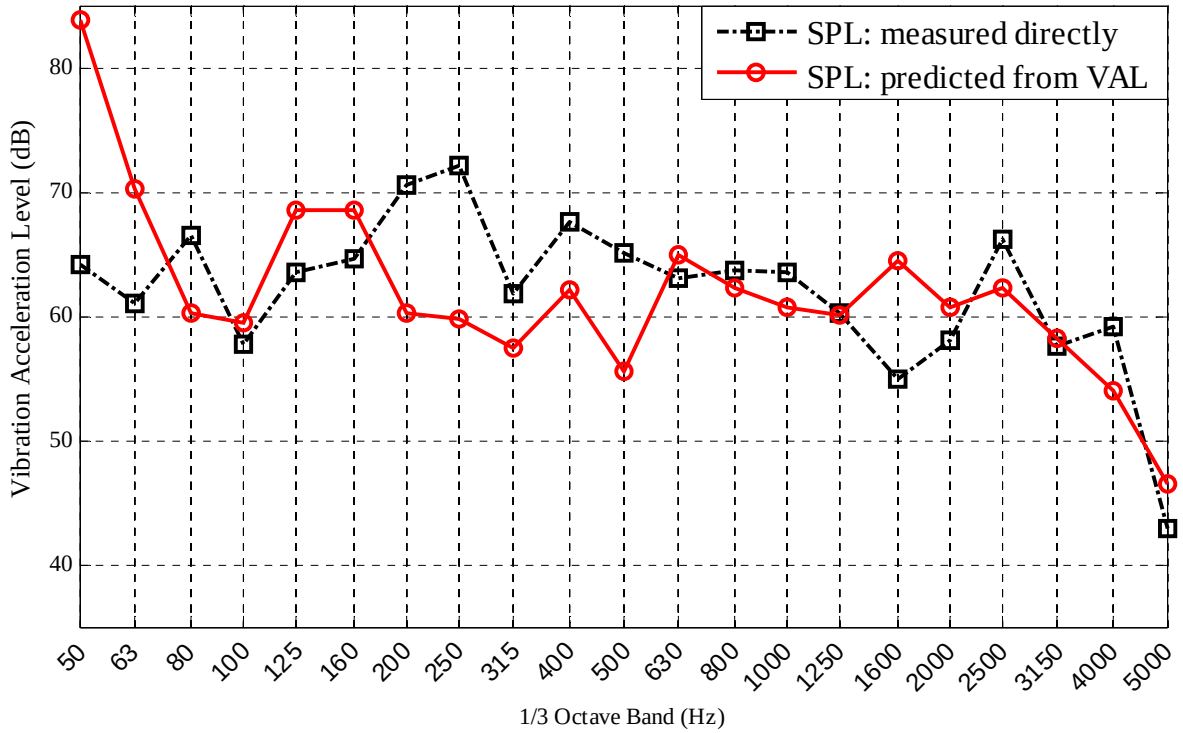


FIGURE 3.4 Measured and predicted time-averaged sound pressure levels at 0.2 meters away from the surface

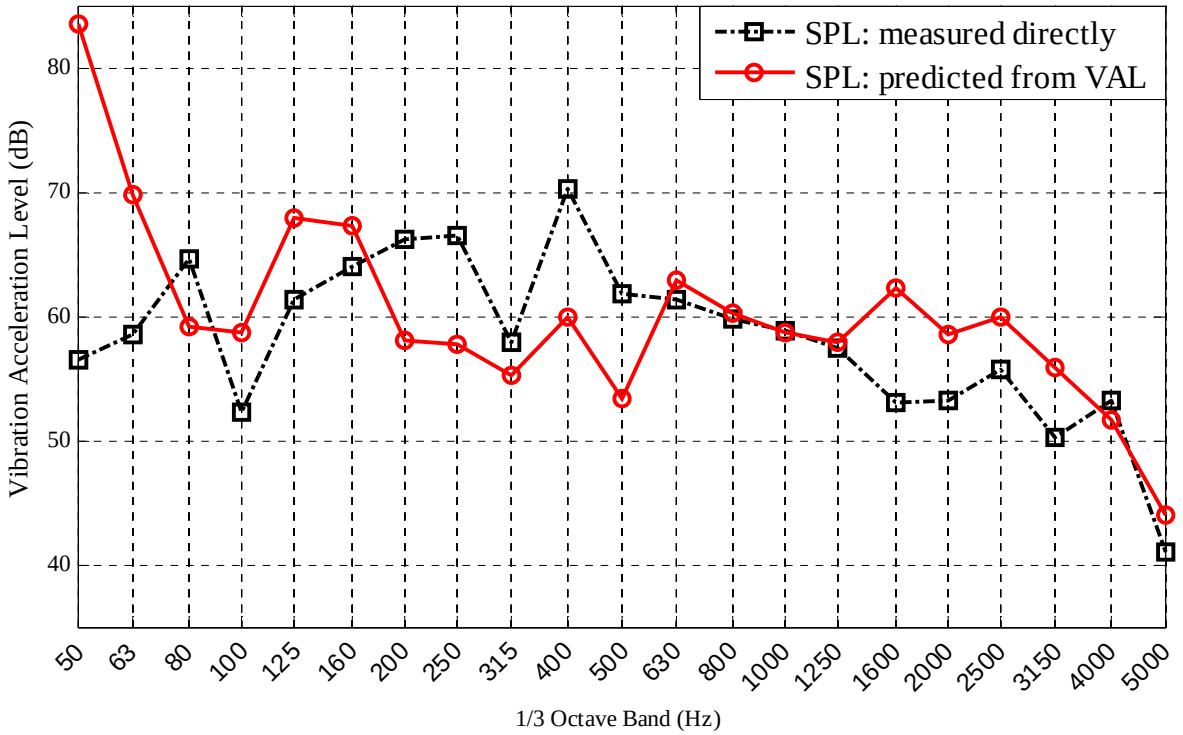


FIGURE 3.5 Measured and predicted time-averaged sound pressure levels at 0.5 meters away from the surface

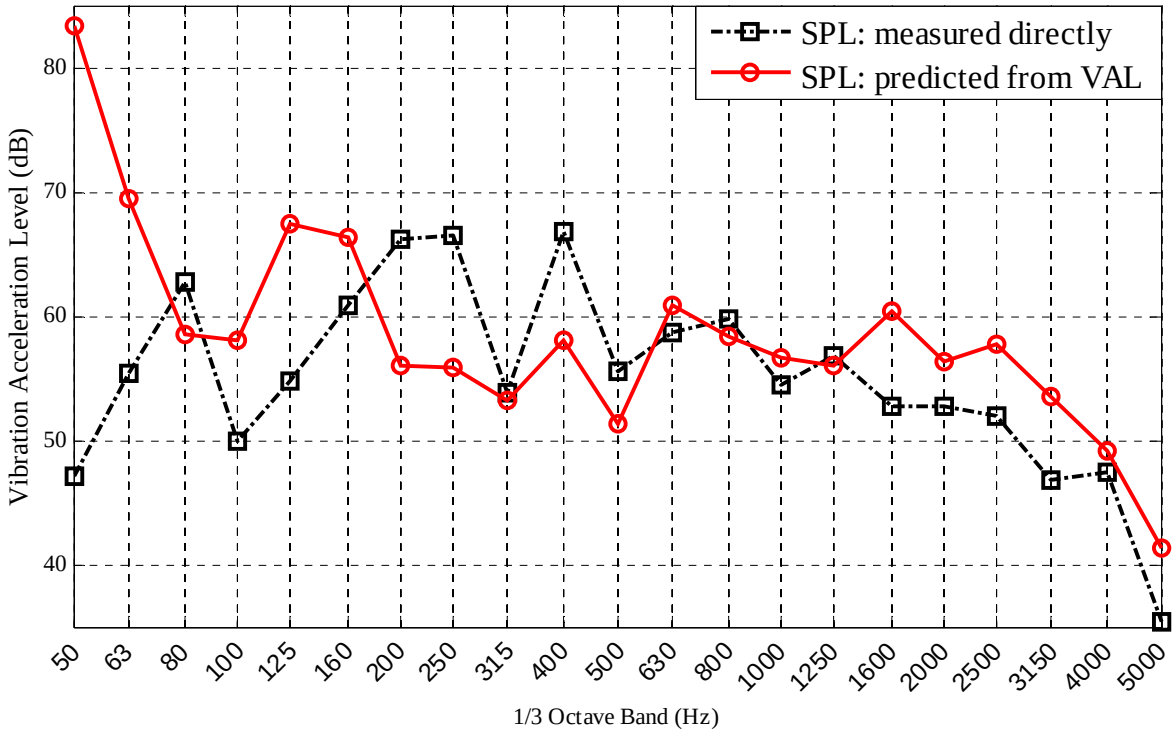


FIGURE 3.6 Measured and predicted time-averaged sound pressure levels at 1.0 meter away from the surface

# CHAPTER 4 ACOUSTIC TEST CHAMBERS AND METHODS

A structural comparison was done between acoustic test chambers recognized in standard acoustic material testing methods and the acoustic chamber located in the Ryerson Aeroacoustic Research Facility. A note on room acoustics and the description of each chamber and transmission loss testing method are given here to assist the reader's comprehension of later sections.

## 4.1 Room Acoustics: Modes of Vibration

Proper functionality of acoustic control rooms such as concert halls, sound mixing studios or reverberation chambers relies on a properly dimensioned space. The reason is that the size and shape of the control room affect its accuracy for sound reproduction. At the most basic level, a room is simply a band-pass filter, or rather three band-pass filters, with one filter for each of the three dimensions: length, width and height (see equation (2.10) at the beginning of sub-section 2.2.2). Each filter is tuned to a specific frequency, determined by the room's dimension, with most of the acoustic energy concentrated at that frequency. The rest of the energy is distributed in Fourier components at harmonically related multiples of the tuned frequencies, hereby labelled as *resonance modes of vibration* or simply *room modes*. Room modes can be identified by peaks and dips in the frequency response. At the nodes, they not only cause a boost of energy, but they also increase their decay time, which we perceive as reduced clarity of sound. Although there is nothing we can do about the existence of the room modes, we can effectively reduce the coloration[14] they add to the reproduced sound by carefully choosing the dimensions of the room. One way to achieve this is to space room modes as evenly as possible. An asymmetrically shaped room is a better choice over a room that is a perfect cube because it distributes energy over more consistently spaced resonance frequencies, rather than superimposing all of it in one frequency. An even better alternative would be to design a room that has densely packed room modes. This is obtained by making the room larger while keeping the proportions the same. Larger rooms are ideal for sound reproduction because the natural response of these rooms contains less energized resonance peaks that start lower in the frequency spectrum and thus are distributed closer apart. The combined effects of these peaks yield a

[14] Coloration is a term used for unwanted extraneous variations in the frequency response of a loudspeaker

reasonably flatter overall response. On the contrary, smaller rooms of the same proportion have only a few high-energy modes which are spaced farther apart, since the first mode starts higher in the frequency spectrum. The number of room modes and the mean modal separation can be predicted using equations (2.11) and (2.11a). As mentioned before, the worst shape of a room with respect to sound reproduction is a perfect cube, because of the high-energy state of the matching frequencies. A similar response would be expected from a room whose dimensions are multiples of each other, since many of the same frequencies would be emphasized [27, 28].

## 4.2 Acoustic Test Chambers and Environments

Acoustic material and component testing can be performed either in a specialized environment or "in situ." The need for a test chamber to assist in acoustical measurements is primarily justified by the suitable grade of accuracy a researcher is trying to achieve. The researcher may choose from a precision, engineering, or survey grade of performance, where each grade would employ a specific type of test chamber and industry-standard procedures. In this thesis, the interest is primarily in engineering and survey grades of performance. The test chambers that are typically used in these grades are hemi-anechoic and free-field chambers. A precision grade of performance uses a full/hemi-anechoic chamber and a reverberation chamber [29].

### 4.2.1 Full/Hemi Anechoic Chamber

A full/hemi anechoic chamber, as depicted in Figure 4.1, is an echo-free enclosure constructed with a noise attenuating outer structure such as concrete, masonry or modular panels and is internally shielded with the cladding of highly sound absorbing material in the shape of a wedge. Anechoic wedges attenuate internal reflections, or echoes, by transforming the acoustic energy into heat energy through the friction mechanism between air and absorbing material. The wedge size determines the lowest frequency, the cut-off frequency[15], that can be attenuated. A hemi anechoic chamber has acoustical treatment on the ceiling and walls only; the floor is intentionally left reflective so that large and heavy objects can be tested [29, 30].

[15] Cut-off frequency is the lowest frequency that can be measured in a room with desirable accuracy. It is the lower bound of the test room's performance range. Sometimes, cut-off frequency simply refers to lowest frequency.

FIGURE 4.1 A typical structure of a full- (left) and hemi- (right) anechoic chamber[16]

### 4.2.2 Free-Field Chamber

A free-field chamber is a practical and economic alternative to a hemi-anechoic chamber. It is similar in design and construction, but rather than having anechoic wedges, the walls and ceiling of a chamber are lined with modules of absorber panels several inches thick (Figure 4.2). The chief advantage of using modular acoustic panels is that the sound attenuation performance of an existing structure can be easily altered by optimising the shape and thickness of the acoustic treatment. For example, a thick layer is used for small rooms and chambers intended for low frequency testing, while a thinner layer is used for larger rooms and chambers intended for high frequency testing. To a large extent, the volume of the room predetermines the necessary amount of acoustic treatment. Further reduction in acoustical treatment would ultimately cause all noise attenuation to be ascribed to air absorption of the enclosed volume - the greater the space the better the absorption. The SPL response of a large room can be compared to the free-field conditions of an outdoor parking lot, which can be regarded as a room of infinite size [29].

### 4.2.3 Reverberation Chamber

A reverberation chamber, as its name suggest, is a screened room that produces a long reverberation time or long lasting echo (Figure 4.3). It is recommended for measuring the acoustic properties of materials which are exposed to diffuse sound fields and whose acoustic properties depend on the size of the material [23]. A diffuse sound field is a hypothetical term used in practice to describe otherwise complicated interference of randomly incident broadband

[16] Image taken from <http://www.noe.co.jp/en/development/dev02.html#contents01>

plane waves as a simple uniform non-directional field [21]. A relatively high level of diffusivity can be achieved if the design of the reverberation room guarantees many modal frequencies with equalized mode spacing. Such conditions can be attained if at least 15 to 25% of a reverberation room's surface area is occupied by diffusers, which are strategically placed reflection panels [23]. Some reverberation rooms are rectangular, where the room dimensions are based on certain ratios which omit multiples or rational fractions of each wall pair. Others employ irregular geometry such as non-parallel vertical walls and slated calling, thus reducing the degenerate effects on room modes caused by overlapped modal patterns [27]. A highly reflective surface finish will be used as well. The design might either incorporate massive masonry or concrete walls several feet in depth coated with reflective paint, laminates of plywood and masonite fiberboard separated with fibreglass insulation or well-damped modular steel panels. The specific construction method depends on the type of testing that the room is designed for. For instance, a reverberation room constructed of concrete is ideal for sound absorption testing[17], but it requires an acoustic absorber such as a base trap to capture low frequency sound to make it suitable for sound power testing[18]. In contrast, a reverberation room constructed of modular steel panels is ideal for sound power level testing, but not as effective for sound absorption testing. The flex in the light construction of modular steel panels provides the correct amount of low frequency absorption for sound power testing purposes, but it elevates the low frequency data for sound absorption testing, especially at frequencies below 200 Hz [29].

In both construction methods, the room volume determines the lower frequency limit. For instance, for measurements down to 125 Hz, a minimum room value of 80 $m^3$ is recommended. For measurements down to 100 Hz, the minimum room volume increases to 125 $m^3$ [23]. In general, doubling the room volume would reduce the cut-off frequency by at least one third-octave center frequency. The design and construction of the reverberation room make it an expensive capital investment for a research institution. Whenever possible, a smaller reverberation chamber is used, where the only major drawback is its high cut-off frequency [31].

---

[17] Sound absorption testing determines the amount of sound absorbed by a material. The amount of sound absorption is represented by product of the absorption coefficient and the surface area of a material. The unit of sound absorption is the Sabin, and the sound absorption coefficient has a practical unit between 0 and 1.

[18] Sound power testing determines the total sound energy radiated by the sound source per unit time. The unit of measurement is the Watt.

FIGURE 4.2 A typical structure of a free-field chamber[19]

FIGURE 4.3 A typical structure of a large (left) and small (right) reverberation chamber[20]

## 4.3 Transmission Loss Testing Methods

Two standard methods that are primarily used today for acoustic material testing are the *impedance tube method* and the *reverberation room* method [34]. These methods alone are adequate for sound absorption testing, from which acoustic properties of material such as absorption[21], refraction[22], impedance[23] and admittance[24] can be extracted, but they need to be

[19] Image taken from < http://www.eckelusa.com/images/stories/legacy/new/york.jpg>

[20] Image taken from <http://www.noe.co.jp/en/development/dev02.html#contents02>

[21] A property of materials that reduces the amount of sound energy reflected. The introduction of an absorbent into the surfaces of a room will reduce the sound pressure level in that room by not reflecting all of the sound energy striking the room's surfaces.

[22] The bending of a sound wave from its original path, either because it is passing from one medium to another with different velocities or by changes in the physical properties of the medium.

paired with other chambers/extensions for sound transmission loss testing [35]. The performance of one method over the other is justified by the type of the material being tested and the frequency range of the tested data. The two methods are compared here to determine which method better suits the design of the acoustic chamber and the test specimen.

### 4.3.1 Impedance Tube Method

The impedance tube, or standing wave tube as it is commonly referred to, is a device that generates "pure tone" stationary waves that propagate as plane waves. It is handy device for measuring the acoustic properties of small test samples including composite and irregular materials. An extended version of an impedance tube used specifically for sound transmission loss measurements is referred to as transmission loss tube (Figure 4.4). It consists of an assembly of modular tubes (source and receiving), a sound source, a test sample holder and a termination. The tube walls are constructed from a dense and sufficiently rigid material with a smooth internal surface. The tubes are straight and long with a uniform cross section area along the length to prolong undisturbed propagation of the plane waves. The source tube is located at the upstream of a sample holder and is terminated by a sound source in the form of a loudspeaker which excites the plane wave field. The receiving tube is located at the opposite end, downstream of a sample holder, and is usually terminated by an anechoic wedge. The modular tubes are of specific length to ensure a uniform pressure field along the cross section of the tube in advance of a plane wave reaching a microphone position. As a rule-of-thumb, microphones are positioned no closer than one effective tube diameter from a termination. In the transmission loss tube, the loudspeaker and the sample radiate sound in the source tube and the receiver tube, respectively. The usable frequency range of a transmission loss tube depends on the diameter of the tube and the spacing between microphone locations. A large tube setup is used for low frequency measurements, while a small tube setup is used for mid/high frequency measurements. The diameter of the transmission loss tube must be chosen with care since the internal plane wave field can only be sustained below the resonant frequency of the first cross mode. This is

[23] The opposition to the flow of acoustic energy measured in ohms. The complex ratio of dynamic pressure to particle velocity at a point in an acoustic medium, measured in rayls (1 rayl = 1 N s/m3).

[24] The reciprocal of impedance.

known as resonance of an air cavity, and it can be calculated using equation (2.12) developed at the end of sub-section 2.2.2 [34, 35].

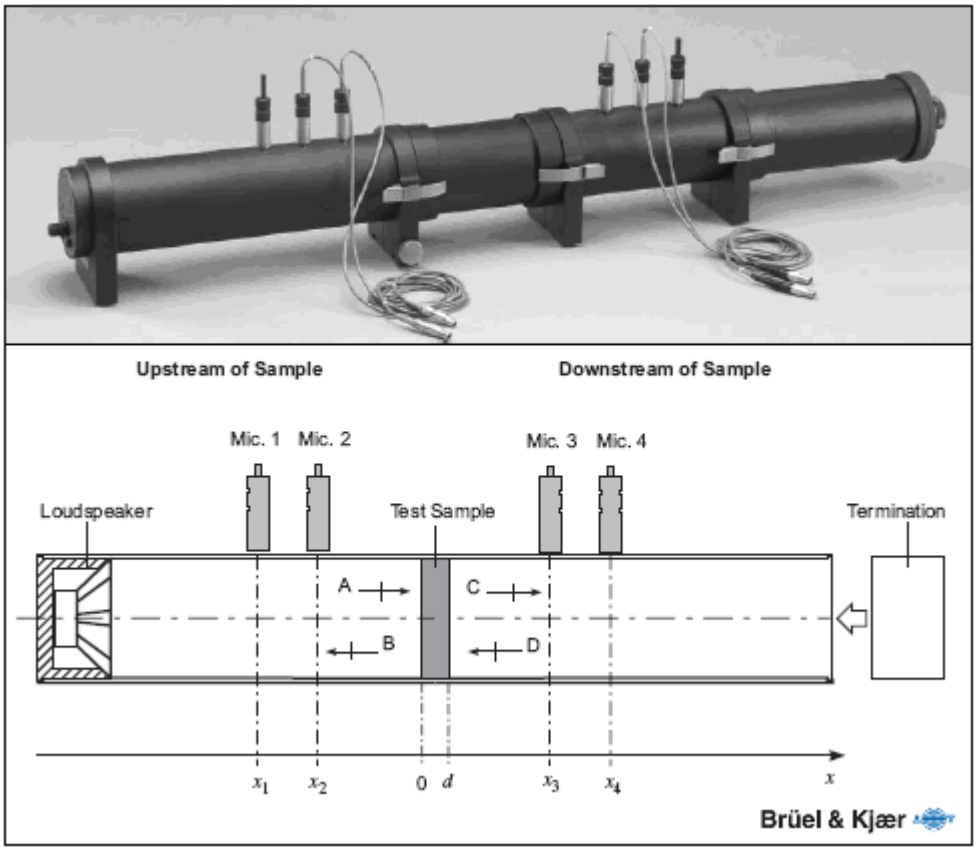


FIGURE 4.4 An actual photo and schematic diagram of the transmission loss tube [35]

The impedance tube method is primary used for porous absorbers because is not suitable for acoustic material testing of those absorbers that depend on their surface area for their effect, such as vibrating panels [32]. For this reason, it is yet to be determined if a conventional transmission loss tube could be integrated to accommodate transmission loss testing of a double-panel structure assembly. Experimental work done by Anderson [36] suggests that it is feasible to accurately obtain the transmission loss of an assembly, in his case a loudspeaker driver in a baffle, as long as the assembly is fully enclosed within a transmission loss tube and the edges of the assembly terminate at the tube walls. Furthermore, a conventional impedance tube proved to be adequate for testing composite panels, which in essence are a panel assembly consisting of core material, possibly an array of point or line connectors, sandwiched between a layer of metal skins [35]. Unfortunately, the performance of the transmission loss tube is dictated by its

dimensions. A large sample requires a source tube of at least the same effective diameter as the sample; for instance, the present acoustic chamber has an effective diameter of 0.813 meters; thus, a sample of the same size would limit the valid frequency range to approximately 211 Hz. The transmission loss measurements of large panels are usually reported in one-third octave bands over a standard range of frequencies, from 100 to 5000 Hz; thus, the results obtained with the transmission loss tube would have been inconclusive due to insufficient data range. However, with regard to vibration isolation measurements of infra sound, this frequency range is very useful. Furthermore, rules regarding microphone spacing suggest at least one tube diameter between terminations. In order to use the impedance tube method with a current sample size, a transmission loss tube of at least five meters in length would have to be constructed, thus failing to comply with the current laboratory's designated space limitations. One thing is for certain, the impedance tube method is a quick and accurate method for verifying transmission loss performance of individual materials before they are manufactured into components, but not a favourable method for testing fully assembled components.

### 4.3.2 Reverberation Room Method

A comprehensive description of test chambers, including the reverberation chamber, was presented in section 4.1.2. The only other requirement necessary to set up a complete test facility for transmission loss measurement is the choice of the receiving chamber. The test facility could either incorporate a twin arrangement of reverberation chambers or a reverberation chamber coupled with either a full/hemi-anechoic chamber or a free-field chamber [29, 31]. The reverberation room method is ideal for testing large structural assemblies and it is recommended that the test specimen should preferably form a whole room surface, wall or floor [35]. The low frequency measurements of sound transmission loss obtained with this method are very sensitive to test specimen size, specimen edge restrains, the location and size of the sound source, as well as the placement of the microphones [29]. For these reasons, the procedure involved in the set up and the extraction of transmission loss data using a reverberation room method is time consuming. The method relies on an omni-directional sound source. An approximation can be obtained, in practice, by mounting an array of full range loudspeakers or a system of multi-driver loudspeakers that cover different frequency ranges on the faces of a polyhedron. Placing the source(s) in trihedral corners of the room will excite room modes more effectively and minimize

the effects of the direct field[25] [23]. For a researcher, a major advantage of using test chambers is the ability to select an accurate test environment to perform specific measurements. Unquestionably, precision grade transmission loss results can be obtained if a reverberation chamber is connected to a full/hemi-anechoic chamber, as is illustrated in Figure 4.5. This is so, of course, if the space restrictions and economics are omitted from the constraints. As was mentioned earlier, whenever possible, small reverberation chambers are used with combination of an anechoic or a free-field chamber, possible even a large room.

FIGURE 4.5 A typical test chamber arrangement for transmission loss measurement: reverberation room connected to adjacent anechoic chamber[26]

[25] A region in which the majority of sound energy arriving from the sound source at a point has traveled a straight line between them, that is, without reflection.

[26] Image taken from <http://www.noe.co.jp/en/development/images/dev02_012.jpg>

# CHAPTER 5 CONSTRUCTION AND PERFORMANCE REQUIREMENTS OF THE TEST FACILITY

## 5.1 Design and Construction of the Test Facility

With the nature of the test specimen in mind, as well as the background knowledge outlined in the previous chapter, the acoustic chamber resembles a small reverberation chamber within a semi-reverberant room environment. The American Society for Testing and Materials (ASTM) and International Organization for Standardization (ISO) issued a number of standards that should be referred to when accrediting or constructing new acoustic research facilities for measuring the transmission loss of building partitions and elements using the reverberation room method. The ones referred for the purpose of the structural assessment were: ASTM E90-09[27], ASTM E1289-08[28] [23, 39].

### 5.1.1 Construction of the Acoustic Chamber

The acoustic chamber is a rectangular box with internal dimensions of 0.775 meters in length and width, and 0.813 meters in height. The design concept for the acoustic chamber was similar to the one that inspired the Wharfedale series of sand filled loudspeaker cabinets designed in late 50's [37]. Birch plywood was the material of choice at the time, even though it exhibited a major problem for speaker designers. The flexible nature of the sandwiched thin-laminate-sheets caused the plywood cabinets to resonate uncontrollably at low frequencies. The designers at Wharfedale pointed out in their "Cabinet Handbook" that the most effective way of reducing cabinet resonance was to line the walls of the cabinet with sound absorbing material or use a sandwich construction of two plywood panels separated with dry sand [37, 38]. Given that compacted sand fills had been used in building construction to reduce ground borne vibration transmitted to the concrete foundation, it is an ideal material to fill the gap between two sheets of ply. The acoustic chamber incorporates a simple design that permitted ease in construction. It was decided that a pair of stiff boxes should be constructed out of ¾ inch (19.05 mm) 5-ply birch plywood and be press fit together with a dry beach sand. The volume of the inner box was 20 $ft^3$

[27] ASTM E90-09 Standard Test Method for Laboratory Measurement of Airborne Sound Transmission Loss of Building Partitions and Elements

[28] ASTM E1289-08 Standard Specification for Reference Specimen for Sound Transmission Loss

(0.566 $m^3$), while the volume of the outer box was 37 $ft^3$ (1.05 $m^3$). For extra support two self-lock steel cable ties were attached to the upper and lower periphery of the outer box. The chamber was also made mobile by mounting four heavy duty compound wheels, which also served as ground born vibration isolators. A 3-way loudspeaker unit was mounted at the bottom of the inner box with a microphone positioned right above it within the volume of the inner box. This setup is depicted in Figure 5.1.

FIGURE 5.1 Construction of the acoustic chamber

### 5.1.2 Construction of the Receiving Room

The Ryerson Aeroacoustic Research Facility was designated as the receiving room for transmission loss testing. In general, laboratories are classified as semi-reverberant enclosures since their supporting walls are constructed from thick masonry blocks and concrete. Also, their interior design is lacking in the significant level of absorption seen in a furnished room. The Ryerson Aeroacoustic Research Facility was constructed in such a way, except from two small storage rooms on each side, which incorporated some gypsum drywall construction. The lab's

floor was coated with highly reflective surface panels. To a large extent, the laboratory is an empty rectangular room with dimensions of 8.23 meters in length, 4.90 meters in width, and 3 meters in height. Even though 15% of the room's volume is occupied by various laboratory equipment and furniture such as filling cabinets, bookcases and desks, this furniture was rearranged in such a way as to optimise their smooth surfaces, as one would do with specially designed diffuser panels used to increase the reverberant environment.

### 5.1.3 Construction and Installation of the Test Specimen

The construction and installation of the hood (i.e., the cover for the current test chamber) were compared with standard specifications given for a reference specimen for sound transmission loss testing in ASTM E1289-08 [39], and good similarities were found. The standard requires constructing the test panel by riveting galvanized steel sheet, 0.62 mm in nominal thickness with a surface mass of 0.5 to 7 kg/m$^3$, to the steel frame of the same outside dimensions as the sheet. Furthermore, the frame should be constructed by notching and welding steel right angles to form the four corners of the frame, which are then smoothened by grinding. The test specimen should be installed in the relevant chamber opening by fastening it into a section of wood-stud frame, which is previously attached around the perimeter of the opening, and all joints should be sealed with duct tape. In comparison, the hood consisted of a weldment between a single square steel sheet of metal, ¼ inch (6.35 mm) in thickness and 36 inch (914 mm) side length, and four sheets, 5 inch (127 mm) in width and corresponding length, to form a rim. Four ½ inch steel flange nuts where welded symmetrically near the corners of hood for sample mounting purposes, again all weldments were smoothened by gridding. To protect the hood from accidental notches and corrosion it was coated with yellow nylon paint. The hood of the chamber had the dual function of a sample holder and an access door to the speaker unit and the measuring equipment. For this reason, no fasteners were used. Furthermore, to prevent flanking transmission[29] and promote only the transmission of the sound borne vibration from the internal pressure wavefront, the hood was press fit into a 1 inch thick layer of foam that was placed on top of the sand filling and then tightly sealed with sandbags that were wedged along

[29] Flanking transmission refers to sound transmission from the source room to the receiving room through paths other than the test panel

the rim of hood's perimeter, as illustrated in Figure 5.2 below. The top edge of the inner box was lined with a foam pipe lagging to further insulate the system.

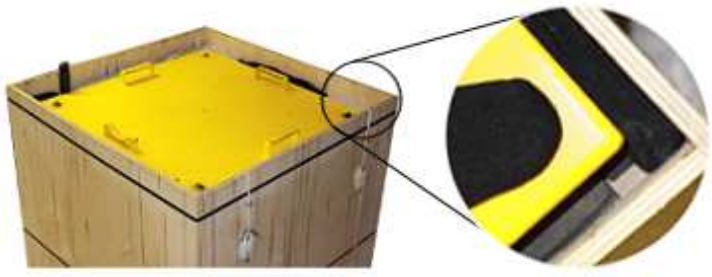

FIGURE 5.2 Fully enclosed acoustic chamber with its hood sealed with foam and sandbags

The main difference between the two specimens (i.e., the hood and the reference specimen) was that the hood had a surface mass about 10 times greater than recommended. This was necessary to provide a solid mounting surface for various connectors. Another difference was how the specimen was installed in the laboratory opening. The hood extended beyond the chamber's inner wall rather than being placed within it (Figure 5.3).

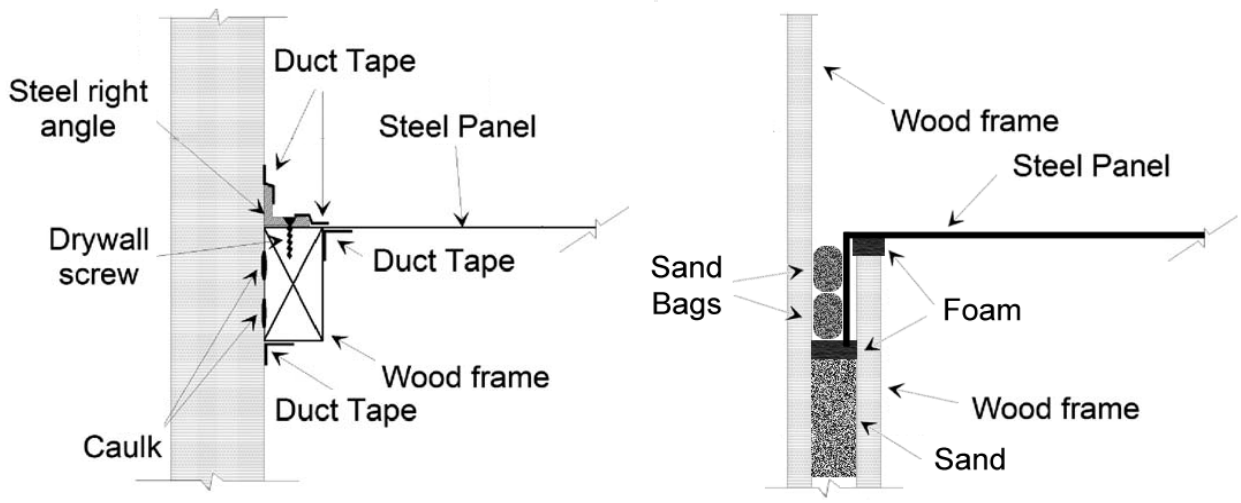


FIGURE 5.3 Installation of the reference specimen (left) vs. the hood in the acoustic chamber (right) [39]

As was indicated in Chapter 1, the second panel of the double-panel assembly was held solely by the connectors, and the perimeter of the panel was not sealed to confine the airspace between the two panels. ASTM E1289-08 suggests two methods of installation for the double-

panel reference specimen, one involving a common wood frame, the other involving a separate frame. The two installations are depicted in Figure 5.4.

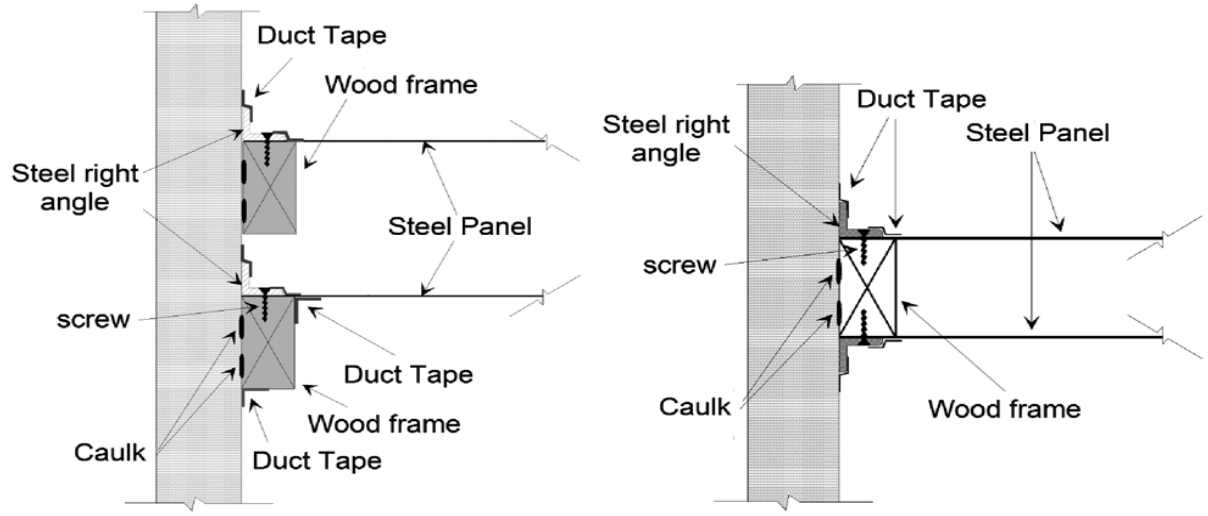


FIGURE 5.4 Double-panel reference specimen with separate wood frames (left) and common wood frame (right) [39]

The two proposed solutions to confine the airspace between the two panels are illustrated in Figure 5.5. Solution (A) requires welding a steel sheet of metal on to each side of the square panel to form a hood. The weldments are then smoothened by gridding. The second hood is installed by placing it above the first hood and press fitting it into the foam base. Just like before, the hood is sealed by wedging sandbags along the rim of hood's perimeter. Solution (B) requires completing the second panel's construction and installation as documented in the ASTM standard. Also, the connector mounting locations have to be moved away from the walls to prevent boundary conditions from affecting the VAL. In comparison, solution (A) is the most favourable solution due to its simplicity in construction and installation. If the flanking transmission experiment reveals that the sound insulation resistance of the first hood is too high for adequate transmission loss measurements, then both hoods need to be constructed from thinner steel sheets.

## 5.2 Performance Requirements for Transmission Loss Measurements

Several tests were conducted based on the notes from ISO and ASTM standards to evaluate the performance of the test facility. These tests verified that the acoustic chamber is

capable of generating a diffuse sound field above an established lower frequency limit with enough sound power to surpass the minimum sound pressure levels in the receiving room to yield valid transmission loss data.

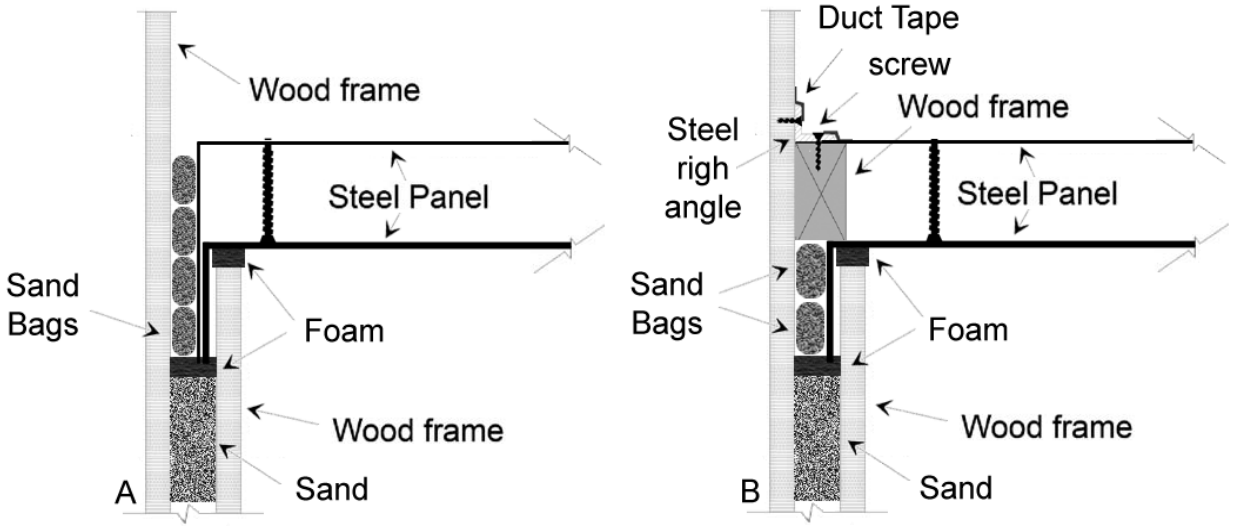


FIGURE 5.5 Proposed adjustments to the double-panel installation: welding a rim to the second panel (A) or constructing the panel as recommended in the standard and moving the connector position (B)

### 5.2.1 Diffusivity Measurements

ASTM E90-09 [23] suggests that a satisfactorily diffuse sound field will be ensured in the room if the same mean modal separation is achieved as required to obtain a minimum of approximately 18 room modes at 125 Hz third-octave in a room with a minimum preferred volume of 80 $m^3$. Inserting these parameters into equations (2.11) and (2.11a) resulted in a mean modal separation of 2.6 Hz. ASTM E336-09[30] [40] is a standard used in survey level testing of building elements, and it suggest that at least 10 room modes at 125 Hz third-octave in a room with a minimal volume of 40 $m^3$ are required for good results. This translates to a mean modal separation of 5.4 Hz. Furthermore, the diffusivity results obtained by Tsui et al [23] with their small twin-reverberation chamber design suggest that approximately a 14.6 Hz mean modal separation would be adequate for accurate transmission loss measurements. Table 5.1

[30] ASTM E336-09 Standard Test Method for Measurement of Airborne Sound Attenuation between Rooms in Buildings

summarises the lower frequency limits when the above calculation is repeated with the set modal separations from various literature for the acoustic chamber and receiving room volume.

TABLE 5.1 Lower frequency limit at a given volume for the set mean modal separation

| Literature Source | Mean modal Separation (Hz) | Lower frequency limit (Hz) | |
|---|---|---|---|
| | | Acoustic Chamber | Receiving Room |
| ASTM E90-09 | 2.6 | 1600 | 100 |
| ASTM E336-09 | 5.4 | 1000 | 80 |
| Tsui et al | 14.6 | 800 | 50 |

In order to support the prediction that the sound pressure distribution in the acoustic chamber is diffuse and to establish the lower frequency limit, the spatial variation in sound pressure levels was examined according to the procedure outlined in ASTM E90-09. Essentially, the standard required placing an omni-directional loudspeaker in a room and exciting the room with various one-third octave band signals. The time-average sound pressure level, $\bar{L}$, was determined at various locations along a linear path and inspected for stability. The loudspeaker was placed near the internal trihedral corner of the chamber angled towards the bottom of the chamber to reduce the direct field effects. The microphone paths were oriented diagonally between opposing corners of the chamber 200 mm below the hood. One-third octave measurements were taken at 100 mm intervals up to 800 mm length. This was a complicated and time consuming process, especially when performed manually; thus, a decision was made to use a RealTime Analyzer to acquire and process the data. Unfortunately, the signal generator of the RealTime Analyzer is incapable of producing a pink noise signal in individual one-third octave bands Therefore, a pink noise signal in the full audible frequency range was used instead, and $\bar{L}$ for a particular one-third octave band was extracted from the full data set (Figure 5.6). From the sound pressure level variation curves, it can be clearly seen that the sound field in the acoustic chamber becomes relatively stable above 1000 Hz. The tolerance limit of +/- 3dB is considered to be accurate for the present work. This result confirms the lower frequency limit predicted from ASTM E336-09 for survey level measurements.

### 5.2.2 Reverberation Time

The reverberation time is one of the most important characteristics of a room. It helps

determine the minimum sound absorption required in the room to obtain good sound reflections. The sound absorption in the room should be as low as possible to achieve adequate diffuse sound field conditions and minimize the direct field region that dominates near radiating surfaces. In the case of the test specimen, this would not only improve the measured sound transmission loss, but also the predictions of the SPL obtained from VAL data at the specimen's surface. The ASTM E90-09 recommendation is to use rooms with the sound absorption no greater than:

$$A = V^{2/3} \tag{5.1}$$

where $A$ = room sound absorption in the frequency range that extends from $f = 2000/V^{2/3}$ to 2000 Hz.

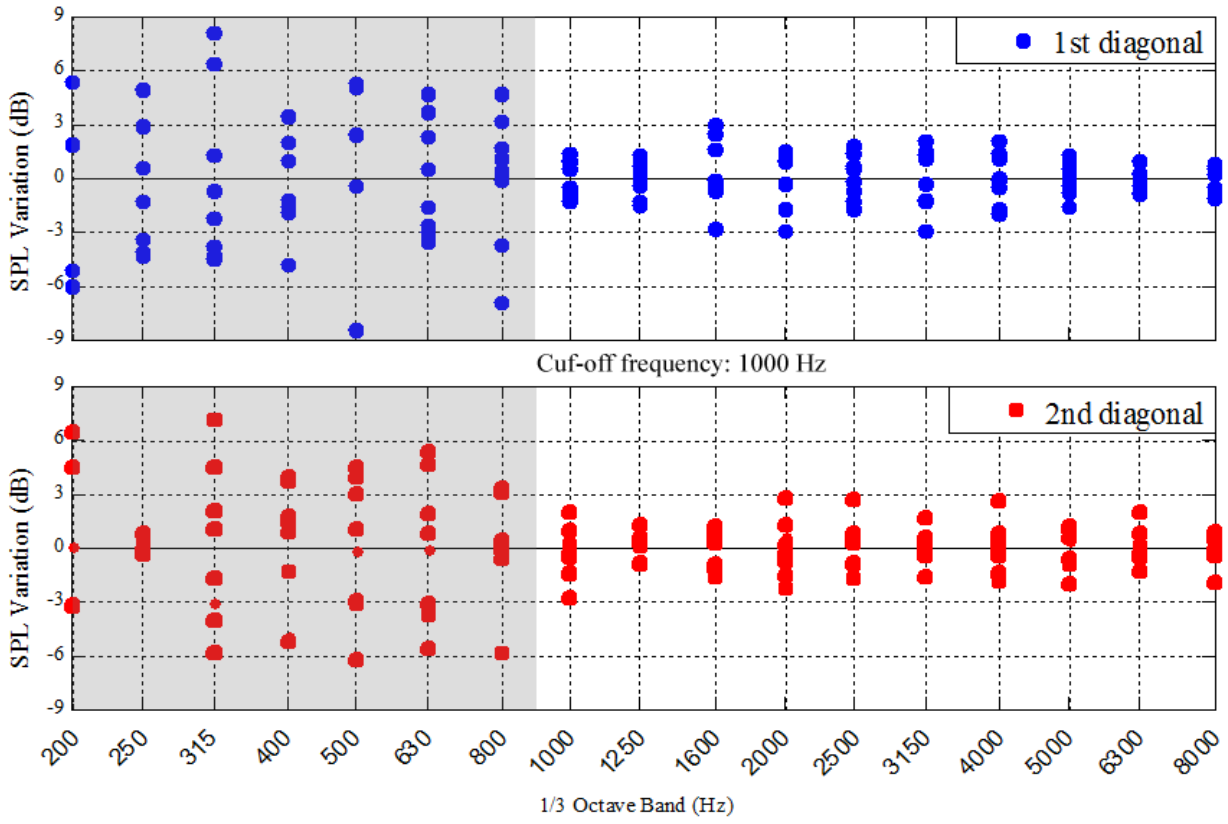


FIGURE 5.6 The sound pressure level variation along the two diagonal paths in the acoustic chamber given between 200 – 8000 Hz one-third octave center frequencies with +/- 3dB tolerance limit

The sound absorption tests were conducted according to the suggestions given in ASTM C423-08a [24], except that the reverberation times of each room were determined from the decay curves of impulse excitation obtained using a Sound Analyzer software package that was based on ISO 3382[31]. The absorption of the room and its contents was calculated from the Sabine formula which was introduced in equation (3.1). The accuracy of the results depends on the precision grade of the test facility. Two ASTM standards were referred to in the previous section which recommended a 2.6 to 5.4 Hz mean modal separation to achieve adequate diffuse sound field conditions in the reverberation chamber and in a common room. In general, there exists a crossover frequency above which room modes start to cluster so closely together that they are no longer seen as resonant peaks; this point is known as the Schroeder frequency [20]:

$$f_S = 2000\sqrt{\frac{T_{60}}{V}} \tag{5.2}$$

Schroeder established a 3-fold overlap criteria which required more than 3 times the mean modal separation within the half-power bandwidth (-3dB) given by:

$$BW = \frac{2.2}{T_{60}} \tag{5.3}$$

Thus, one can predict mean modal spacing directly from reverberation time data using the following equation:

$$df = \frac{BW}{3} = \frac{0.733}{T_{60}} \tag{5.4}$$

The measured reverberation time and calculated results for the abovementioned parameters are shown in Table 5.2. The volume of the acoustic chamber (source room) and that the laboratory (receiving room) are 0.488 and 121.8 $m^3$, respectively. With these volumes, the

[31] ISO 3382 is a standard for acoustics measurement of the reverberation time of rooms with reference to other acoustical parameters

room absorption should not fall above 0.620 $m^2$ Sabine in the chamber and 24.57 $m^2$ Sabine in the laboratory, except above 2000 Hz where atmospheric absorption may make it impossible to avoid a slightly higher value than those calculated from equation (5.1). Reverberation time measurements obtained in a typical room are known to have little significance below 200 Hz as they are affected by the energy build-up of room modes. This behaviour is seen in the tabulated results for the receiving room. Schroeder frequency calculations suggest that a satisfactorily diffuse field will occur around the 1600 Hz third-octave in the acoustic chamber and the 200 Hz third-octave in the receiving room, with a mean modal spacing of 2.89 Hz and 0.63 Hz, respectively. When compared with the lower frequency limits suggested in ASTM standards, the Schroeder frequency represents a conservative value. For a given mean modal separation, both equation (2.11a) and (5.4) will provide similar results, one will help in estimating the room dimensions, while the other will help in determining surface finish and the room's content for correct sound absorption. The absorption of both rooms, was on average, within the recommended limits.

### 5.2.3 Flanking Transmission

To ensure that the walls of the chamber are properly insulated and to establish the upper bound for reliable transmission loss results, a test was conducted to determine the degree of flanking transmission. Flanking transmission loss or noise reduction measurements are obtained by testing various specimens of high sound insulation resistance. A lack of significant variance between transmission loss results indicate that the sound is transmitted through flanking mechanism rather than through the test specimen. The threshold of reliable transmission loss results is reached when the sound insulation resistance of the test specimen approaches the resistance of the walls that make up the reverberation chamber [23]. At that point, sound is transmitted from the source to the receiving location by a path other than that under consideration. If the test specimen has a sound insulation resistance greater than that of walls that make up the reverberation chamber, then all the sound perceived in the receiving side will be from flanking transmission. The necessary precaution was taken every time the hood was removed to place it back in such a way as to minimize flanking. One aspect of the acoustic chamber that was not documented was the noise reduction specification of the wall construction used in building the chamber. If the noise reduction ratio between the ply-sand-ply walls of the

chamber and hood reaches unity, then the upper bound for reliable transmission loss measurements has been reached and the transmission loss results for the hood and the double-panel assembly will be incorrect. To find the upper bound for reliable transmission loss, the decision was made to complete the box structure of the chamber by closing off its opening with the same ply-sand-ply sandwich of materials (Figure 5.7). This way all the sides of the chamber will be constructed symmetrically and from the same materials. The transmission loss and noise reduction measurements will be consistent throughout its surface. The results of this experiment are shown in Figure 5.8.

TABLE 5.2 Summary of the space-time averaged room parameters

| One-third-octave center frequency (Hz) | Source Room V = 0.488 $m^3$ | | | | Receiving Room V = 121.8 $m^3$ | | | |
|---|---|---|---|---|---|---|---|---|
| | T60* | A | $f_s$ | df | T60 | A | $f_s$ | df |
| 50 | 11.92±6.588 | 0.01 | 9885 | 0.061 | 12.90±0.729 | 1.50 | 651 | 0.057 |
| 63 | 0.215±0.022 | 0.36 | 1328 | 3.409 | 9.725±0.654 | 2.00 | 565 | 0.075 |
| 80 | 1.230±0.058 | 0.06 | 3175 | 0.596 | 3.991±0.615 | 4.86 | 362 | 0.184 |
| 100 | 0.059 | 1.31 | 697 | 12.38 | 4.752±0.807 | 4.09 | 395 | 0.154 |
| 125 | 0.043 | 1.81 | 594 | 17.05 | 6.896±0.797 | 2.82 | 476 | 0.106 |
| 160 | 0.042 | 1.85 | 587 | 17.45 | 2.725±0.396 | 7.12 | 299 | 0.269 |
| 200 | 0.451±0.003 | 0.17 | 1922 | 1.627 | 1.076±0.022 | 18.0 | 188 | 0.681 |
| 250 | 0.145±0.003 | 0.54 | 1092 | 5.041 | 1.203±0.032 | 16.1 | 199 | 0.609 |
| 315 | 0.166±0.002 | 0.47 | 1165 | 4.424 | 1.147±0.020 | 16.9 | 194 | 0.639 |
| 400 | 0.182 | 0.43 | 1223 | 4.019 | 1.152±0.021 | 16.8 | 195 | 0.636 |
| 500 | 0.188 | 0.41 | 1242 | 3.897 | 1.171±0.015 | 16.6 | 196 | 0.626 |
| 630 | 0.372 | 0.21 | 1745 | 1.972 | 1.186±0.009 | 16.4 | 197 | 0.618 |
| 800 | 0.315 | 0.25 | 1606 | 2.331 | 1.182±0.008 | 16.4 | 197 | 0.620 |
| 1000 | 0.230 | 0.34 | 1373 | 3.188 | 1.187±0.009 | 16.4 | 197 | 0.618 |
| 1250 | 0.210 | 0.37 | 1311 | 3.495 | 1.161±0.008 | 16.7 | 195 | 0.631 |
| 1600 | 0.165 | 0.47 | 1162 | 4.448 | 1.133±0.006 | 17.1 | 193 | 0.647 |
| 2000 | 0.201 | 0.39 | 1284 | 3.643 | 1.086±0.006 | 17.9 | 189 | 0.675 |
| 2500 | 0.268±0.002 | 0.29 | 1482 | 2.734 | 1.026±0.007 | 18.9 | 184 | 0.715 |
| 3125 | 0.130 | 0.60 | 1032 | 5.638 | 0.956±0.005 | 20.3 | 177 | 0.767 |
| 4000 | 0.122 | 0.64 | 1000 | 6.013 | 0.884±0.004 | 22.0 | 170 | 0.829 |
| 5000 | 21.18±0.060 | -- | 13177 | 0.035 | 0.772±0.003 | 25.1 | 159 | 0.949 |
| 6300 | 75.02±0.082 | -- | 24797 | 0.010 | 0.667±0.003 | 29.1 | 148 | 1.099 |
| 8000 | 34.67±0.054 | -- | 16857 | 0.021 | 0.536±0.002 | 36.2 | 133 | 1.367 |
| **All** | **0.254** | **0.31** | **1442** | **2.888** | **1.166±0.143** | **16.7** | **196** | **0.629** |

* Three decimal place 95% confidence interval for individual qualities

FIGURE 5.7 Acoustic chamber sealed with the same ply-sand-ply sandwich as the wall construction

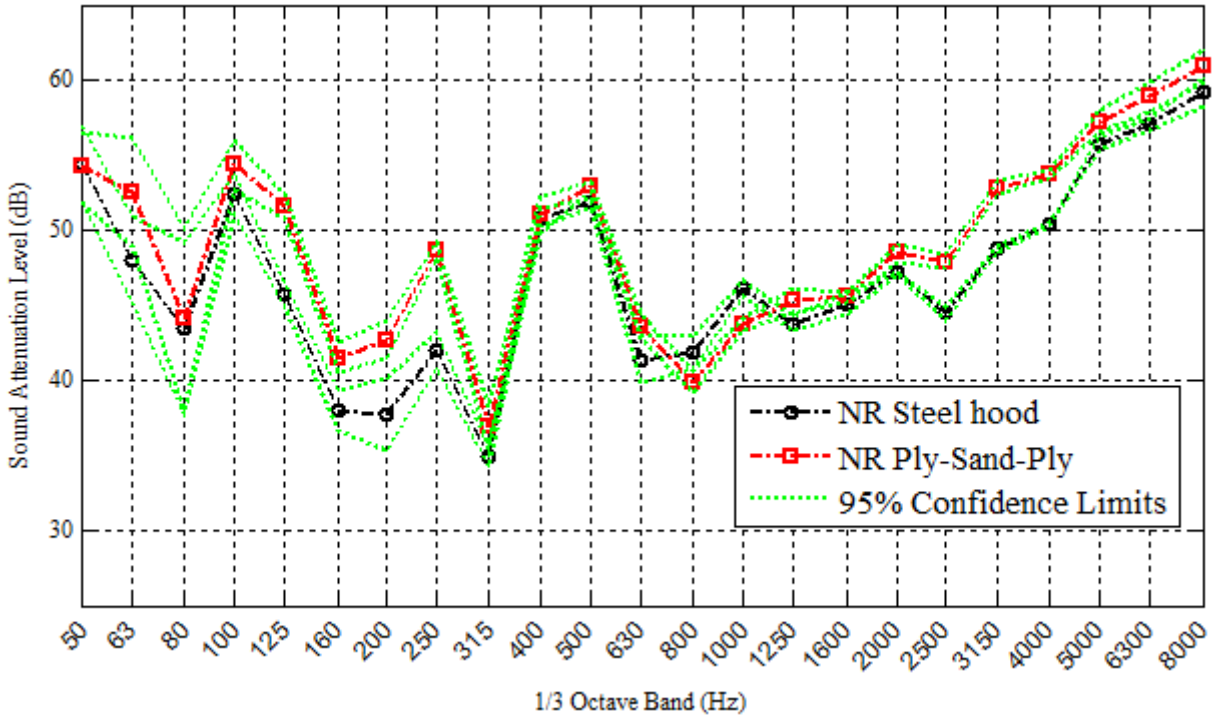


FIGURE 5.8 Noise reduction of the ply-sand-ply wall relative to the noise reduction of the steel hood

The sound attenuation results are considered to be accurate if the measured levels are at least 10 dB lower than the flanking transmission levels. The comparison of the noise reduction levels between the steel hood and ply-sand-ply sample revealed a remarkably similar response with levels within the 10 dB headroom range. Unquestionably, the sound insulation resistance of the hood is in close proximity to that of walls that make up the reverberation chamber. In consequence, the sound is transmitted almost equally through the flanking mechanism and through the test specimen.

### 5.2.4 Sound Power Requirements

The aforementioned ASTM standards suggest that the difference between the sound pressure levels of the signal-plus-background noise and the background noise alone should not fall below 10 dB. If the background noise level is between 5 and 10 dB below the combined level, the following correction should be used:

$$\bar{L}_a = 10 \log_{10}\left(10^{\bar{L}_{sb}/10} - 10^{\bar{L}_b/10}\right) \tag{4.5}$$

where $\bar{L}_a$ = adjusted signal level, dB

$\bar{L}_{sb}$ = level of signal and background combined, dB

$\bar{L}_b$ = background noise level, dB

Levels up to 5dB from the background noise level should be omitted from the results. The Ryerson Aeroacoustic Research Facility housed the test facility; its hard walls confined the semi-reverberant field to which the source sound was transmitted. The nominal power output (master volume) of the loudspeaker had to be determined to produce enough sound power to overcome the background noise levels surrounding the chamber. Figure 5.9 illustrates the range in the time-averaged sound pressure levels of signal-plus-background noise and the background noise alone along the measurement grid, as well as corresponding space-average sound pressure levels. The space-averaged source headroom is plotted in Figure 5.10. The headroom is adequate for the frequency range that extends from 50 to 10000 Hz. During the daytime hours, the background noise in the laboratory contains distinctive peaks. A constant noise at 20 Hz is emitted from the exhaust of the HVAC system and about 35 Hz is emitted from a compressor in the adjacent laboratory. Transient noise at 130 Hz is occasionally emitted by the hand dryer in the adjacent washroom; other transient noises included high frequency machine shop noise and mid frequency pedestrian conversation. To eliminate the influence of most of these noise sources, the measurements were performed late at night during the shutdown period.

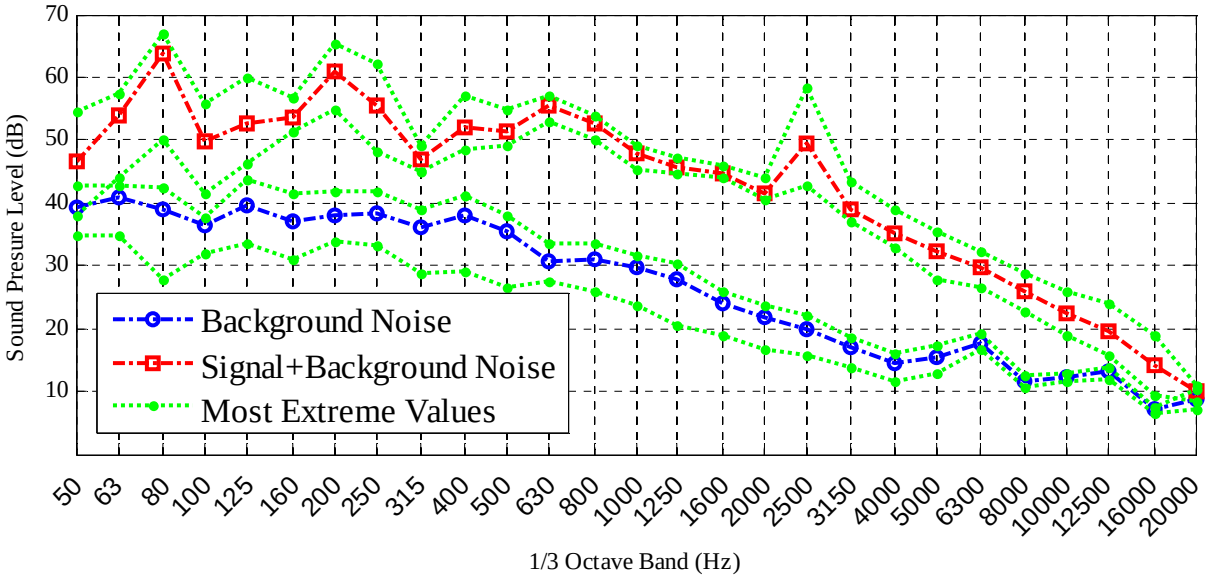


FIGURE 5.9 Range of time-averaged sound pressure levels along the measurement grid

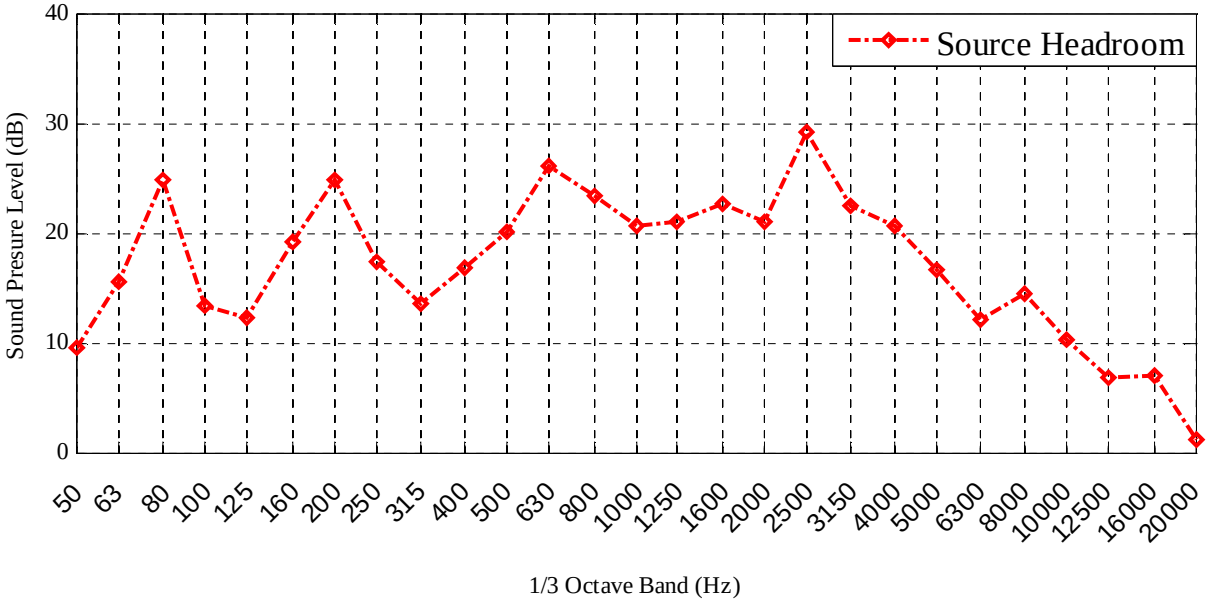


FIGURE 5.10 Space-averaged Source Headroom

# CHAPTER 6 INSTRUMENT SETUP AND SIGNAL PROCESSING

This chapter provides the reader with a description of the instrument setup and signal processing techniques: hardware and software used in the signal generation, acquisition, and processing of sound transmission data obtained from the acoustic material testing. Due to substantial time span between the completion of this thesis and the preliminary work, a number of tests were performed on the existing equipment and software to update them if necessary to support current methods. The laboratory equipment used in the current setup in illustrated in Figure 6.1 below.

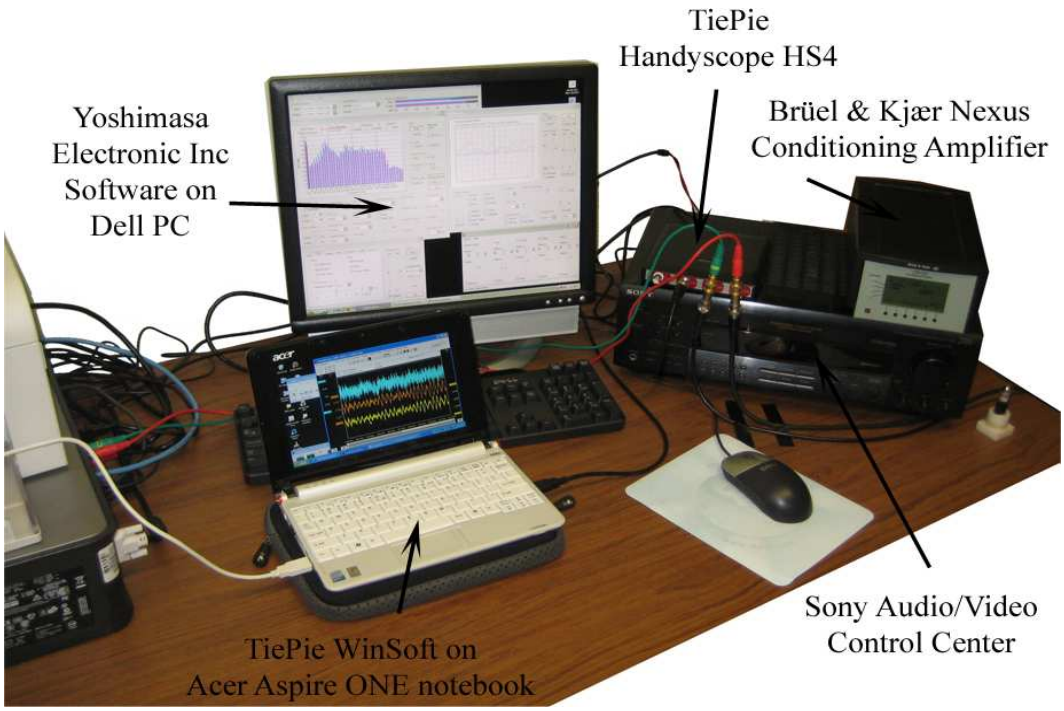


FIGURE 6.1 Signal generation, acquisition, and processing center

## 6.1 Signal Generation System

Proper acoustic measurements rely not only on accurate placement of source drivers and measurement transducers but also on the quality and “cleanness” of the test signal. Significant distortion of the test signal might not only corrupt the measurements but also harm the equipment by supplying dangerous, high-energy sound levels in the high frequency range of the

device. The research made use of the Yoshimasa Electronic Inc. Digital Signal Generator, computer software that relies on Dell PC's sound card as its O/I device. In most cases, any distortion to the output signal will occur near the maximum levels of the analog amplifier built into the D/A converter of the sound chip; for that reason, one has to adjust the digital output to appropriate levels. The major drawbacks in decreasing the level of the digital output are the reductions in the resolution and the dynamic range (the range in volume levels) of the signal. The digital level of the signal generator was adjusted to fine tune the amplitude of the output signal. For the sole purpose of transmission loss research, the resultant sound quality was considered to be adequate, and the digital level setting was omitted as a factor in distortion measurements. On the other hand, the dynamic range was a critical factor in noise measurements due to the fact that transmission loss experiments rely on sufficient signal-to-noise ratio, which in this case can be obtained only with high power test signals; as a result, a digital output device should be able to deliver large amounts of power for short periods of time. The analog amplifier in the D/A converter of a computer sound card is incapable of such power output; thus, an external power amplifier was used. In the early stages of this work, Brüel & Kjær Power Amplifier Type 2706 was used, but after testing its amplified signal, distortions were noticed in the response and the power amplifier had to be replaced with the Sony Audio/Video Control Center, a high level home theatre digital signal processing receiver. Refer to the Appendix A for the source signal distortion analysis. [41]

Inevitably, the loudspeaker driver was by far the most important hardware component of the signal generating system, but it also played a crucial role in test chamber design. The transmission loss measurements of the walls and partitions are usually done in one-third-octave bands over a standard range of mid-band frequencies, from 100 Hz to 5000 Hz. For accurate measurements, it is recommended to use an omni-directional full range speaker unit with a wide flat frequency response range. A full range speaker is also known as a coaxial or 2-way speaker, which incorporates a high frequency driver known as a tweeter inside a cone of the low frequency driver known as a woofer. Another variation, such as a 3-way speaker, may also add a midrange driver. The most important loudspeaker specifications are the rated input power, sensitivity rating and reproduction frequency response. Input power refers to the maximum amount of power a speaker can handle on a continuous basis. It is crucial that the power amplifier output does not exceed this number. The sensitivity rating, given in decibels per Watt

at one meter from the source, refers to the speaker's efficiency in converting power (Watts) to volume (decibels). The higher the rating, the higher the sound pressure level at one meter from the speaker with a given amount of amplifier power. High sensitivity not only reduces the power requirements of the amplifier, but also allows for high sound pressure levels to be produced if necessary. The frequency response is the range of frequencies the speaker unit is capable of reproducing with a certain accuracy. The accuracy is determined by a standard amplitude tolerance given by plus or minus 3 dB. The flat response is the ideal case, where all tones in the specified frequency range are treated equally with no coloration imposed by the speaker (Figure 6.2 A). A speaker whose response curve lies within the tolerance limits is regarded as a reasonably accurate speaker; reasonably, because the nature of the response varies between speakers even though they satisfy the +/- 3 dB standard. A close look at Figure 6.2 B-thru-D, reveals that all three response curves satisfy the +/- 3 dB standard but response curve C has smoother amplitude variations than B, while response curve D has a smooth response with low amplitude variations [42].

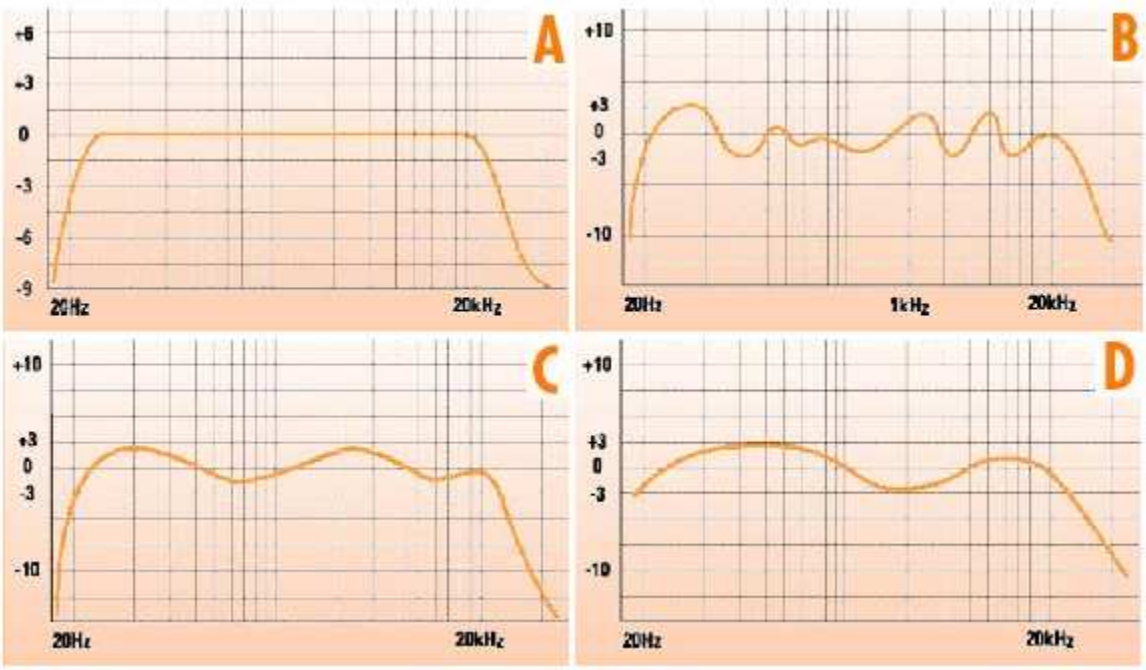


FIGURE 6.2 Examples of loudspeaker 20 – 20,000 Hz frequency response: a) flat; b) with +/- 3 dB AT; c) with +/- 3 dB AT and smoother amplitude variations; d) with +/- 3 dB AT, smoother response, and low amplitude variations [42].

Selecting a proper loudspeaker is a difficult task if the loudspeaker data sheet only specifies the frequency response range without the curve. Sometimes, even the amplitude tolerance is omitted. Omitting these crucial details might make the engineering data specifications more appealing, but it actually seriously misleads the potential user. For this reason, two 3-way loudspeaker units were used in the study: the Electro-Voice 15TRX and the RFT Carrera loudspeaker. The frequency response of each of the loudspeakers may vary depending on the acoustic environment and the loudspeaker cabinet qualities. For instance, Figures 6.3 and 6.4 illustrate the frequency response[32] curves for both loudspeakers under various environment conditions. There are three noticeable changes to the response, best seen in Figure 6.3.

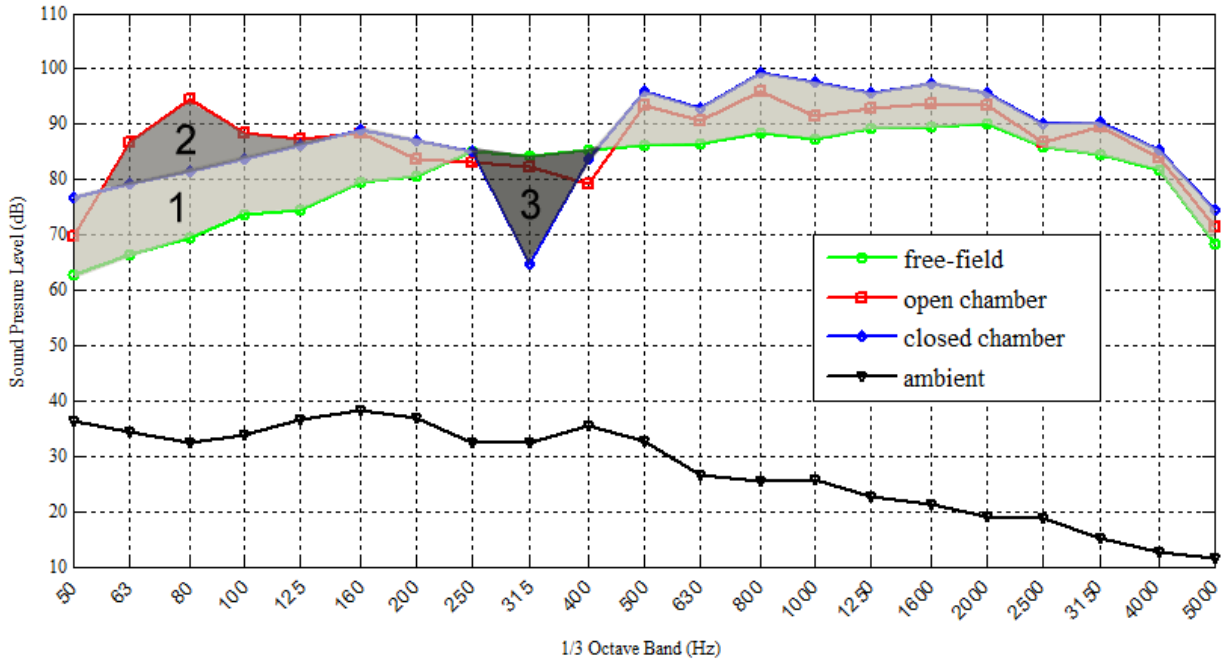


FIGURE 6.3 Electro-Voice TRX loudspeaker frequency response curves for various environmental conditions

[32] Frequency response measurements are based on the ratio of amplitudes of the output signal (speaker output) to that of the input signal (generated white noise). The vertical axis in Figures 6.3 and 6.4 are not normalized with respect to the input signal as in Figure 6.2.

- First is the change in response between the free-field and closed-chamber configuration. The increase in acoustic energy (sound pressure build up) is a direct result of enclosing the sound source within a package (inside a chamber).

- Second is the increase in low frequency sound pressure levels resulting from the sound reflected by the walls and corners of the confined space. The Electro-Voice 15TRX loudspeaker specifications documented optimum increase in low frequency response of the woofer when the driver is installed in a baffle with a minimum volume of 0.57 $m^3$ [43]. The driver was not enclosed in its own cabinet for this purpose.

- Third is the dip seen in the closed-chamber configuration response caused by destructive interference from both floor and wall reflections and as such is fairly wide. This is a very common occurrence seen in fairly reflective small to moderate spaces. There is only one dip because of the symmetry between the walls and floors which cram all the losses into a single third-octave band. The only feasible treatment to alleviate the dip is to move the loudspeaker and/or the microphone position away from the center of the chamber.

Standards recommend that the volume occupied by the sound source (loudspeaker enclosed in a cabinet) should not exceed 1% of the room volume. The Electro-Voice 15TRX loudspeaker is not the best choice, not only because it is massive, but also because it has no cabinet and poor high frequency response. An alternative sound source should be used, preferably one with a smooth response curve extending to at least the 8000 Hz octave band, so that coincidence effects of the hood can be clearly noticeable. The source should be small with respect to the chamber's volume, yet powerful enough to produce sound pressure levels of at least 45 dB above the background noise levels at each measurement band [44]. The RFT Carrera loudspeaker was the best available alternative, its response is plotted in Figure 6.4.

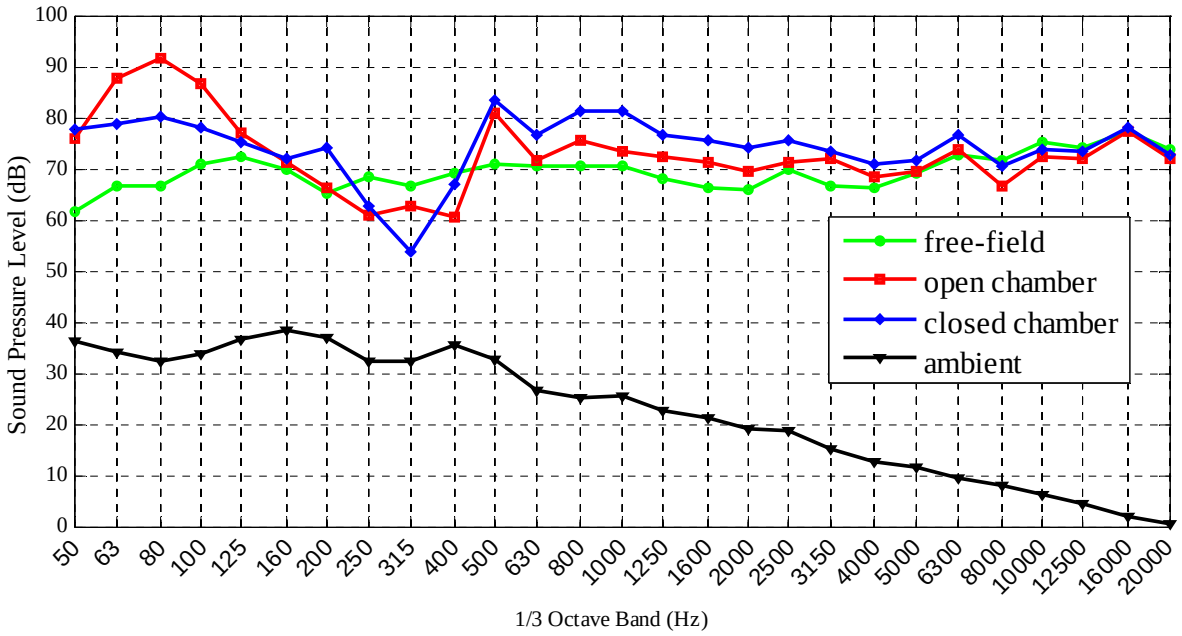


FIGURE 6.4 RFT Carrera loudspeaker frequency response curves for various environmental conditions

## 6.2 Data Acquisition System

In a semi-reverberant environment, a large number of microphone positions and additional source positions are recommended for accurate measurements. Many averages are taken because the uncertainty of the space averaged sound pressure levels increase with decreasing frequency and with decreasing room volume [40]. For this reason, measured values of sound transmission loss may change significantly, especially at lower frequencies. The change in position of the sound source also affects the results. A typical setup requires a large number of microphones connected to a multi-channel simultaneous data acquisition [29], a requirement beyond the capabilities of the Ryerson Aeroacoustic Research Facility. The most feasible alternative was to fix a single microphone at an appropriate location within the acoustic chamber while manually relocating the receiving room microphone to the various key locations along the measurement grid (Figure 6.5). The data acquisition for acoustic measurements consisted of two precision microphones: the Brüel & Kjær type 4190, 1/2" free-field microphones with Brüel & Kjær Nexus Conditioning Amplifier Type 2690 A0S2 to power the microphones and post amplify microphone signals. The TiePie USB Oscilloscope: Handyscope HS4 was used with WinSoft, TiePie windows software, to digitize the microphone signals and store the data files on an Acer Aspire ONE notebook. The digital oscilloscope was connected to the notebook rather than the Dell PC, because Dell's AC power supply corrupted oscilloscope signals. The

microphone signals were also directed to the Line In port of the Dell's onboard sound card to be processes by the Yoshimasa Electronic Inc. Acoustic Analyzing System software. The data acquisition system for vibration measurements consisted of a single LIVM accelerometer from Dytran Instruments Inc. The accelerometer, model 3030B, is lightweight (6.8 gram) and only ¼ inch (6.35 mm) in diameter. It has sensitivity[33] of 10 mV/g and frequency range from 5 – 10000 Hz. It was connected to an imc Cronos-PL2 modular measurement system, which was used with the imc FAMOS data analysis software to digitize the microphone signals and store the data files on a notebook.

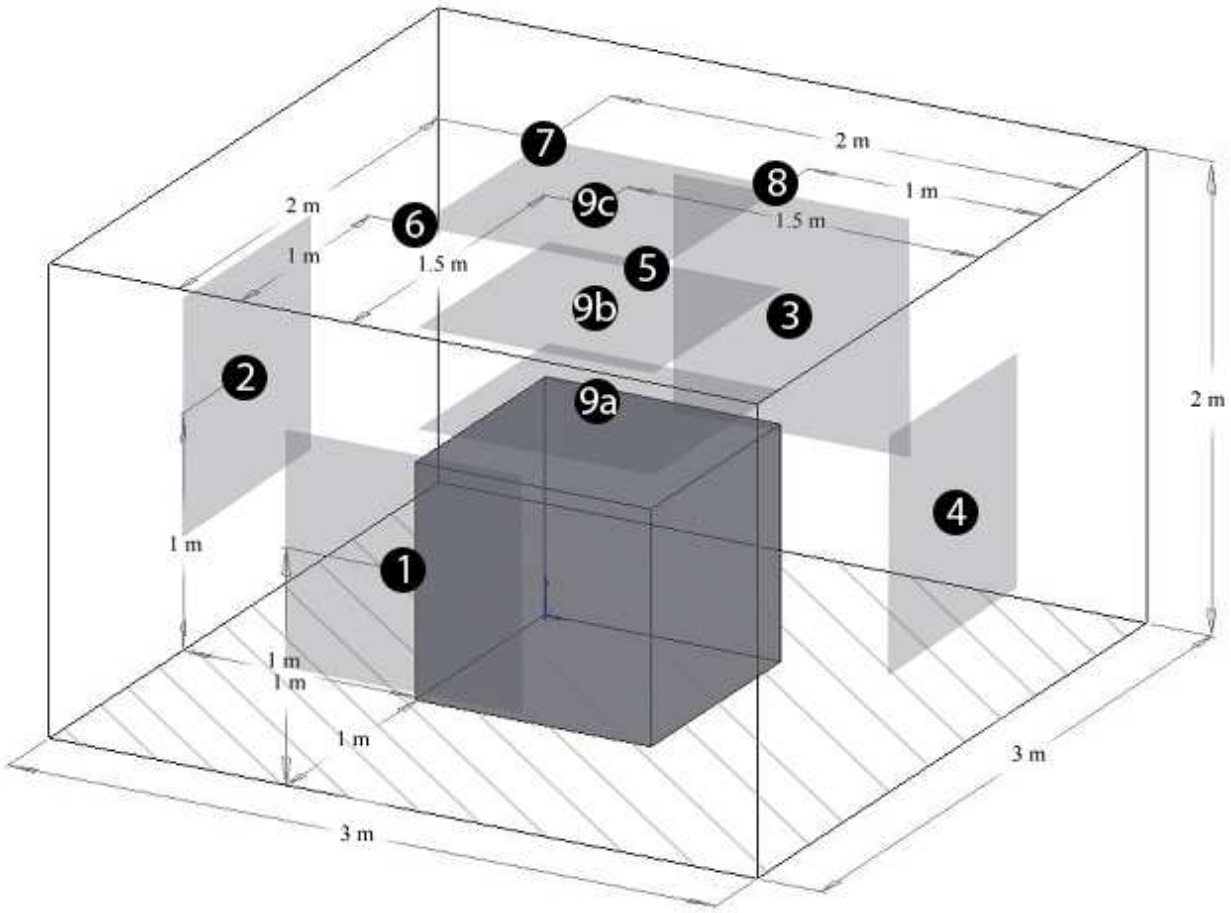


FIGURE 6.5 Microphone positions for a rectangular measurement surface. All locations are at least 1 meter from the sound emitting or reflecting surface, except position 9a and 9b which are located 0.2 and 0.5 meters from the hood respectively.

## 6.3 Signal Processing and Representation

[33] Sensitivity of the accelerometer is the ratio of the sensor's electrical output to mechanical input, typically rated in terms of mV/g. The volt (symbol: V) is the SI derived unit of electromotive force. The g-force (symbol: g) is not one of the SI derived units, but a unit of measure commonly referred to the acceleration due to gravity: 9.806 $m/s^2$.

WinSoft allows digitized microphone signals to be exported in an ASCII file format. These data files were then imported into a MATLAB interface and processed by custom algorithms. The MATLAB software is a high-level technical computing language developed by MathWorks for algorithm development, data analysis, and data visualization. Many algorithms were written over the course of this work, the most important ones are for the calculation of spectrum, total signal energy, and the equivalent continuous sound pressure level. The *spectrum* algorithm is based on the FFT algorithm and calculates the relative levels of signal energy within equally divided frequency bins. The frequency bins could be narrowband, i.e., include a "couple" of frequencies, or broadband, i.e., contain a wide range of frequencies. A time weighting function or "time window" was integrated into the spectrum algorithm. A weighting function changes the nature of the signal in the time domain, thereby implicitly changing the nature of the spectrum in the frequency domain. When the time window is applied to a continuous signal it slices the data into sections which are later analyzed. No weighting is represented by a "rectangular window", otherwise known as the "flat window". This type of window simply cuts the data when the sample size is reached and should not be used with broadband continuous signals, unless the frequency of the signal contains an integer number of cycles. For the case of a signal with a non-integer number of cycles, discontinuities at the boundaries of the time limited data cause leakage of energy from the main frequencies of a broadband signal into neighbouring frequencies. The leakage is reduced when the discontinuities are eliminated using a smoother termination between time data sections. For most applications, a "hanning window" is used in the frequency response measurements excited by true random excitation, such as white or pink noise. The *total signal energy* algorithm compares the energy of the signal in the time domain to the one in the frequency domain and serves as a total energy monitoring tool. This algorithm tested the capacity of the s*pectrum* algorithm in generating valid results. It is important to remember that a time weighted signal should be used when comparing the total signal energy of a spectrum where a time window was applied. The *equivalent continuous sound pressure level* algorithm is an extension of the *spectrum* algorithm; it further manipulates the results to an alternative form commonly used by noise control engineers [45].

Following the ASTM recommendation, an average of 10 decay rates was used for reverberation time and room absorption calculations. For sound pressure level measurements at each microphone position, a time average of 30 seconds was used. Time averaging was used to

filter any abnormalities in the signal caused by transient events. This average time was sufficient to yield a 95% confidence limit of the time-averaged sound pressure level to ±0.5dB at each one-third octave band. The sound pressure level data consisted of 22 samples, each of 1.34 seconds in length with a 97656.25 Hz sampling rate and a 131072 sample size with 16 bits instrument resolution. The sample size was the largest one available with the oscilloscope set to 16 bits instrument resolution. For the vibratory acceleration levels measurements at each accelerometer location, an average of 50 samples was used, each of 1.31 seconds in length with a 100000 Hz sampling rate and a 131072 sample size with 16 bits instrument resolution. Shannon's sampling theorem states that a continuous time signal can be completely reconstructed from its sampled values if the sampling rate (Hz) is equal to or greater than twice the highest frequency of interest; otherwise, the accuracy in reconstruction is diminished and the high-frequency spectral components of the original signal will be misinterpreted as lower-frequency components. In the current study, the transmission loss measurements are to be taken up to the upper limit of the 8000 Hz octave band; thus, a high sampling rate was required to allow reasonable accuracy of the high frequency components. The ratio of sampling rate to highest frequency of interest (8910 Hz) was approximately 11 for both the sound and the vibration measurements. In combination with the corresponding sampling size, this allowed for a frequency resolution of 0.745 Hz and 0.763 Hz, respectively. Such narrowband frequency spacing insures minimal energy losses within the sampling period between the sampled signal and the actual continuous signal. Also, it prevents any significant dips in the spectrum to go unnoticed. Further details in the signal processing are given in Appendix B, and the Matlab algorithms developed herein are given in Appendix C.

Throughout this work, the sound pressure levels and sound attenuation levels results were visualized either using the spaced-averaged sound pressure levels or time-averaged sound pressure levels also known as *equivalent continuous sound pressure level.* The algorithm used for this purpose was set to "broadband spectrum" with octave and third-octave band filters. Theses filters have passbands which are a fractional ratio of the filter's center frequency. The preferred centre frequencies and passbands are defined in following standards: ISO R 266:1997 and ANSI S1.6-1984. It is a common practice to indentify the center frequencies of each band by its nominal value; however, exact center frequencies are used in calculations. In acoustic

analysis, it is preferred to use the third-octave bands; Table 6.1 lists the third-octave bands with their nominal and exact center frequencies and the corresponding passbands [46].

Although the processing time of MATLAB algorithms is relatively short, the time required to assembly a complete set of data takes a long time, approximately 40 seconds per sample. This time constraint is directly linked with the performance of the data acquisition system. To obtain a quick real time spectrum, one-third octave and reverberation time analysis of the sound field, free trial Acoustic Analyzing System software was used, developed by the Yoshimasa Electronic Inc. To verify that the sound pressure levels results obtained at single microphone location with this software and with the MATLAB algorithm were indeed equivalent, these sound pressure levels were compared with those from a standard hand held octave spectrum analyser, CESVA SC-160. Figure 6.6 illustrates the findings. From this comparison, one can conclude that MATLAB algorithm is quite precise and much more accurate than the results obtained using the RealTime Analyzer feature of the Acoustic Analyzing System software, but it does not refute the fact that this software can be quickly and easily used within its accuracy region, 125 Hz to 4000 Hz, to measure various aspects of the sound field during time consuming calibration experiments.

TABLE 6.1 Properties of third-octave bands [46]

| Center Frequency (Hz) | | Passband (Hz) |
|---|---|---|
| Nominal | Exact | |
| 125 | 125.89 | 112 - 141 |
| 160 | 158.49 | 141 - 178 |
| 200 | 199.53 | 178 - 224 |
| 250 | 251.19 | 224 - 282 |
| 315 | 316.23 | 282 - 355 |
| 400 | 398.11 | 355 - 447 |
| 500 | 501.19 | 447 - 562 |
| 630 | 630.96 | 562 - 708 |
| 800 | 794.33 | 708 - 891 |
| 1000 | 1000.0 | 891 - 1120 |
| 1250 | 1258.9 | 1120 - 1410 |
| 1600 | 1584.9 | 1410 - 1780 |
| 2000 | 1995.3 | 1780 - 2240 |
| 2500 | 2511.9 | 2240 - 2820 |
| 3150 | 3162.3 | 2820 - 3550 |
| 4000 | 3981.1 | 3550 - 4470 |

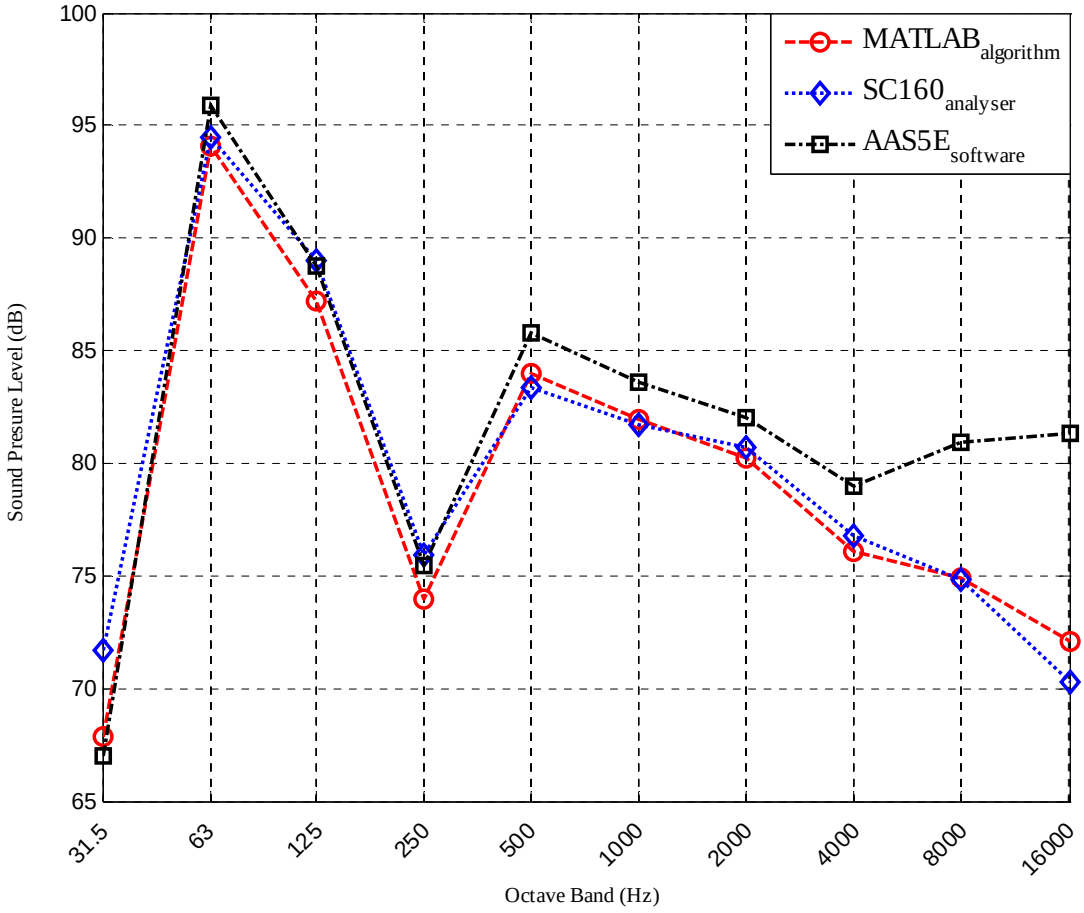


FIGURE 6.6 Comparison of results obtained by different spectrum analysers

# CHAPTER 7 RESULTS

## 7.1 Vibratory Acceleration Levels Results

The present results lead to the conclusion that the acoustical effects of varying the structure-borne vibration cannot be measured directly because the acoustic chamber was not designed to confine the airspace between the two panels to focus the acoustic energy radiated from the hood at the second panel, as originally suggested by Raasch [11]. Since the structure-born vibration transmitted through the connectors is the main source of excitation, the noise reduction at the surface of the double-panel assembly can be estimated by establishing a link between VAL and SPL (theory described in section 3.2). The assumption here is that by lowering the structure-born vibration, measured by VAL, there would be a corresponding reduction in noise. To demonstrate this hypothesis and the performance of the acoustic chamber in its double-panel configuration, acceleration measurements were conducted with rubber, neoprene, polyurethane and super-soft-polyurethane vibration isolators. The description and the appearance of these commercially available vibration isolators are demonstrated in Table 7.1 and Figure 7.1 below.

TABLE 7.1 Properties of vibration isolators

| # | Isolator Type | Description | Temperature Range |
|---|---|---|---|
| 1 | Solid | Alloy steel threaded fasteners | |
| 2 | Rubber | Superior resistance to tear and abrasion;<br>good flexibility in cold temperatures | -45°C to 65°C |
| 3 | Neoprene | Resistant to weather, ozone, and acids.<br>It has moderate resistance to oils. | -29°C to 82°C |
| 4 | polyurethane | Used in both compression and shear applications,<br>Durometer is 58A. | 13°C to 41°C |
| 5 | super-soft-polyurethane | Recommended use in compression application only.<br>Durometer is 8A. | -40°C to 82°C |

The double-panel configuration, partially illustrated in Figure 5.5A, consisted of a assembly of the hood, custom-made threaded fasteners onto which various types of vibration isolators were attached and a second panel made out of a square steel sheet of metal, 1/8 inch (3.175 mm) in thickness and 36 inch (914 mm) side length coated with yellow nylon paint,

which was also used for the hood. All parts were assembled by first screwing the threaded fasteners into the four steel flange nuts located near the corners of hood until all were secure and levelled. Each threaded fastener had a threaded hole machined at one end for attaching 5 mm bolts found on each side of vibration isolators. After attaching one end of the vibration isolator to the threaded fastener, the other end was fit through a screw hole in the second panel and fastened tightly by a nut over self-locking steel washers. This procedure was used throughout the VAL measurements except for the solid connection, where a hexagonal steel nut was screwed on the threaded fasteners to provide a load bearing surface. The connection between the hood and the second panel was completed by screwing a bolt with washers onto the threaded fastener. Acceleration measurements were taken at the center of the second panel and at one of the corner connections. Figure 7.2 illustrates the findings. The ambient line in both of the plots represents the accelerometer measurement in the absence of acoustic loading. The performance of each vibration isolator can be easily ranked according to the amount of reduction in VAL when compared with the VAL for a solid connection. Note that the latter (which serves as a reference) is above the VAL for all other connectors. Furthermore, the performance rank between vibration isolator follows the same trend regardless of the measurement location, center or corner of the panel. As suggested from the literature [10], the vibration isolator proved to be more effective in the high frequency region.

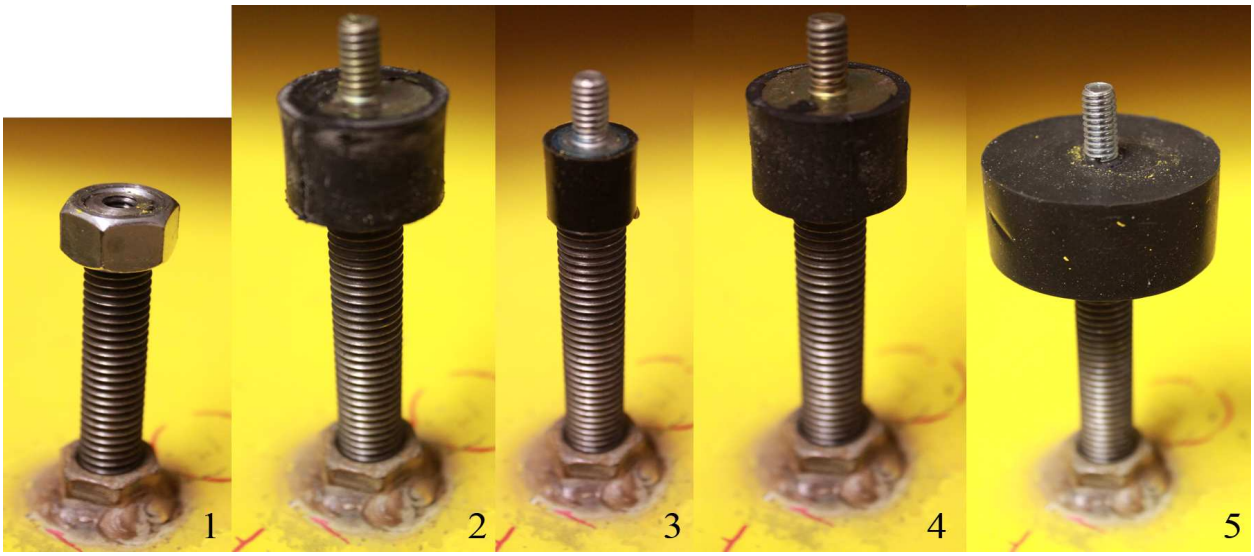


FIGURE 7.1 Various types of commercially available vibration isolators used in this thesis.

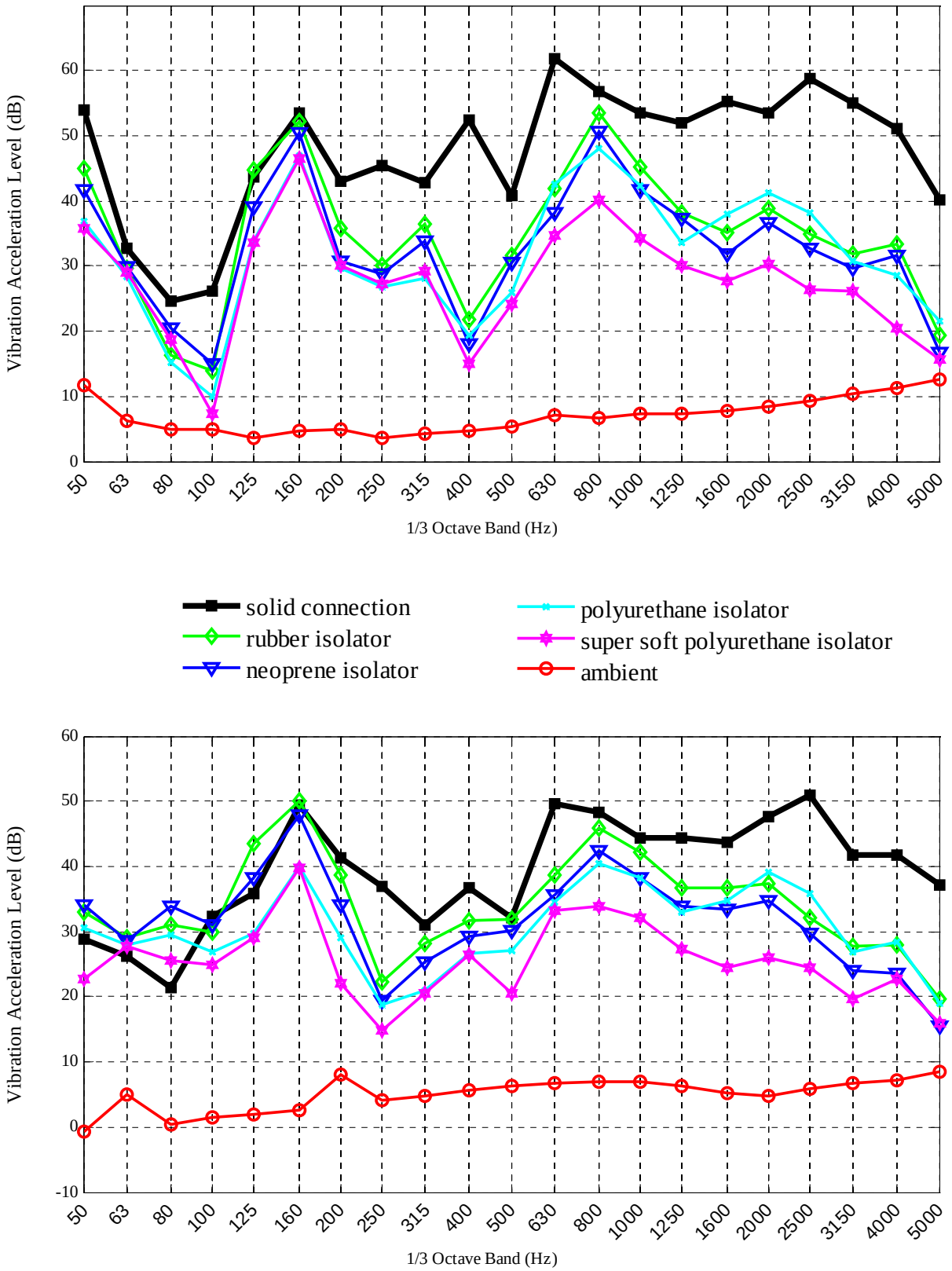


FIGURE 7.2 Vibratory acceleration levels at the center of the panel (top) and at the corner connection (bottom).

## 7.2 Transmission Loss Results

Three performance measures were used to describe sound attenuation of the hood. Two of them, noise reduction and transmission loss, will inevitably deviate from the theoretical predictions due to the fact that the space limitations of the acoustic chamber did not allow for the sound pressure level measurements to be taken at sufficient distance from the reflective surface to omit the near-field fluctuation in pressure. Although the receiving room could accommodate such measures, its semi-reverberant environment caused systematic variations in sound pressure levels with position within the permissible measurement region. These variations are depicted in Figure 7.3. In such situations, noise reduction becomes meaningless and should not be used. Fortunately, these variations occurred outside the established reliable frequency range.

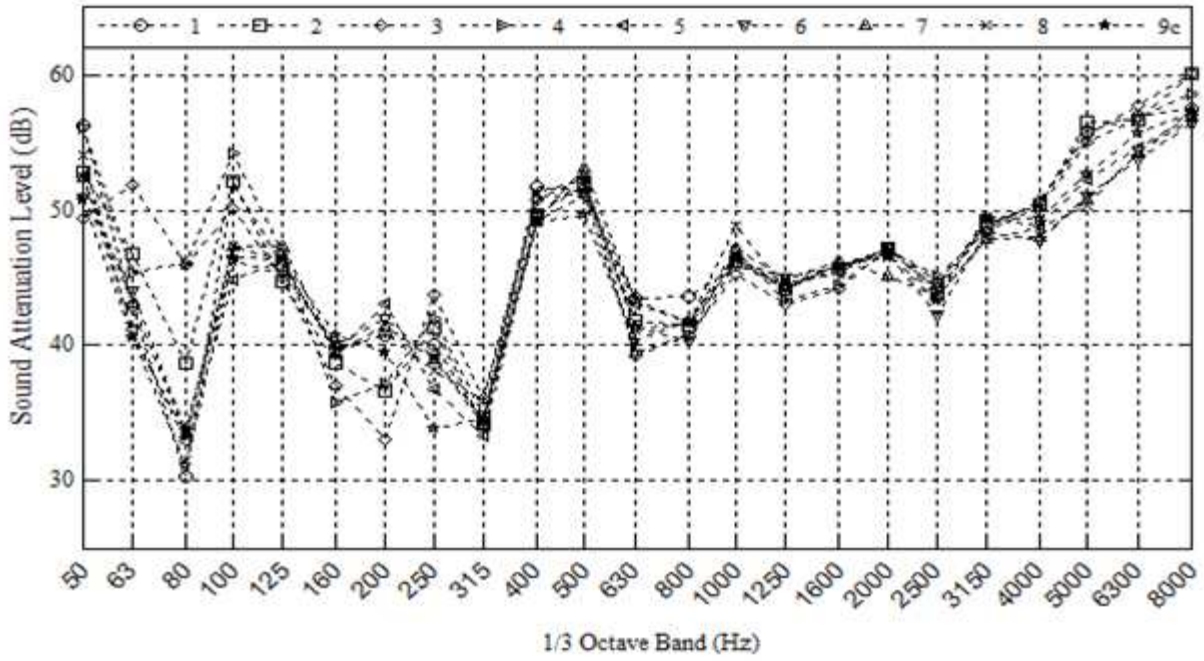


FIGURE 7.3 Variations in noise reduction caused by systematic variation in sound pressure level with position within the measurement grid.

The transmission loss relation is a more appropriate measure than noise reduction because it takes into account the parameters of the room such as room absorption (Table 5.2). Noise reduction results are used in the transmission loss calculations; thus, caution must be exercised when interpreting the transmission loss results. The sound attenuation results obtained from the insertion loss relation are the most accurate for this set up because the sound pressure

level measurements are only taken in the permissible measurement region of the receiving room before and after hood installation. It is worth noting that, during the sound pressure level measurements with the acoustic chamber in its open configuration, the laboratory equipment and furniture began to resonate in a frequency region that extended between 63 to 100 Hz third-octave. The corresponding building up of energy in this region resulted in elevated insertion loss values. Figure 7.4 compares the space-averaged transmission and insertion loss results within the predicted transmission loss confidence region.

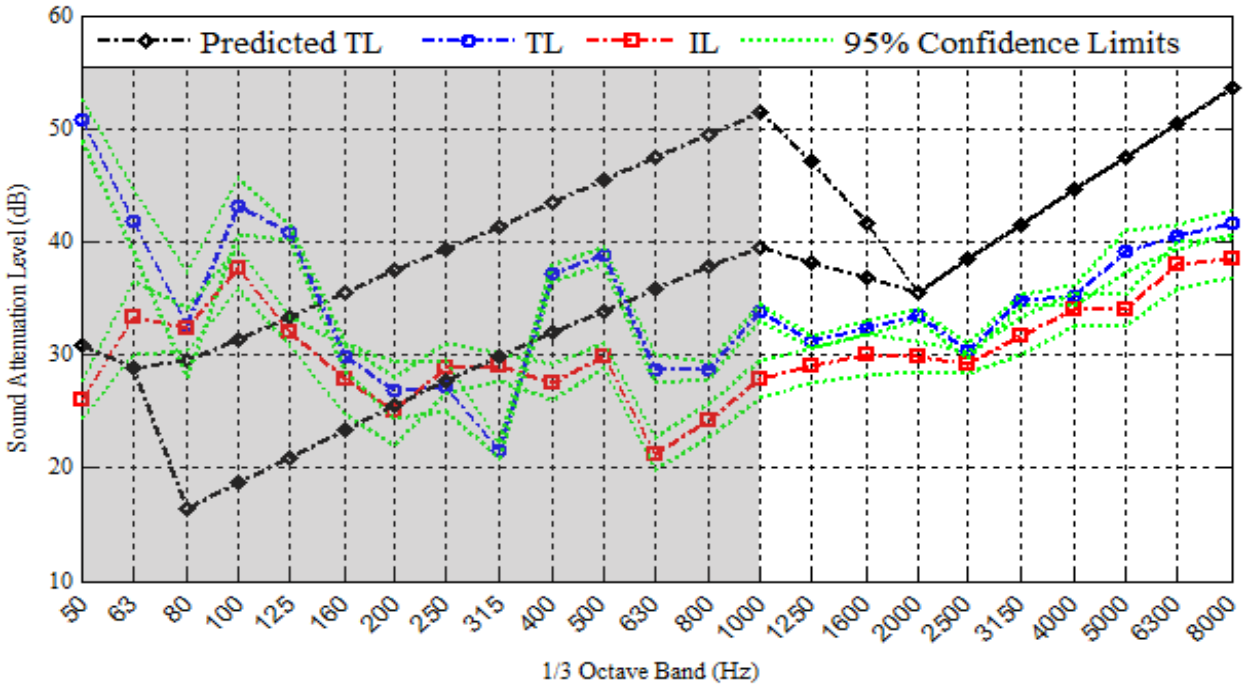


FIGURE 7.4 Comparison of the theoretical and experimental space-averaged transmission and insertion loss.

The assessment of the test facility established a 1000 Hz lower frequency limit for reliable survey level results, and a significant discrepancy between the theoretical transmission loss predictions and the measured values is seen below this limit. Above it, both transmission and insertion loss follow the trend established by the predicted values with the upper limit controlled by the theoretical transmission loss. The coincidence dip seems to occur within a band one-third-octave higher than predicted. To be sure, two more measurements were taken a lot closer to the hood, at 0.2 and 0.5 meters from the hood, location 9a and 9b respectively in Figure

6.5. Figure 7.5 supports this speculation. The coincidence dip takes place at 2500 Hz third-octave.

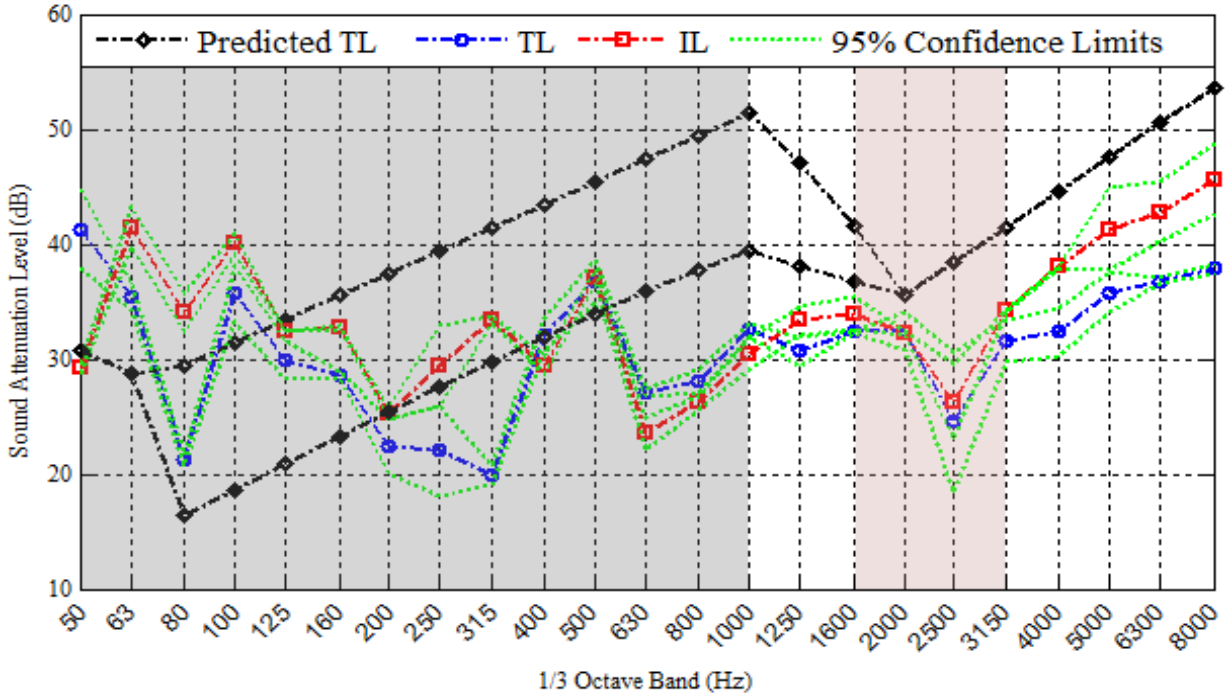


FIGURE 7.5 Comparison of the theoretical and experimental space-averaged transmission and insertion loss at locations 9a and 9b on the measurement grid.

# CHAPTER 8 SUMMARY, CONCLUSIONS AND RECOMMENDATIONS

## 8.1 Summary and Conclusions

An acoustic chamber was designed for testing structure-borne sound transmission in a double-panel assembly induced by point connectors. The structure-borne sound transmission dominated over the air-borne sound transmission, because the airspace between the two panels was not confined to focus the acoustic energy radiated from the hood at the second panel. Rubber, neoprene, polyurethane and super-soft-polyurethane vibration isolators were tested and ranked, from the least effective to most effective, in reducing the vibratory acceleration level (VAL) on the second panel. (Refer to figure 7.2). All vibration isolators proved to be more effective in the high frequency region and hold their performance ranks regardless of the measurement location.

The main focus of this thesis was the structural assessment of an acoustic chamber and its receiving room. It was concluded that the performance of the enclosures of the Ryerson Aeroacoustic Research Facility should be evaluated using the ASTM and ISO standards pertaining to the reverberation room method. The performance of the test facility for transmission loss measurements was examined by means of diffusivity measurements, reverberation time measurements, flanking transmission tests and sound power measurements. The diffusivity measurements indicated that the lower reliable frequency limit for the acoustic chamber was about 1000 Hz. This frequency was confirmed from the theoretical modal density calculations based on the size of the chamber and mean modal spacing requirements needed to sustain a diffuse sound field. The Schroeder frequency limit determined from the reverberation times of the room demanded a much lower mean modal spacing, and thus a higher lower frequency limit. The Schroeder frequency limit is a conservative value for precision grade acoustic environments; thus, for survey level measurements, the lower frequency limit measured from the diffusivity test is considered to be adequate. The flanking transmission test revealed that the sound insulation resistance of the hood is in close proximity to that of walls that make up the reverberation chamber. In consequence, the sound is transmitted through the flanking mechanism rather than through the test specimen. This indicates that caution must be exercised when interpreting any of the performance indicators like transmission loss or insertion loss of the

single-panel because the upper bound for reliable values has been reached. Structural assessment of the test facility revealed that the performance of the double-panel assembly cannot be directly measured with this set up because the second panel needs to be modified to enclose the air cavity between the two panels. In addition, the flanking transmission test indicates that the hood also needs to be modified so that the overall sound insulation resistance of the double-panel assembly is below the sound insulation resistance of the walls that make up the reverberation chamber. The sound power measurements indicate that the current sound generation system has enough sound power to overcome the minimum sound pressure levels in the receiving room to yield valid sound attenuation data.

To better estimate the sound pressure levels (SPL) from the measurement of the vibratory acceleration levels (VAL) on the plate's surface, the equation describing the relationship between VAL and SPL was revisited and adjusted to account for distance, radiation efficiency, and room effects. The estimation of sound pressure levels appears to be in good agreement with the measured sound pressure levels at various distances from the specimen. This result supports the hypothesis that it is feasible to predict sound attenuation level of a specimen using the sound pressure difference between measured SPL and those estimated from VAL.

Acoustic performance of a single-panel (hood) was evaluated using various performance measures to verify the potential of this test facility. Both the transmission loss and the insertion loss follow the trend established by the predicted values, with the upper limit controlled by the theoretical transmission loss. Although these results appear favourable, a final decision regarding their accuracy must be postponed until the structural adjustments are made to the test facility.

## 8.2 Recommendations

Throughout the course of this research, many important variables regarding the acoustic properties of the enclosures have been identified. Although the application of the changes proposed in the body of the thesis would enhance the acoustic chamber performance, a better approach would be to apply the lessons learned from the current design into a new design of the acoustic chamber; one that would not only overcome the frequency limitations due to the chamber's volume, but also incorporate different orientations and size of the test specimen. The functionality of the acoustic chamber can be enhanced through application of the following suggestions:

- Investigating the response of the specimens to low frequency excitation is primarily dependent on the large volume of the enclosure. A new design should be of adequate volume: optimize equation (2.11) and (2.11a) to result in a low frequency limit and a mean modal separation of 1-to-3 Hz (precision-to-survey). If the entire Ryerson Aeroacoustic Research Facility was reconstructed to accommodate a reverberation chamber and a receiving chamber, the lowest frequency limit would still only be about 150 Hz, which is inadequate to study the low frequencies (30-90 Hz) encountered in gas turbine exhaust installations.

- The specimen mounting plane should be oriented vertically instead of horizontally so that shearing effects of the various vibration isolators can be investigated as well. For instance, although the super-soft-polyurethane had best vibration isolation, the arrangement of four connectors of this kind is just too weak to withstand the weight of the mounted panel.

- The enclosures of turbine-generator exhaust systems are subjected to extremely high temperatures: 300-to-600 degrees Celsius. It would be beneficial to test connectors that do not become soft and irreversibly deformed when subjected to high temperatures, e.g., silicone mounts (maximum temperature range: -62°C to 288°C) or wire mesh mounts (alloy steel spring damped with metal mesh; maximum temperature range: -73°C to 204°C), and heat them while they are being tested.

# APPENDIX A: SOURCE SIGNAL DISTORTION

Testing the sound card digital output

Signals with sound levels near the extremity of D/A converter capabilities will result in a distortion in the form of clipping, where the peaks of the waveform will be cut off and appear as flat lines on an oscilloscope display. This type of distortion will also redistribute power to component frequencies (harmonics) of the fundamental frequency of the input signal. Figure A.1 and Figure A.2 demonstrate such distortion.

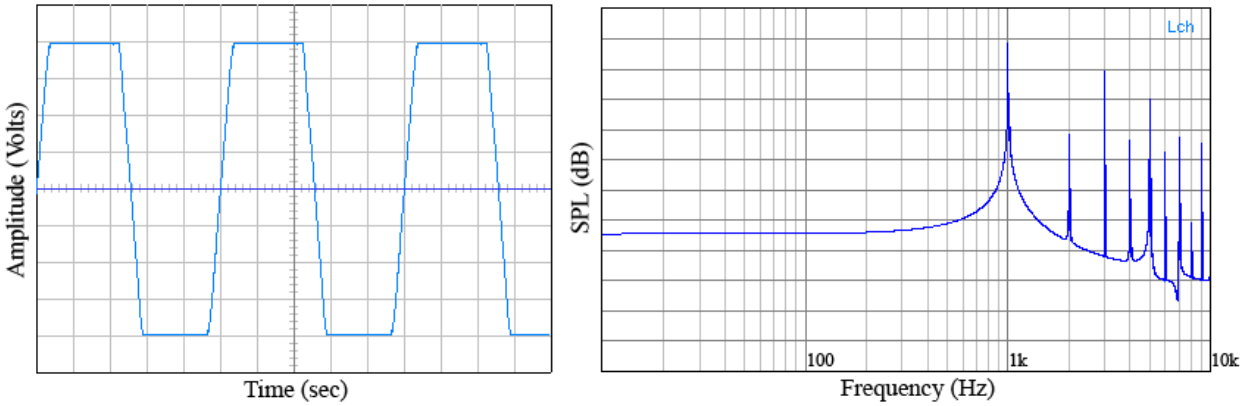


FIGURE A.1 Oscilloscope and FFT Analyzer Power Spectrum display of a clipped signal

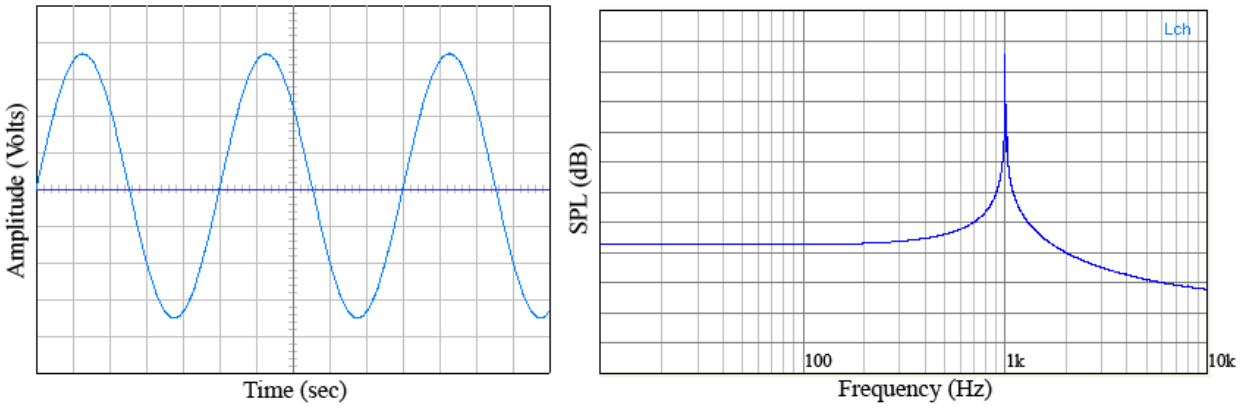


FIGURE A.2 Oscilloscope and FFT Analyzer Power Spectrum display of a proper signal

The power spectrum display of Figure A.2 represents the frequency response of an output signal routed back to the input of the computer sound card. No amplifier was connected.

Testing the power amplifier analog output

From the power spectrum, display of Figure A.3, it is evident that the Sony Audio/Video Control Center introduced minor spikes at 60 Hz and 180 Hz as well at harmonics of the input signal frequency. These distortions diminish as the power output of the amplifier is increased.

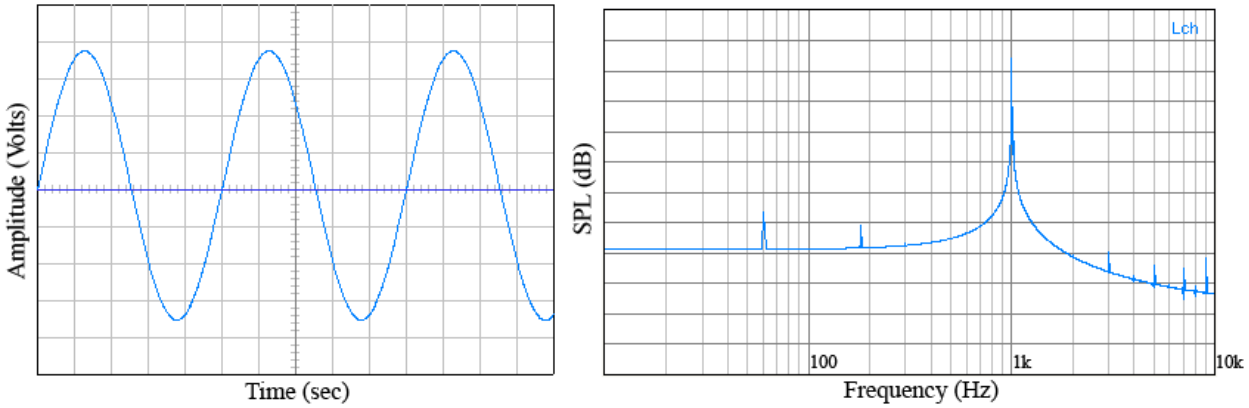


FIGURE A.3 Oscilloscope and FFT Analyzer Power Spectrum display of analog output of a Sony Audio/Video Control Center

From the power spectrum of Figure A.4, it is evident that the Bruel&Kjcer Power Amplifier Type 2706 introduced extra spikes and a lot more profound spikes at the low frequency range than the Sony Control Center, but a lot smoother response thereon. These distortions diminish as the power output of the amplifier is increased, but not as nicely as in former case.

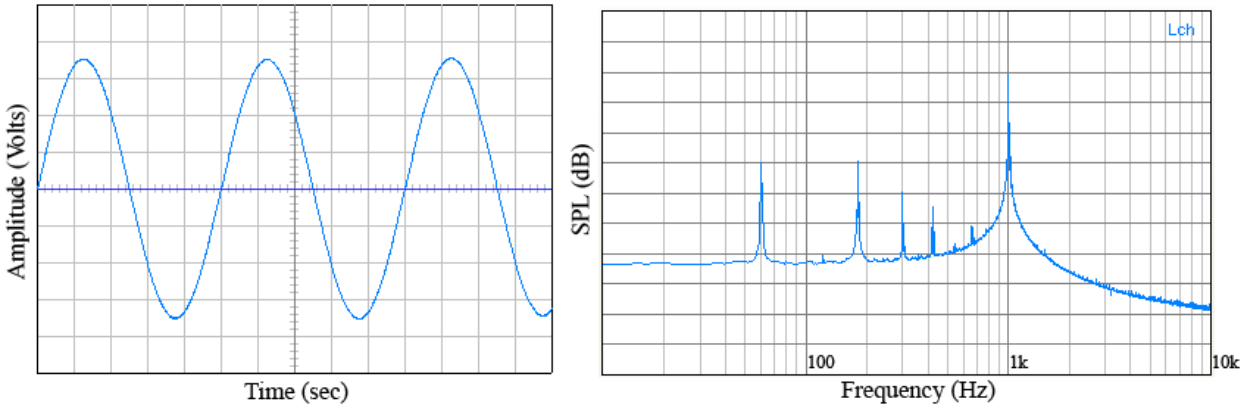


FIGURE A.4 Oscilloscope and FFT Analyzer Power Spectrum display of analog output of a Bruel&Kjcer Power Amplifier Type 2706

# APPENDIX B: SIGNAL PROCESSING THEORY

This appendix provides the reader with a comprehensive step by step derivation of the signal's spectrum, total signal energy and the equivalent continuous sound pressure level equation used in signal analysis to represent the sound transmission data obtained from the acoustic material testing.

## B.1 Spectrum

The Fourier transform (FT) maps a signal f(t) into complex "spectrum" values at a series of frequencies given by:

$$F\left(\omega_n\right) = \int_0^{\mathrm{T}} \mathrm{f}(t)\,\mathrm{e}^{-i\omega_n \mathrm{t}}\,dt \tag{B1.1}$$

where $\omega_n = 2\pi n / T$ = n$^{th}$ angular frequency instant, (rad/s)

$T$ = period of a sampled signal, s

$t$ = time, s

$i = \sqrt{-1}$ = imaginary number

Digitized signals are discrete in nature and finite in duration. Hence, the integral symbol is replaced by the summation symbol and time limits are replaced by integer (positive) numbers, and the discrete Fourier transform (DFT) results. The DFT is given by:

$$X_n = \sum_{k=0}^{N-1} x\left(t_k\right)\mathrm{e}^{-i\omega_n \mathrm{t}_k} \tag{B1.2}$$

where $X_n = X\left(\omega_n\right)$ = complex spectrum value at frequency $\omega_n$

$N$ = number of sampling points

$x\left(t_k\right)$ = time series

$t_k = k\Delta t$ = discrete-time or $k^{th}$ sampling instant, s

$\Delta t$ = T / N = sample spacing, s

The relationship between the FT and the DFT at the frequency $\omega_n$ is given by:

$$F_n = \frac{\mathrm{T}}{N} X_n \tag{B1.3}$$

Matlab software uses the fast Fourier transform (FFT) algorithm to calculate the DFT. Substituting the definitions of $\omega_n$ and $t_k$, we have:

$$X_n = \sum_{k=0}^{N-1} x_k \mathrm{e}^{-i2\pi nk/N},\ n = 0,\ \ldots,\ (N-1) \tag{B1.4}$$

where $x_k = x\left(t_k\right)$ = input signal amplitude (real or complex) as a function of time.

Matlab does not permit the use of zero or a negative index; thus, the DFT is adjusted to the following form:

$$X_n = \sum_{k=1}^{N} x_k \mathrm{e}^{-i2\pi(n-1)(k-1)/N},\ n = 1,\ 2,\ \ldots,\ N \tag{B1.5}$$

The norm (magnitude) of the Fourier amplitudes is called the Fourier spectrum (FS), and it is equal to the square root of the FFT times its conjugate, $\bar{X}_n$. FS represents the signal amplitude at each frequency bin, and for the DFT is given by:

$$\left|X_n\right| = \sqrt{X_n \bar{X}_n} \tag{B1.6}$$

Multiplying the above relation by the constant $\frac{T}{N}$, we get the FS:

$$\left|F_n\right| = \frac{\mathrm{T}}{N}\sqrt{X_n \bar{X}_n} \tag{B1.7}$$

The square of the norm is called the spectral density function, or the spectrum as it is commonly referred to. It describes relative levels of energy within equally divided frequency bins.

$$\left|F_n\right|^2 = \left(\frac{\mathrm{T}}{N}\right)^2 \left|X_n\right|^2 \tag{B1.8}$$

## B.2 Total Signal Energy

The total signal energy, i.e., the mean square value, is generally given by:

$$\overline{x^2} = \frac{1}{T}\int_0^T \mathrm{x}(t)^2\, dt \tag{B2.1}$$

The definite integral can be expressed as a sum by using the following definition:

$$\int_a^b f\, dx = \lim_{\Delta x \to 0} \sum_{x=a}^{b} f(x)\,\Delta x \tag{B2.2}$$

Hence,

$$\overline{x^2} = \frac{1}{N}\sum_{k=0}^{N-1} x_k^2 \tag{B2.3}$$

The root mean square value (RMS) for two sided FFT is given by:

$$\sqrt{\overline{x^2}} = \sqrt{\frac{1}{N}\sum_{k=0}^{N-1} x_k^2} \tag{B2.4}$$

The energy of the signal, as represented in the time and frequency domains, is related by the use of Parseval's theorem. The theorem states that the total signal energy contained in a time domain waveform $x(t)$ is equal to the total energy of the waveform's Fourier Transform $X(f)$, i.e.,

$$\int_{-\infty}^{\infty} |\mathrm{x}(t)|^2 dt = \int_{-\infty}^{\infty} |X(f)|^2 df \tag{B2.5}$$

Adopting the theorem to finite signals yields:

$$\frac{1}{T}\int_0^T |x(t)|^2 dt = \int_0^{fmax} |F(f)|^2 df \tag{B2.6}$$

where $|F(f)|^2 = \left(\frac{\mathrm{T}}{N}\right)^2 |X(f)|^2$

Expressing the definite integral as a sum:

$$\frac{\Delta t}{T}\sum_{k=0}^{N-1} x_k^2 = \Delta f \left(\frac{T}{N}\right)^2 \sum_{n=0}^{N/2-1} |X_n|^2 \tag{B2.7}$$

Substituting the definitions of $\Delta t$ and $\Delta f$ yields:

$$\overline{x^2} = \frac{1}{N}\sum_{k=0}^{N-1} x_k^2 = \frac{T}{N^2} \sum_{n=0}^{N/2-1} |X_n|^2 \tag{B2.8}$$

for the one-sided Spectrum

$$\overline{x^2} = \frac{1}{N}\sum_{k=0}^{N-1} x_k^2 = \frac{T}{N^2}\sum_{n=0}^{N-1} |X_n|^2 \qquad \text{(B2.9)}$$

for the two-sided Spectrum

It is convenient to represent the total signal energy (TSL) in logarithmic units called decibels (dB):

$$\text{TSL} = 10\log_{10}\left(\overline{x^2}\right) \qquad \text{(B2.10)}$$

## B.3 Equivalent Continuous Sound Pressure Level

The equivalent continuous sound pressure level is widely used by spectrum analyzers as an index for noise. It is defined as sound pressure level of a noise fluctuating over a period of time *T* and is expressed as the average (mean-squared) energy:

$$L_{eq} = 10\log_{10}\left(\frac{1}{T}\int_0^T \frac{P^2}{P_0^2}\,dt\right) \qquad \text{(B3.1)}$$

where $P_0$ is reference pressure level = 20μPa

Adjusting the above expression to the nomenclature used in this thesis, yields:

$$L_{eq} = 10\log_{10}\left(\frac{1}{T}\int_0^T \frac{|x(t)|^2}{P_0^2}dt\right) \qquad \text{(B3.2a)}$$

$$= 10\log_{10}\left(\frac{1}{P_0^2}\frac{1}{T}\int_0^T |x(t)|^2 dt\right) \qquad \text{(B3.2b)}$$

$$\approx 10 \log_{10}\left( \frac{1}{P_0^2} \frac{1}{N} \sum_{k=0}^{N-1} \left| x_k \right|^2 \right) \tag{B3.2c}$$

$$\approx 10 \log_{10}\left( \frac{1}{P_0^2} \frac{\mathrm{T}}{N^2} \sum_{n=0}^{N-1} \left| X_n \right|^2 \right) \tag{B3.2d}$$

# APPENDIX C: MATLAB ALGORITHMS

Algorithms written for this thesis incorporated various subprograms, listed in Table C.1, that were originally published by Edward Zechmann under a file name titled "Nth_Oct_Hand_Arm_&_AC_Fi," file ID# 22512, last updated on January 7th, 2009. This file was downloaded from Matlab Cental, an open file exchange for the Matlab and the Simulink user community. All other relevant algorithms are summarized below.

TABLE C.1 Subprograms downloaded from Matlab Central

| Program | Description |
|---|---|
| nth_freq_band<br><br>Dependent Subprograms:<br>sd_round | This program calculates the 1/N-octave band center frequencies and also the lower and upper band edge limits of every frequency band from min_f to max_f (Hz).<br><br>Input Variables:<br>N is the number of frequency bands per octave; min_f is the minimum frequency band to calculate (Hz); max_f is the maximum frequency band to calculate (Hz).<br><br>Output Variables:<br>fc is the vector of nominal center frequency bands (Hz); fc_ext is the vector of exact center frequency bands (Hz); fc_l is the vector of nominal lower bounds of the frequency bands (Hz); fc_ext_l is the vector of exact lower bounds of the frequency bands (Hz); fc_u is the vector of nominal upper bounds of the frequency bands (Hz); fc_ext_u is the vector of exact upper bounds of the frequency bands (Hz). |
| pressure_spectra<br><br>Dependent Subprograms:<br>flat_top<br>number_of_averages<br>spectra_estimate<br>sub_mean<br>window_correction_factor | This function calculates an accurate estimate for the spectra.<br><br>Input Variables:<br>x is the input time record of sound or vibrations data; Fs is the sampling rate (Hz); bin_size is the number of points in each fft should be divisible by 2; win_type is the type of window for smoothing the time records to zero before computing the FFTs. |

```
function MovingAverage
% ========================================================================
% Program imports .DAT files in time domain and calculates fft. It then
% computes moving average for multiple runs. The results are combined and
```

```
% saved to a single .DAT file
% ========================================================================

% data sampling specs
bin_size = 131072;                  % record length
Fs = 97656.25;                      % sampling rate
Bmax = round(22500/(Fs/bin_size));  % upper bound index number
wd = ('hann');                      % filter window type
Scale = 1/0.0316;                   % Nexus gain set to 31.6mV/Pa

%% file reading and fft
cd('C:/Users/Documents/MATLAB/...');      % changes directory to data folder
dataDir = dir('*.DAT');                   % omits all but .DAT files
M = zeros(bin_size/2,length(dataDir));    % space pre-allocation
for j = 1:length(dataDir)                 % counts # of .DAT files the folder
    currFile = dataDir(j).name;           % sequential file reading
    x_t = dlmread(currFile,',',5,0);      % loads data omitting first 5 lines
    % HS4 data output contains insignificant info at those 5 lines
    sx = x_t*Scale;                       % correction to Nexus scaled data
    % FFT calculation
    cd('C:/Users/Documents/MATLAB/...')
    % changes directory to main algorithm folder
    [SP, f, x, bin_size] = pressure_spectra(sx, Fs, bin_size,1,wd);
    % FFT algorithm; SP output contains the amplitudes in frequency domain
    P = (bin_size*SP').^2./2;             % FFT algorithm output modification
    % the correction converts the root-mean-square energy (SP) to energy (P)
    M(:,j)= P; % data matrix which stores SP from each run in separate column
    cd('C:/Users/Documents/MATLAB/...');
    % changes directory back to data folder
end

%% Parseval's Theorem, total signal energy comparison
tse_td = 1/bin_size*sum((sx).^2);   % energy in time domain: eq'n (b.29)
tse_fd = Fs/bin_size*sum(P);        % energy in frequency domain: eq'n (b.29)
er = tse_td - tse_fd;

%% moving average code
P_old_sum = zeros(length(M),1);         % space pre-allocation, starting sum
```

```
P_old_avg = zeros(length(M),1);          % space pre-allocation, starting avg
P_new_sum = zeros(length(M),1);          % space pre-allocation, ending avg
for i = 1:length(dataDir)
    P_new_sum = P_old_sum + M(:,i);      % new, i sum
    P_new_avg = P_new_sum/i;             % average after i sums
    P_old_sum = P_new_sum;               % old = new
    P_old_avg = P_new_avg;               % old avg = new avg
end
cd('C:/Users/Documents/MATLAB/...')      % changes directory to a new folder
savedata = [f', A_new_avg];              % saves moving average result
save('MovingAverageData.DAT','savedata', '-ASCII'); % file name and format
cd('C:/Users/Documents/MATLAB/...)
% changes directory back to main algorithm folder



function Octave(N, min_f, max_f);
% ========================================================================
% Program imports .DAT files in frequency domain and groups the data to
% 1/N-octave band and computes equivalent continuous sound pressure level
% per 1/N-octave
% ========================================================================

%% input variables:
% N is the number of frequency bands per octave. Can be any number greater
%     than 0. Default is 3 for third octave bands.
% min_f is the minimum frequency band to calculate (Hz). Must be greater than
%     0. Default is 20;
% max_f is the maximum frequency band to calculate (Hz). Must be greater than
%     0.  Default is 20000;

%% output variables:
% fc is the vector of nominal center frequency bands in Hz.
% fc_ext is the vector of exact center frequency bands in Hz.
% fc_l is the vector of nominal lower bounds of the frequency bands in Hz.
% fc_ext_l is the vector of exact lower bounds of the frequency bands in Hz.
% fc_u is the vector of nominal upper bounds of the frequency bands in Hz.
% fc_ext_u is the vector of exact upper bounds of the frequency bands in Hz.
```

```
%% constants if no input arguments are specified by the user
if (nargin < 1 || isempty(N)) || ~isnumeric(N)
    N = 3;          % number of bands per octave.
end
if (nargin < 2 || isempty(min_f)) || ~isnumeric(min_f)
    min_f = 20;     % the minimum frequency band to calculate (Hz).
end
if (nargin < 3 || isempty(max_f)) || ~isnumeric(max_f)
    max_f = 20000;  % the maximum frequency band to calculate (Hz).
end
if (nargin < 4 || isempty(max_f)) || ~isnumeric(max_f)
    method = 1;     % 1-random incidence; 2-field incidence; 3-Sewell.
end

% reference constant
bin_size = 131072;      % record length
Fs = 97656.25;          % sampling rate
Pref = 20*10^(-6);      % reference sound pressure threshold of hearing (Pa)

% load data
cd('C:/Users/Documents/MATLAB/...');      % changes directory to data folder
data = load('MovingAverageData.DAT');     % moving average data
f = data(:,1);          % frequency
Amp = data(:,2);        % amplitude

%% nth frequency band
cd('C:/Users/Documents/MATLAB/...')
% changes directory to main algorithm folder
[fc,fc_l,fc_u,fc_ext,fc_ext_l,fc_ext_u] = nth_freq_band(N, min_f, max_f);
% this algorithm calculates the 1/nth octave frequency bands center, lower,
% and upper band edge limits

%% 1/N-octave band PSD calculator
P_band = zeros(length(fc),1);             % space pre-allocation
P_Leq = zeros(length(fc),1);              % space pre-allocation
for i=1:length(fc)
    indices = find(fc_ext_l(i,1) < f & f < fc_ext_u(i,1));
```

```
    % number of pressure points that fall in a given band width
    BinP  = zeros(length(indices),1);
    % number of pressure bins in a band, space pre-allocation
    for j = 1:length(indices)
        BinP(j,1) = Amp(indices(j));
        % pressure (energy) at a given frequency bin
    end
    P_band(i,1) = sum(BinP);
    % pressure (energy) in a given frequency band
    P_Leq(i,1) = 10*log10(P_band(i,1)/Fs/bin_size/Pref^2);
    % equivalent continuous sound pressure level per octave
end
```

# REFERENCES


[1] Godish, Thad., Air Quality 4th ed. Boca Raton: Lewis Publishers, 2004.

[2] Bradley, J.S."Sound in Rooms." National Research Council Institute for Research in Construction. 18 August 2009. (18 August 2009) <http://www.nrccnrc.gc.ca/eng/ibp /irc/bsi/85-sound-rooms.html>

[3] ASTM E1686-03, Standard Guide for Selection of Environmental Noise Measurement and Criteria, Philadelphia.

[4] Frank, Leslie. "Noise Control Engineering Objectives for Compressor Station Turbo-Compressor Units." Industrial Application of Gas Turbines Committee. (7 June 2009). <http://www.iagtcommittee.com/downloads/3.3paper.doc>

[5] Evans, J.B. "Vibration Control for a 25 MW Steam-Turbine Generator Installation Near Academic Teaching and Research Laboratories" The 12th International Congress on Sound and Vibration Portugal: Lisbon, 2005.

[6] Tran, Josepth & Carley, John. "Passive Noise Control – an Engineering Challenge" Sound and Vibration Articles. August 2005. (10 September 2009). <http://findarticles. com/p/articles/mi_qa4075/is_200508/ai_n15613172/pg_2/?tag=content;col1>

[7] ONSB_1_23_07.pdf [2850K], (3 May 2009). <http://www.sce.com/NR/rdonlyres/3DA1 CA40-42EB-4056-866C-FE4E5BB6B586/0/PKRBDS_1_15_07.pdf>

[8] Parzych, D. J. "Estimating Community Sound Levels of Large Industrial Equipment" Proceedings of the Air & Waste Management Association's 94th Annual Conference & Exhibition Orlando, FL, 2001.

[9] y225.pdf [190K], (3 May 2009). <http://www.gp.com/BUILD/DocumentViewer.aspx? repository=BP&elementid=3804>

[10] "Exhaust Systems." ATCO Noise Management Higgott-Kane Division. (15 April 2009). <http://www.higg-kane-atco.com/products_exhaust_read_more.htm>

[11] Raasch, David A., "An Investigation Into Structure-borne Transmission Loss" B.Eng. thesis, Ryerson University, 2003.

[12] De Silva, Clarence W. Vibration and Shock Handbook Boca Raton: Taylor & Francis, 2005.

[13] Harris, Cyril M. (Editor) Shock and Vibration Handbook 3nd ed. New York: McGraw-Hill, 1988.

[14] Norton, M. P. Fundamentals of Noise and Vibration Analysis for Engineers. 2nd ed. New York: Cambridge University Press, 2003.

[15] Sewell, E. "Transmission of Reverberant Sound Through a Single-Leaf Partition Surrounded by an Infinite Rigid Baffle" Journal of Sound and Vibration 12.1, 1970, pp. 21-32.

[16] Callister, J. "An Empirical Scheme to Predict the Sound Transmission Loss of Single-Thickness Panels" Journal of Sound and Vibration 222.1, 1999, p. 145.

[17] Fahy, Frank. Sound and Structural Vibration : Radiation, Transmission and Response. Ed. P. Gardonio and Knovel (Firm). 2nd ed. Boston: Elsevier/Academic, 2007.

[18] Cremer, L. "Theorie der Schalldämmung Wände bei schrägem Einfall" Akustische Zeitschrift, 7 (1942): 81-104. Reprinted in Benchmark Papers in Acoustics Vol 10, Northwood, T. D., (Editor) "Theory of the Sound Attenuation of Thin Walls with Oblique Incidence" Architectural Acoustics Dowden, Hutchinson and Ross, Stroudsburg, Pennsylvania, 1977, pp. 367–399.

[19] Sharp, B.H. "Prediction Methods for the Sound Transmission of Building Elements" Noise Control Engineering 11.2, 1978, pp. 53-63.

[20] Long, Marshall. Architectural Acoustics Boston: Elsevier/Academic Press, 2006.

[21] Beranek, L., & Ver, I., (Editors) Noise and Vibration Control Engineering: Principles and Applications 2nd ed. Hoboken, N.J.: John Wiley & Sons, 2006.

[22] Kuttruff, Heinrich. Room Acoustics 4th ed. London: Spon, 2000.

[23] ASTM E90-09, Standard Test Method for Laboratory Measurement of Airborne Sound Transmission Loss of Building Partitions and Elements, American Society for Testing and Materials, Philadelphia.

[24] ASTM C423-08a, Standard Test Method for Sound Absorption and Sound Absorption Coefficients by the Reverberation Room Method, American Society for Testing and Materials, Philadelphia.

[25] ASTM C634-09, Standard Terminology Relating to Building and Environmental Acoustics, American Society for Testing and Materials, Philadelphia.

[26] Walker, J. G. & White, R. G. (Editors) Noise and Vibration Chichester, Eng.: Ellis Horwood; New York: Halsted Press, 1982.

[27] Winer, Ethan."How to Tune Your Room" RealTraps® Articles. August 2004. (1 March 2009). <http://www.realtraps.com/art_tuning.htm>

[28] "Room modes and Standing Waves" State of the Art Acoustik. (1 March 2009). <http://www.sota.ca/

[29] NI Developer Zone, "Acoustic Test Chambers and Environments" National Instruments. 15 November 2006. (26 June 2009). <http://zone.ni.com/devzone/cda/tut/p/id/264>

[30] "Full/Hemi Anechoic Chambers." ECKEL Noise Control Technologies. (26 June 2009). <http://www.eckelusa.com/products/test-chambers/anechoic-chambers.html>

[31] Tsui, Chung Y., Carl R. Voorhees, and Jackson C. S. Yang., "The Design of Small Reverberation Chambers for Transmission Loss Measurement" Applied Acoustics 9.3, 1976, pp. 165-175.

[32] Everest, F. Alton., Master Handbook of Acoustics 4th ed. Blue Ridge Summit, Pa.: Tab Books, 1981.

[33] Product Description "LMS Test.Lab Acoustic Material and Component Testing." LMS® Engineering Innovation. (26 June 2009). <http://www.lmsintl.com/testing/testlab/acoustics/material-component-testing>

[34] Applications, "Material Testing Standards." Brüel & Kjær. (26 June 2009). <http://www.bksv.com/Applications/MaterialTesting/MaterialTestingStandards.aspx>

[35] bp1039.pdf [816K], (26 June 2009). <http://www.bksv.com/doc/bp1039.pdf>

[36] Anderson, Brian E., "Derivation of Moving-Coil Loudspeaker Parameters Using Plane Wave Tube Techniques" Master's thesis, Brigham Young University, 2003.

[37] Comeau, Peter J. "Speaker Cabinets – a material history – Part1" Speaker-Parts Blog. 31 August 2007. (30 June 2009). <http://speaker-parts.worldomain.net/info/speakers/speaker_cabinets-pt1.php>

[38] Wharfedale_CabinetModels_1962_page1-8.pdf [17020KB], (3 May 2009). <http://www.troelsgravesen.dk/Wharfedale_cat_files/Wharfedale_CabinetModels_1962_page1-8.pdf>

[39] ASTM E 1289-08 Standard Specification for Reference Specimen for Sound Transmission Loss, American Society for Testing and Materials, Philadelphia.

[40] ASTM E336-09, Standard Test Method for Measurement of Airborne Sound Attenuation between Rooms in Buildings, American Society for Testing and Materials, Philadelphia.

[41] "RA Program Manual." Yoshimasa Electronic Inc. 13 July 2005. (24 March 2008) < http://www.ymec.com/manual/era/operation.htm#basic_inout>

[42] Dicomo, Paul. "Understanding Speaker Frequency Response." ecoustics Articles. 9 April 2009. (30 June 2009). <http://forum.ecoustics.com/bbs/messages/34579/131062.html>

[43] 15TRX & 15TRXB EDS.pdf [539K], (15 July 2009). <http://archives.telex.com/archives/EV/Speakers/EDS/15TRX%20&%2015TRXB%20EDS.pdf>

[44] Rivera, Dean. "Standardized Testing." Sound & Video Articles. 1 September 2001. (24 June 2009). <http://svconline.com/mag/avinstall_standardized_testing/>

[45] Application Note, "Time Windows." Brüel&Kjær. 1994. (7 May 2009) <http://www.bksv.com/Library/Application%20Notes.aspx>

[46] "Science & Engineering Encyclopedia Version 2.3." Dirac Delta Consultants Ltd. (24 March 2008) <http://www.diracdelta.co.uk/science/source/o/c/octave/source.html>